

Numerical Simulation of Ground- Water Flow in the Central Part of the Western San Joaquin Valley, California

United States
Geological
Survey
Water-Supply
Paper 2396

Prepared in cooperation
with the San Joaquin
Valley Drainage Program



AVAILABILITY OF BOOKS AND MAPS OF THE U.S. GEOLOGICAL SURVEY

Instructions on ordering publications of the U.S. Geological Survey, along with the last offerings, are given in the current-year issues of the monthly catalog "New Publications of the U.S. Geological Survey." Prices of available U.S. Geological Survey publications released prior to the current year are listed in the most recent annual "Price and Availability List." Publications that are listed in various U.S. Geological Survey catalogs (see **back inside cover**) but not listed in the most recent annual "Price and Availability List" are no longer available.

Prices of reports released to the open files are given in the listing "U.S. Geological Survey Open-File Reports," updated monthly, which is for sale in microfiche from the U.S. Geological Survey Books and Open-File Reports Sales, Federal Center, Box 25286, Denver, CO 80225.

Order U.S. Geological Survey publications **by mail or over the counter** from the offices given below.

BY MAIL

Books

Professional Papers, Bulletins, Water-Supply Papers, Techniques of Water-Resources Investigations, Circulars, publications of general interest (such as leaflets, pamphlets, booklets), single copies of periodicals (Earthquakes & Volcanoes, Preliminary Determination of Epicenters), and some miscellaneous reports, including some of the foregoing series that have gone out of print at the Superintendent of Documents, are obtainable by mail from

**U.S. Geological Survey, Books and Open-File Reports Sales
Federal Center, Box 25286
Denver, CO 80225**

Subscriptions to periodicals (Earthquakes & Volcanoes and Preliminary Determination of Epicenters) can be obtained **ONLY** from

**Superintendent of Documents
U.S. Government Printing Office
Washington, DC 20402**

(Check or money order must be payable to Superintendent of Documents.)

Maps

For maps, address mail orders to

**U.S. Geological Survey, Map Sales
Federal Center, Box 25286
Denver, CO 80225**

Residents of Alaska may order maps from

**U.S. Geological Survey, Map Sales
101 Twelfth Ave., Box 12
Fairbanks, AK 99701**

OVER THE COUNTER

Books

Books of the U.S. Geological Survey are available over the counter at the following U.S. Geological Survey offices, all of which are authorized agents of the Superintendent of Documents.

- **ANCHORAGE, Alaska**—4230 University Dr., Rm. 101
- **LAKEWOOD, Colorado**—Federal Center, Bldg. 810
- **MENLO PARK, California**—Bldg. 3, Rm. 3128, 345 Middlefield Rd.
- **RESTON, Virginia**—National Center, Rm. 1C402, 12201 Sunrise Valley Dr.
- **SALT LAKE CITY, Utah**—Federal Bldg., Rm. 8105, 125 South State St.
- **SPOKANE, Washington**—Rm. 135, U.S. Post Office Bldg., W. 904 Riverside Ave.
- **WASHINGTON, D.C.**—U.S. Department of the Interior Bldg., Rm. 2650, 1849 C St., NW.

Maps

Maps may be purchased over the counter at the U.S. Geological Survey offices where books are sold (all addresses in above list) and at the following Geological Survey offices:

- **ROLLA, Missouri**—1400 Independence Rd.
- **FAIRBANKS, Alaska**—New Federal Building, 101 Twelfth Ave.

Numerical Simulation of Ground- Water Flow in the Central Part of the Western San Joaquin Valley, California

By KENNETH BELITZ, STEVEN P. PHILLIPS, and
J.M. GRONBERG

Prepared in cooperation with the
San Joaquin Valley Drainage Program

U.S. GEOLOGICAL SURVEY WATER-SUPPLY PAPER 2396

U.S. DEPARTMENT OF THE INTERIOR
BRUCE BABBITT, Secretary

U.S. GEOLOGICAL SURVEY
DALLAS L. PECK, Director



Any use of trade, product, or firm names in this publication is for descriptive purposes only and does not imply endorsement by the U.S. Government

UNITED STATES GOVERNMENT PRINTING OFFICE: 1993

For sale by the
Books and Open-File Reports Sales
U.S. Geological Survey
Federal Center, Box 25286
Denver, CO 80225

Library of Congress Cataloging in Publication Data

Belitz, Kenneth.

Numerical simulation of ground-water flow in the central part of the western San Joaquin Valley, California / by Kenneth Belitz, Steven P. Phillips, and J.M. Gronberg.

p. cm. — (U.S. Geological Survey water-supply paper ; 2396)

Includes bibliographical references (p.).

1. Groundwater flow—California—San Joaquin River Valley—Mathematical models. I. Phillips, Steven P. II. Gronberg, Jo Ann M. III. Title. IV. Series. TC176.B45 1993

551.49'097948—dc20

93-20359
CIP

FOREWORD

This report was prepared by the U.S. Geological Survey in cooperation with the San Joaquin Valley Drainage Program and as part of the Regional Aquifer-System Analysis (RASA) Program of the U.S. Geological Survey.

The San Joaquin Valley Drainage Program was established in mid-1984 and is a cooperative effort of the U.S. Bureau of Reclamation, U.S. Fish and Wildlife Service, U.S. Geological Survey, California Department of Fish and Game, and California Department of Water Resources. The purposes of the program are to investigate the problems associated with the drainage of agricultural lands in the San Joaquin Valley and to develop solutions to those problems. Consistent with these purposes, program objectives address the following key concerns: (1) public health, (2) surface- and ground-water resources, (3) agricultural productivity, and (4) fish and wildlife resources.

The RASA Program of the U.S. Geological Survey was started in 1978 following a congressional mandate to develop quantitative appraisals of the major ground-water systems of the United States. The RASA Program represents a systematic effort to study a number of the Nation's most important aquifer systems, which in aggregate underlie much of the country and which represent an important component of the Nation's total water supply. In general, the boundaries of these studies are identified by the hydrologic extent of each system, and accordingly transcend the political subdivisions to which investigations were often arbitrarily limited in the past. The broad objectives for each study are to assemble geologic, hydrologic, and geochemical information, to analyze and develop an understanding of the system, and to develop predictive capabilities that will contribute to the effective management of the system. The Central Valley RASA study, which focused on the hydrology and geochemistry of ground water in the Central Valley of California, began in 1979. Phase II of the Central Valley RASA began in 1984 and was completed in 1990. The focus during this second phase was on more detailed study of the hydrology and geochemistry of ground water in the San Joaquin Valley, which is the southern half of the Central Valley.

CONTENTS

Foreword	III
Abstract	1
Introduction	2
Previous Work	2
Physical Hydrogeology	4
Modeling Approach.....	5
Governing Equation.....	6
Discretization.....	6
Transmissivity and Leakance	7
Sources and Sinks.....	9
Storage Coefficient.....	10
Boundary Conditions.....	10
Simulation Period, Model Time-step Size, and Initial Conditions.....	10
Parameter Estimation and Available Data Base	11
Land-Surface Altitude and System Geometry	11
Water Levels.....	12
Distribution of Texture, Semiconfined Zone	12
Hydraulic Conductivity of Lithologic End Members.....	13
Transmissivity of the Confined Zone.....	16
Specific Storage.....	17
Specific Yield.....	17
Recharge and Pumping.....	18
Drains.....	20
Bare-Soil Evaporation	23
Head-Dependent Boundary Condition	23
Model Calibration	24
Steady-State Calibration.....	24
Transient Calibration	26
Comparison of Simulated and Measured Conditions.....	27
Water Budget.....	34
Discussion of Model Assumptions	35
Summary	40
References Cited	41
Appendix A: Specific Yield	47
Appendix B: Bare-Soil Evaporation.....	48
Appendix C: Selected Model Input Data	49
Appendix D: Data Generated from Measured Water Levels and Used for Comparison with Simulation Results	61

FIGURES

1. Map showing topography and location of model boundary in study area	3
2. Generalized hydrogeologic section of study area.....	4
3. Map showing model grid and lateral boundary conditions.....	7
4. Generalized hydrologic section and vertical layers representing numerical model of ground-water flow system	8
5-10. Maps showing:	
5. Location of wells used to map water table.....	13
6. Location of lithologic and geophysical logs used to map distribution of texture	14
7. Location of well cluster sites used for model calibration, slug tests, and selected hydrographs.....	16
8. Water-budget subarea boundaries	19
9. Subareas used for evaluating vertical distribution of ground-water pumpage	20
10. Location of drainage-system subareas, wells in and around area underlain by regional-collector system, and field sites by Lord (1988).....	22

11. Graph showing bare-soil evaporation as a function of water-table depth	23
12-16. Maps showing:	
12. Root mean square error and bias as a function of two dimensionless parameters, K' and K''	26
13. Change in water-table altitude, 1972-84	28
14. Measured and simulated depth to water, October 1984	31
15. Measured areas subject to bare-soil evaporation, 1984	32
16. Measured and simulated areas subject to bare-soil evaporation, 1984	33
17. Graph of measured and simulated number of model cells subject to bare-soil evaporation, 1972-88	34
18. Maps showing change of head in confined zone, 1972-84	35
19. Hydrographs of measured and simulated altitude of water table and head in confined zone for selected model cells in areas where water table is within 20 feet of land surface, 1972-88	37
20. Hydrographs of measured and simulated altitude of water table and head in confined zone for selected model cells in areas where water table is more than 50 feet below land surface, 1972-88	38
21. Diagram showing water budget for study area, 1981-84	39
22. Axes of minimum root mean square error for different values of ratio of hydraulic conductivities of coarse-grained material derived from Sierra Nevada (K_{C-S}) to that from Coast Ranges (K_{C-CR})	39
23. Map showing flux across the Corcoran Clay Member in 1984 mapped as a function of hydraulic conductivity of coarse-grained material (K_C) and that of the Corcoran Clay Member of the Tulare Formation of Pleistocene age (K_{CORC})	39
24. Hydrographs of simulated semiconfined and confined zone heads for selected locations where thickness of semi-confined zone is large	40

TABLES

1. U.S. Geological Survey 7.5-Minute Topographic Maps Used in Remapping Land-Surface Altitude	11
2. Statistical Summary of Distribution of Texture of Coast Ranges Alluvium and Sierran Sand	15
3. Hydraulic Conductivity Evaluated from Slug Tests Using Method of Cooper and Others (1967)	15
4. Water-Budget Data for 1980	18
5. Summary of Percentage of Ground-Water Pumpage by Subarea	21
6. Drainage-System Characteristics and Regression Parameters	23
7. Location of U.S. Geological Survey Well Cluster Sites Used in Calculating Estimated Values of Head in Model Cells	25
8. Mean and Standard Deviation of Water-Level Changes, 1972 to 1984	30

CONVERSION FACTORS AND VERTICAL DATUM

Multiply	By	To obtain
acre	4,047.0	square meter
acre-foot (acre-ft)	1,233	cubic meter
acre-foot per year (acre-ft/yr)	1,233	cubic meter
foot (ft)	0.3048	meter
foot per mile (ft/mi)	0.1894	meter per kilometer
foot per second (ft/s)	0.3048	meter per second
foot per year (ft/yr)	0.3048	meter per year
foot squared per second (ft ² /s)	0.0929	meter squared per second
gallon per day per foot (gal/d)/ft	0.0124	cubic meter per day per meter
inch (in.)	25.4	millimeter
mile (mi)	1.609	kilometer
square mile (mi ²)	2.590	square kilometer

Temperature is given in degrees Fahrenheit (°F), which can be converted to degrees Celsius (°C) by the following equation:

$$\text{Temp } ^\circ\text{C} = 5/9 (^\circ\text{F}) - 32.$$

Sea level: In this report "sea level" refers to the National Geodetic Vertical Datum of 1929—a geodetic datum derived from a general adjustment of the first-order level nets of the United States and Canada, formerly called Sea Level Datum of 1929.

VI Contents

Numerical Simulation of Ground-Water Flow in the Central Part of the Western San Joaquin Valley, California

By Kenneth Belitz, Steven P. Phillips, and J.M. Gronberg

Abstract

The occurrence of selenium in agricultural drain water in the central part of the western San Joaquin Valley, California, has focused concern on strategies for managing shallow, saline ground water. To assess alternatives to agricultural drains, a three-dimensional, finite-difference numerical model of the regional ground-water flow system was developed. This report documents the mathematical approach used to model the flow system, the data base on which the model is based, and the methods used to calibrate the model.

The 550-square-mile study area includes parts of the Panoche Creek alluvial fan and parts of the Little Panoche Creek and Cantua Creek alluvial fans. The model simulates transient flow in the semiconfined and confined zones above and below the Corcoran Clay Member of the Tulare Formation of Pleistocene age. The model incorporates areally distributed ground-water recharge, areally and vertically distribut-

ed pumping, regional-collector drains in the Westlands Water District (operative from 1980 to 1985), on-farm drains in parts of the Panoche, Broadview, and Firebaugh Water Districts, and bare-soil evaporation (which occurs if the water table is within 7 feet of land surface). The model also incorporates texture-based estimates of hydraulic conductivity, where texture is defined as the fraction of coarse-grained deposits present in a given subsurface interval.

The numerical model was developed using hydrologic data from 1972 to 1988. Most of the parameters incorporated into the model were evaluated independently of the model, including system geometry, the distribution of texture, the altitudes of the water table and potentiometric surface of the confined zone in 1972 (initial condition), the hydraulic conductivity of coarse-grained deposits derived from the Coast Ranges, the hydraulic conductivity of coarse-grained deposits derived from the Sierra Nevada, specific storage, recharge, pumping, and param-

eters needed to incorporate drains and bare-soil evaporation. Four parameters were calibration variables: the hydraulic conductivity of fine-grained deposits in the semiconfined zone, the hydraulic conductivity of the Corcoran Clay Member, specific yield, and the transmissivity of the confined zone.

The model was calibrated in two phases. In the first phase, a steady-state model of the ground-water flow system in 1984 was used to constrain the relation between the hydraulic conductivity of fine-grained deposits in the semiconfined zone and the hydraulic conductivity of the Corcoran Clay Member, thus reducing the number of independent variables from four to three. In the second phase of calibration, the change in altitude of the water table from 1972 to 1984, the change in altitude of the potentiometric surface of the confined zone from 1972 to 1984, and the number of model cells subject to bare-soil evaporation from 1972 to 1988 were used to evaluate the remaining three variables.

The calibrated model reproduces the average change in water-table altitude (1972–84) to within 0.4 foot (average measured change 11.5 feet) and the average change in confined zone head (1972–84) to within 19 feet (average measured change 120 feet). The simulated time-series record of the total number of model cells subject to bare-soil evaporation (each cell is 1 mile square) is within the range of the measured data. The measured values are at a minimum in October and a maximum in July. The October values ranged from 103 in 1972 to 132 in 1984 (the drains were closed in 1985) to 151 in 1988. The July values ranged from 144 in 1973 to 198 in 1984, to 204 in 1988. The simulated values ranged from 103 in 1972 to 161 in 1984, to 208 in 1988.

INTRODUCTION

Agricultural productivity in California's western San Joaquin Valley is subject to the potentially adverse effects caused by the occurrence of saline ground water at shallow depths. Of the more than 2.2 million acres under irrigation in the western San Joaquin Valley, nearly 850,000 acres is underlain by a water table that is within 5 ft of land surface (San Joaquin Valley Drainage Program, 1989). Historically, subsurface tile drains have been used to control the altitude of the water table and to manage subsurface water quality. In the early 1980's, subsurface regional-collector drains were installed in a 42,000-acre area in the central part of the western San Joaquin Valley. Selenium-bearing water, pumped from these drains and exported to the Kesterson Wildlife Refuge, led to deaths and deformities of waterfowl and aquatic biota (Deverel and others, 1984; Presser and Barnes, 1985; Ohlendorf and others, 1986). The occurrence of selenium toxicity at Kesterson resulted in the closure of the regional-collector drains, which began in March 1985 and was completed in April 1988 (Phillips and Belitz, 1991). In the absence of drains, there is considerable concern as to how to maintain agricultural productivity in the presence of shallow, saline ground water (San Joaquin Valley Drainage Program, 1989). In particular, there is a need to evaluate alternative strategies for controlling the altitude of the water table.

This report documents the development of a three-dimensional, finite-difference numerical model

of the ground-water flow system in the central part of the western San Joaquin Valley (fig. 1). The study area is about 550 mi² and includes the Panoche Creek alluvial fan and parts of the Little Panoche Creek and Cantua Creek alluvial fans. The study area also includes the 42,000-acre area (about 67 mi²) underlain by the closed regional-collector drains. The model described in this report can be used to evaluate the response of the water table to changes in management practices that affect recharge to or discharge from the ground-water flow system. Because the flow system is complex, development of the model requires synthesis of a large data base and evaluation of several model parameters. The accuracy of the model is constrained by the assumptions and simplifications incorporated in the analysis and by the accuracy of the input data. Thus, this report emphasizes the mathematical approach used to model the flow system, the data base on which the model is based, and the methods used to calibrate the model. In addition, this report documents the ability of the model to reproduce measured hydrologic conditions. An evaluation of management alternatives is given in Belitz and Phillips (1992).

The model was developed as part of the comprehensive investigation by the U.S. Geological Survey of the hydrology and geochemistry of the San Joaquin Valley. The studies are being done as part of the Regional Aquifer-System Analysis Program of the U.S. Geological Survey and in cooperation with the San Joaquin Valley Drainage Program.

PREVIOUS WORK

Several previous studies provided a foundation for the development of a model of the ground-water flow system in the central part of the San Joaquin Valley. Belitz and Heimes (1990) described the hydrogeology of the ground-water flow system in the central part of the western San Joaquin Valley, including the area of this report. They synthesized previous work and presented new data to describe the geology of the flow system, the evolution of the flow system since the development of irrigated agriculture, and the state of the flow system in 1985. Gronberg and others (1990) used a geographic information system to evaluate the hydrogeologic distribution of 5,860 water wells in the same study area as Belitz and Heimes (1990). Laudon and Belitz (1991) mapped the distribution of texture (defined as the

fraction of coarse-grained deposits in a given subsurface interval) in the uppermost 50 ft of deposits in an

area somewhat larger than the area of this report. Phillips and Belitz (1991) developed a preliminary,

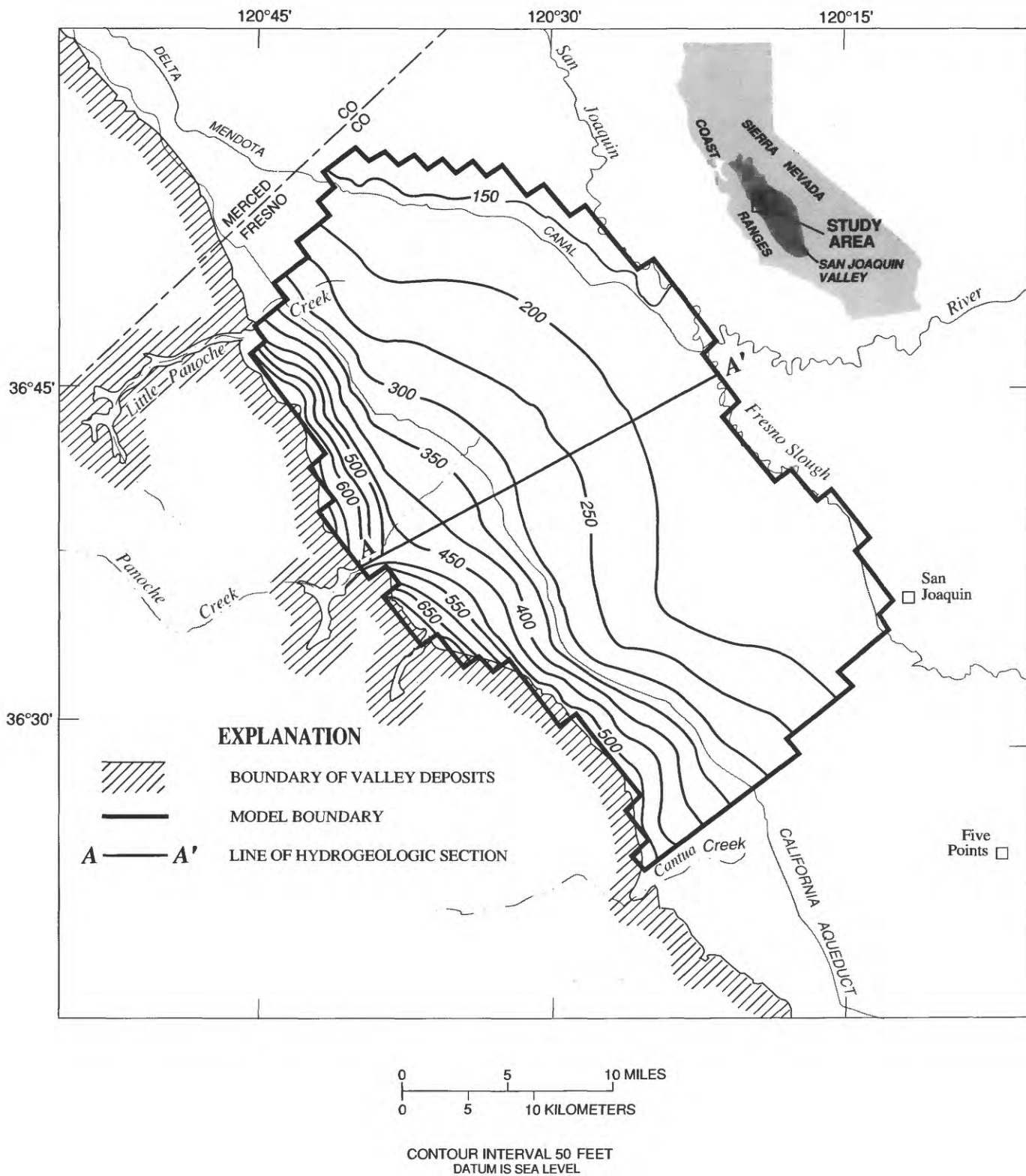


Figure 1. Topography and location of model boundary in study area.

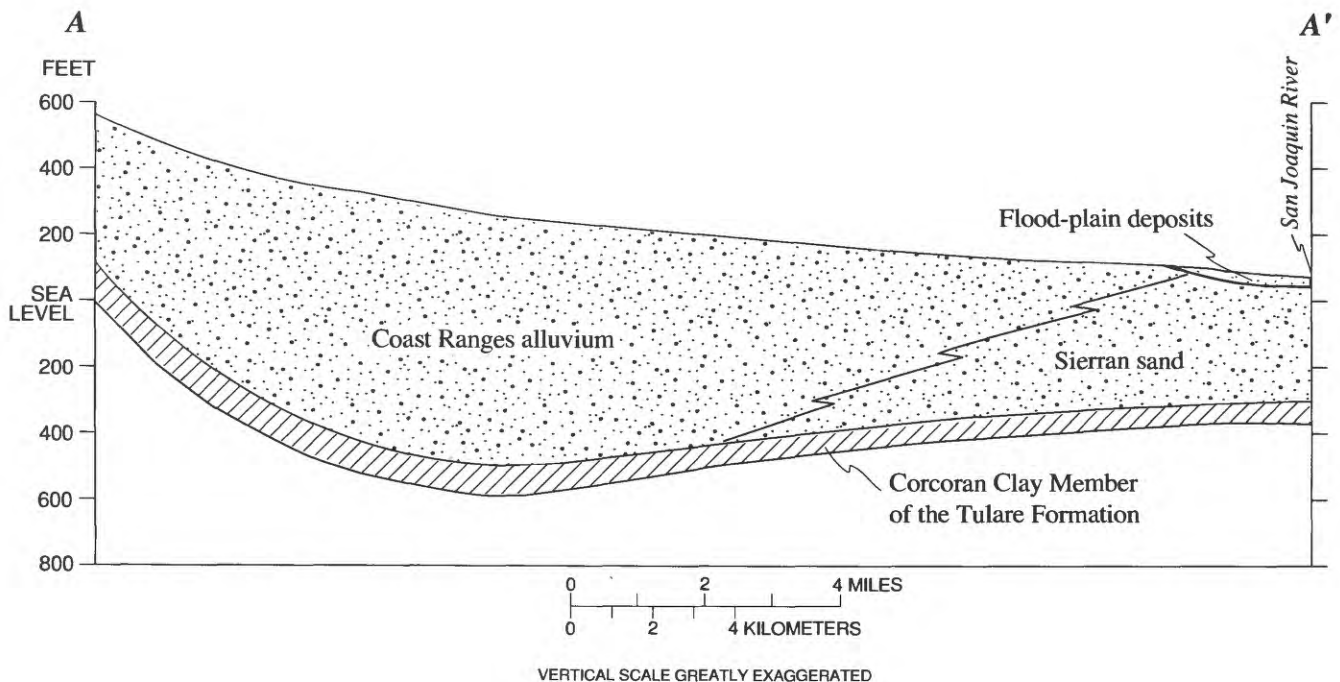
steady-state model of the semiconfined ground-water flow system in the area of this report. The purpose of that work was to develop a method for optimizing texture-based estimates of hydraulic conductivity. Gronberg and Belitz (1992) developed a water budget for 11 subareas in the study area of this report. Belitz and Heimes (1990) presented a more complete discussion of previous hydrogeologic studies that focus on or include the present study area. Gilliom and others (1989) presented the results of several studies concerning the sources, distribution, and mobility of selenium in the San Joaquin Valley.

Williamson and others (1989) developed a numerical model of the regional ground-water flow system of the Central Valley of California, an area of about 20,000 mi². That model was calibrated with hydrologic data from 1961 to 1971 and provides a quantitative description of the flow system for the entire Central Valley, including the study area, but at a relatively coarse scale. It divided the 550-mi² area into 16 cells of 36 mi² each and represented the semiconfined zone as a single layer.

PHYSICAL HYDROGEOLOGY

The physical hydrogeology of the study area has been previously described (Belitz and Heimes, 1990). The following discussion is based on that report. The study area is underlain by the Corcoran Clay Member of the Tulare Formation of Pleistocene age, which divides the ground-water flow system into an upper semiconfined zone (Davis and De Wiest, 1966) and a lower confined zone (Davis and Poland, 1957) (fig. 2). The Corcoran Clay Member is an areally extensive lacustrine deposit of low permeability (Johnson and others, 1968). The base of the Corcoran Clay Member ranges in depth from 400 ft in the valley trough to more than 800 ft along the Coast Ranges (Bull and Miller, 1975); its thickness ranges from 20 to 120 ft (Page, 1986).

The semiconfined zone above the Corcoran Clay Member consists of three hydrogeologic units: Coast Ranges alluvium, Sierran sand, and flood-plain deposits. The Coast Ranges alluvium comprises oxidized alluvial-fan deposits derived from the Coast



EXPLANATION

- | | | | | | |
|---|-------------------|---|-----------------|---|---------------|
|  | SEMICONFINED ZONE |  | CONFINING LAYER |  | CONFINED ZONE |
|---|-------------------|---|-----------------|---|---------------|

Figure 2. Generalized hydrogeologic section of study area (modified from Belitz and Heimes, 1990).

Ranges to the west. The deposits are primarily sand and gravel at the fanheads and along stream channels and are primarily silt and clay in the interfan and distal-fan areas (Laudon and Belitz, 1991). The thickness of the Coast Ranges alluvium is more than 800 ft along the Coast Ranges and thins to zero near the valley axis (Miller and others, 1971), where it interfingers with Sierran sand. The Sierran sand consists of well-sorted, medium- to coarse-grained fluvial sand derived from the Sierra Nevada to the east; these deposits typically are chemically reduced. The Sierran sand is 400 to 500 ft thick in the valley trough and thins eastward and westward (Miller and others, 1971). The flood-plain deposits overlie the Sierran sand and consist primarily of clay and silt of variable oxidation state. The flood-plain deposits are derived from the Coast Ranges to the west and the Sierra Nevada to the east and range in thickness from 5 to 35 ft (Laudon and Belitz, 1991).

The confined zone beneath the Corcoran Clay Member consists primarily of poorly consolidated flood-plain, deltaic, alluvial-fan, and lacustrine deposits of the Tulare Formation (Bull and Miller, 1975). The thickness of the confined zone, defined as the interval from which ground water historically has been pumped, ranges from 570 to 2,460 ft (Williamson and others, 1989).

The climate in the central part of the western San Joaquin Valley is semiarid; annual precipitation ranges from 6 to 8 in. (Rantz, 1969). Rain occurs primarily from October to April. Temperature varies seasonally from an average daily minimum of 35° F to an average daily maximum of 102° F. Under natural conditions, recharge to the ground-water flow system was primarily from infiltration of stream water from intermittent streams (Little Panoche, Panoche, and Cantua Creeks; fig. 1) and perhaps from smaller ephemeral streams located between the larger intermittent streams. None of the streams in the study area reach the valley trough; streamflow is lost to infiltration and evapotranspiration. Discharge from the ground-water flow system was primarily by evapotranspiration and streamflow along the valley trough. Ground-water gradients in the area were typically from southwest to northeast, reflecting the general topographic trend of the area; the magnitude of the gradients ranged from 1 to 3 ft/mi, reflecting the arid climate and low rates of recharge to the system.

The present-day hydrology of the area is dominated by agricultural activities. Percolation of irrigation water past crop roots and ground-water pumping

are the dominant hydraulic stresses on the flow system. Presently, most of the irrigation water applied in the area is imported from the Sierra Nevada through the Delta-Mendota Canal (operative since the early 1950's) and from the California Aqueduct (operative since 1967). Ground water and the San Joaquin River also are sources of irrigation water. Most of the ground water is pumped from the lower confined zone; lesser quantities are pumped from the Sierran sand in areas where it is more than 200 ft thick and where the water quality is adequate for agricultural use (Gronberg and others, 1990; Gronberg and Belitz, 1992).

Until the completion of the California Aqueduct in 1967, ground water was the only source of irrigation water for most of the central part of the western valley. Several decades of ground-water pumping has lowered hydraulic heads in the confined zone several hundred feet (Ireland and others, 1984) and caused land subsidence of more than 1 ft across the entire area and as much as 29 ft locally (Poland and others, 1975). In 1967, surface-water delivery from the California Aqueduct became available; by 1974, surface water had replaced ground water as the principal source of irrigation water. From 1974 to 1988, ground-water pumping was relatively constant, except for an increase in 1977 (the second year of a 2-year drought in California). Although ground-water pumping had been relatively constant since 1974, irrigation has increased.

The reduction in ground-water pumping and increase in total irrigation since 1967 has had two important results: (1) an increase in the altitude of the potentiometric surface in the confined zone and (2) an increase in the altitude of the water table. From 1967 to 1984, the potentiometric surface rose 100 to 200 ft across the entire study area, representing a recovery of nearly half the total drawdown that occurred from predevelopment conditions to 1967 (Belitz and Heimes, 1990). From 1967 to 1984, the water table rose more than 10 ft across nearly half the study area and as much as 100 ft locally, which increased the area underlain by a shallow water table (for example, water table within 10 ft of land surface) and consequently the need for drainage.

MODELING APPROACH

The U.S. Geological Survey's three-dimensional, finite-difference ground-water flow model (McDonald

and Harbaugh, 1988) was used to simulate the regional flow system in the central part of the western San Joaquin Valley. The ground-water flow model was calibrated in two phases, the first phase under steady-state conditions and the second phase under transient conditions.

Steady-state modeling was an extension and refinement of work presented by Phillips and Belitz (1991). In the steady-state model, the semiconfined zone was divided vertically into five layers, and the altitude of the water table (1984) and the confined zone heads (1984) were treated as specified-head boundaries. The purpose of the steady-state model was to constrain the hydraulic properties of the lithologic end members. The steady-state model was not used to develop an initial condition for input to the transient model.

The transient model was calibrated using hydrologic data from 1972 to 1988. It incorporated the semiconfined and confined zones and also included areally distributed sources and sinks of water not explicitly represented in the steady-state model, including recharge to the water table, subsurface drains, bare-soil evaporation, and ground-water pumping. The transient model uses a modified version of the U.S. Geological Survey code, which allows for the activation and deactivation of model cells as the water table rises above or declines below the bottom of the cells (McDonald and others, 1992). In the following subsections, the approach for mathematically modeling transient flow in the central part of the western San Joaquin Valley is presented and, where appropriate, the requirements of the steady-state and transient models are distinguished.

Governing Equation

Three-dimensional, transient ground-water flow in an anisotropic porous medium can be evaluated by solving the following equation with appropriate initial and boundary conditions:

$$\frac{\partial}{\partial x} \left(K_H \frac{\partial h}{\partial x} \right) + \frac{\partial}{\partial y} \left(K_H \frac{\partial h}{\partial y} \right) + \frac{\partial}{\partial z} \left(K_V \frac{\partial h}{\partial z} \right) + W = S_s \frac{\partial h}{\partial t}, \quad (1)$$

where

- h = hydraulic head (L),
- K_H = horizontal hydraulic conductivity (L/t),
- K_V = vertical hydraulic conductivity (L/t),
- W = external sources/sinks of water (t^{-1}),

- S_s = specific storage (L^{-1}),
- x, y, z = cartesian coordinates (L), and
- t = time (t).

If an anisotropic flow system is discretized vertically into multiple layers, the flow equation can be expressed in a quasi-three-dimensional framework:

$$\frac{\partial}{\partial x} \left(T_k \frac{\partial h_k}{\partial x} \right) + \frac{\partial}{\partial y} \left(T_k \frac{\partial h_k}{\partial y} \right) + \lambda_{k+1} (h_{k+1} - h_k) + \lambda_{k-1} (h_{k-1} - h_k) + W_k = S_k \frac{\partial h_k}{\partial t}, \quad (2)$$

where

- T_k = transmissivity of layer k (L^2/t),
- h_k = vertically integrated hydraulic head of layer k (L),
- λ_{k+1} = leakance between layers k and $k+1$ (t^{-1}),
- h_{k+1} = vertically integrated hydraulic head of layer $k+1$ (L),
- λ_{k-1} = leakance between layers k and $k-1$ (t^{-1}),
- h_{k-1} = vertically integrated hydraulic head of layer $k-1$ (L),
- W_k = sources or sinks of water in layer k (L/t),
- S_k = storage coefficient of layer k (dimensionless),
- x, y = cartesian coordinates (L), and
- t = time (t).

Discretization

Areally, the model grid is 36 rows by 20 columns with each model cell 1 mi on a side (fig. 3). Vertically, the semiconfined flow system was divided into five layers (fig. 4). The upper two layers are of constant thickness (20 and 30 ft, respectively), reflected by the distribution of monitoring wells (Gronberg and others, 1990) and the need for accurate simulation of the altitude of the water table in shallow areas. A large number of wells were drilled to a depth of 20 ft to monitor the water table where it is shallow. Also, a large number of wells were drilled to a depth of 50 ft along the California Aqueduct. The remaining thickness of deposits at a depth below 50 ft but above the Corcoran Clay Member was divided into three layers of varying thickness; layers 3 to 5 are three-sixteenths, five-sixteenths, and one-half of the remaining thickness, respectively (Phillips and Belitz, 1991). The vertical division of the semiconfined zone allowed for modeling of

vertical anisotropy and vertical head gradients. The confined zone beneath the Corcoran Clay Member was represented by a single layer, and the Corcoran Clay Member was incorporated into the leakage term between the lowermost layer of the semiconfined zone (layer 5) and the confined zone (layer 6).

Transmissivity and Leakage

Within the semiconfined zone (layers 1 to 5), transmissivity varies spatially as a function of the thickness of the layer (or wetted thickness if the water-table altitude is below the altitude of the top of

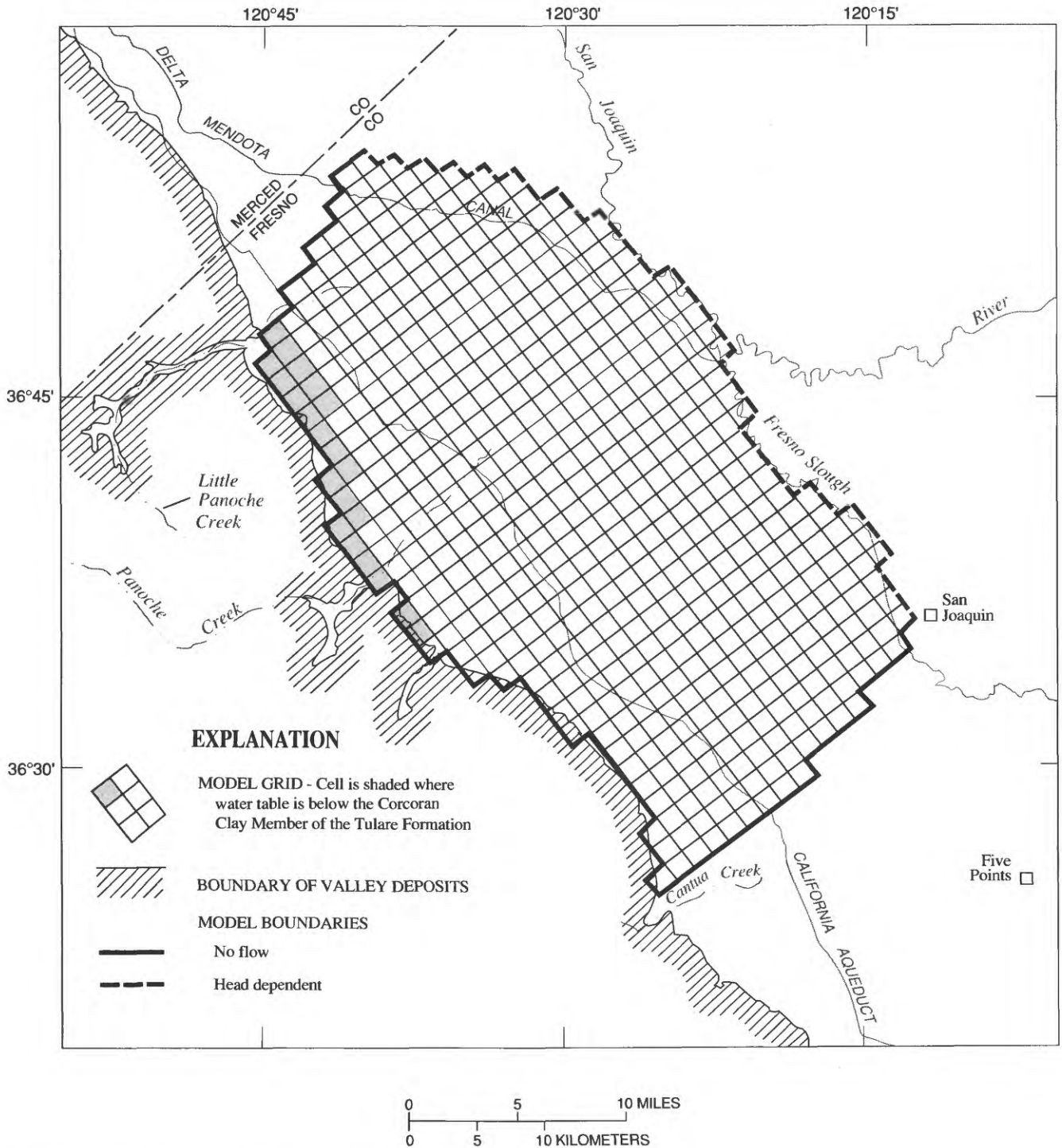


Figure 3. Model grid and lateral boundary conditions.

the layer) and the equivalent horizontal hydraulic conductivity of the deposits within the layer:

$$T_k = K_{H,k} b_k, \quad (3)$$

where

$K_{H,k}$ = equivalent horizontal hydraulic conductivity of layer k (L/t), and

b_k = thickness of layer k (L).

Phillips and Belitz (1991) concluded that the equivalent horizontal hydraulic conductivity was best calculated as a weighted arithmetic average of the hydraulic conductivities of coarse- and fine-grained lithologic end members:

$$K_{H,k} = (K_c \cdot F_{c,k}) + (K_f \cdot F_{f,k}), \quad (4)$$

where

K_c = hydraulic conductivity of coarse-grained end member,

$F_{c,k}$ = fraction of coarse-grained end member, spatially variable,

K_f = hydraulic conductivity of fine-grained end member,

$F_{f,k}$ = fraction of fine-grained end member, spatially variable, and

$$F_{c,k} + F_{f,k} = 1.$$

The leakance between layers also varies spatially, but as a function of the equivalent vertical hydraulic conductivity and thickness of deposits present between the midplanes of adjacent layers. The leakance between layers k and $k+1$ is

$$\lambda_{k+1} = K_{v,k+\frac{1}{2}} / b_{k+\frac{1}{2}}, \quad (5)$$

where

$K_{v,k+\frac{1}{2}}$ = equivalent vertical hydraulic conductivity between layers k and $k+1$ (L/t) and

$$b_{k+\frac{1}{2}} = (b_k + b_{k+1}) / 2.$$

Phillips and Belitz (1991) concluded that the equivalent vertical hydraulic conductivity could be calculated using either a weighted harmonic mean or

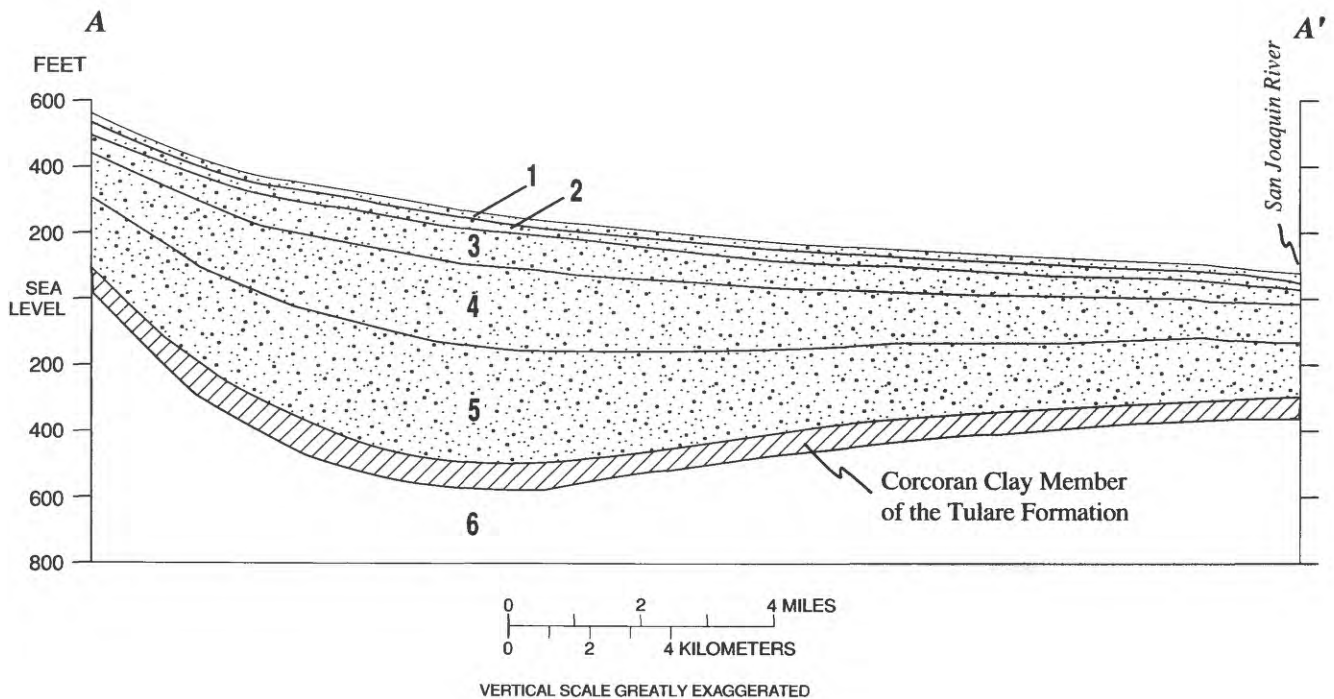


Figure 4. Generalized hydrologic section and vertical layers representing numerical model of ground-water flow system.

weighted geometric mean of the hydraulic conductivities of coarse- and fine-grained lithologic end members. This study used a weighted harmonic mean:

$$K_{v, k + \frac{1}{2}} = \frac{1}{\left(F_{c, k + \frac{1}{2}} / K_c\right) + \left(F_{f, k + \frac{1}{2}} / K_c\right)}, \quad (6)$$

where

$F_{c, k + \frac{1}{2}}$ = fraction of coarse-grained end member present between the midplanes of layers k and $k+1$ and

$F_{f, k + \frac{1}{2}}$ = fraction of fine-grained end member present between the midplanes of layers k and $k+1$.

Similar expressions can be written for the leakance and equivalent vertical hydraulic conductivity between layers k and $k-1$.

In this study, coarse-grained sediment is defined as sediment consisting principally of sand, clayey and silty sand, gravel, and clayey, silty, and sandy gravel. Fine-grained sediment is defined as sediment consisting principally of clay, silt, and sandy clay and silt. These definitions are identical to those of Laudon and Belitz (1991). Within the semiconfined zone, two coarse-grained lithologic end members and one fine-grained lithologic end member were identified: coarse-grained sediment derived from the Coast Ranges, coarse-grained sediment derived from the Sierra Nevada, and fine-grained sediment independent of the source area. These distinctions reflect the hydrogeology of the ground-water flow system and the location of wells that can be used to test hydraulic conductivity.

The leakance between the lowermost layer of the semiconfined zone and the confined zone (layers 5 and 6, respectively) was assumed to be a function of the thickness and hydraulic conductivity of the Corcoran Clay Member (K_{corc}). The transmissivity of the confined zone beneath the Corcoran Clay Member (T_{confined}) was not modeled as a distributed parameter and hence was not evaluated on the basis of lithologic end members. This generalization of the confined zone reflects the primary focus on the semiconfined zone, in particular, the focus on the response of the water table to potential changes in hydrologic conditions.

Sources and Sinks

Sources and sinks in the ground-water flow model of McDonald and Harbaugh (1988) can

include specified fluxes, such as pumping, as well as head-dependent fluxes. Two types of head-dependent sinks, subsurface drains and bare-soil evaporation from a shallow water table, as well as ground-water pumping, were incorporated into the transient model.

The McDonald and Harbaugh (1988) model uses linear head-dependent functions to simulate the influence of drains on the ground-water flow system. If the hydraulic head in a model cell is higher than the altitude of the drain in that cell, then the volumetric flux to the drain can be calculated:

$$QD_{i,j,k} = C_{i,j,k} (h_{i,j,k} - E_{i,j,k}) \quad \text{if } h_{i,j,k} > E_{i,j,k}, \quad (7a)$$

where

$QD_{i,j,k}$ = volumetric flux to a drain in cell i,j,k ;
 $C_{i,j,k}$ = conductance of the cell/drain system in cell i,j,k ;
 $h_{i,j,k}$ = head in cell i,j,k ; and
 $E_{i,j,k}$ = altitude of drain in cell i,j,k .

If the hydraulic head in a model cell is at or lower than the altitude of the drain in that cell, then

$$QD_{i,j,k} = 0 \quad \text{if } h_{i,j,k} \leq E_{i,j,k}. \quad (7b)$$

Equation 7a can be interpreted as a modified form of Darcy's Law in which the conductance term accounts for hydraulic conductivity, cross-sectional area, and the distance across which the head difference occurs.

The McDonald and Harbaugh (1988) model incorporates a linear head-dependent function to simulate bare-soil evaporation or evapotranspiration or both. In any given model cell, the bare-soil evaporation rate (QE) is at a constant and maximum rate (QE_{max}) if the water table (or hydraulic head, h) is above the altitude of some reference surface (Z_{ref}):

$$QE = QE_{\text{max}} \quad \text{if } h > Z_{\text{ref}}. \quad (8a)$$

If, however, the water table is at a depth below the reference surface, the bare-soil evaporation rate is zero:

$$QE = 0 \quad \text{if } h < Z_{\text{ref}} - D_{\text{ext}}, \quad (8b)$$

where

D_{ext} = the extinction depth.

If the water-table altitude is between the reference surface and the extinction depth, the bare-soil evaporation rate decreases linearly from the maximum rate to zero:

$$QE = QE_{\text{max}} [h - (Z_{\text{ref}} - D_{\text{ext}})] / D_{\text{ext}} \quad \text{if } Z_{\text{ref}} - D_{\text{ext}} \leq h < Z_{\text{ref}}. \quad (8c)$$

Storage Coefficient

The McDonald and Harbaugh (1988) model allows for a storage coefficient that depends on the relative altitude of the hydraulic head of a layer and the top of that layer. If the head is higher than the top of the layer, then the change in storage caused by hydraulic head changes is a function of the elastic properties of the aquifer:

$$S_k = S_s b_k, \quad (9a)$$

where

S_k = storage coefficient of layer k (dimensionless),

S_s = specific storage (L^{-1}), and

b_k = thickness of layer k (L).

If the hydraulic head is lower than the top of the layer, then changes in head correspond to changes in water-table altitude, and thus changes in storage are a function of the drainable porosity:

$$S_k = S_y, \quad (9b)$$

where

S_y = specific yield (dimensionless).

Boundary Conditions

In both phases of calibration (steady-state and transient), the lateral boundary conditions were treated identically (fig. 3). The contact between the Coast Ranges and the unconsolidated alluvium was modeled as a no-flow boundary. The northern and southern boundaries of the study area approximate flow lines and also were treated as no-flow boundaries. Along the northeastern and eastern boundaries, the study area is not hydraulically isolated from adjacent areas. To account for the interaction of the flow system with adjacent areas, the northeastern and eastern boundaries were treated as head-dependent boundaries (McDonald and Harbaugh, 1988):

$$QB_{i,j,k} = C_{i,j,k} (HB_{i,j,k} - h_{i,j,k}), \quad (10)$$

where

$QB_{i,j,k}$ = flux across the boundary of cell (i,j,k) (L^3/t),

$C_{i,j,k}$ = conductance of the deposits at the boundary of cell (i,j,k) (L^2/t),

$HB_{i,j,k}$ = externally specified head (L), and

$h_{i,j,k}$ = head in the model cell (i,j,k) (L).

The head-dependent boundary condition allows for flow into or out of the study area and can be seen as a modified form of Darcy's Law:

$$C_{i,j,k} = (A_{i,j,k} K_{i,j,k}) / L_{i,j,k}, \quad (11)$$

where

$A_{i,j,k}$ = area of cell face adjacent to the boundary (L^2),

$K_{i,j,k}$ = hydraulic conductivity of material between cell (i,j,k) and the externally specified head (HB) (L/t), and

$L_{i,j,k}$ = distance between model cell and specified head (L).

The boundary conditions at the top and bottom of the model were treated differently in the first and second phases of calibration. In the first phase of calibration, the semiconfined zone was modeled under steady-state conditions with the altitude of the water table (1984) and confined zone heads (1984) treated as specified-head boundaries. Distributed sources and sinks at the top of the ground-water flow system (recharge, subsurface drains, bare-soil evaporation) were not explicitly incorporated; but ground-water pumping was implicitly incorporated into the specified-head boundary at the bottom of the ground-water flow system. Thus, the specified-head boundary below the Corcoran Clay Member accounted for flux across the Corcoran Clay Member and for ground-water pumping from the semiconfined zone. The limitations of the steady-state model were removed in the second phase of calibration: the semiconfined and confined zones were modeled under transient conditions, the water table was treated as a free surface, and distributed sources and sinks were explicitly incorporated. In the transient model, the confined zone was assumed to be 1,000 ft thick, and the bottom of the confined zone was treated as a no-flow boundary.

Simulation Period, Model Time-Step Size, and Initial Conditions

The transient model began in October 1972 and ran until October 1988. For numerical stability and convergence, the first year was divided into 450 time steps: 0.2 year divided into 200 time steps, 0.3 year divided into 150 time steps, and 0.5 year divided into 100 time steps. Subsequent years were divided into 100 time steps each. The initial head distribution in the semiconfined zone was specified as hydrostatic

beneath the water table; the altitude of the water table in 1972 was mapped from water-level data compiled by Gronberg and others (1990). The initial head distribution in the confined zone (1972) was obtained from a previously published map (Ireland and others, 1984).

PARAMETER ESTIMATION AND AVAILABLE DATA BASE

A large quantity of data is available for the central part of the western San Joaquin Valley that can be used to evaluate model parameters. Many of the parameters were evaluated independent of the model, including geometry, texture, altitudes of the water table and the potentiometric surface in 1972 (initial condition) and in 1984 (specified-head boundaries for the steady-state phase of modeling), hydraulic conductivity of coarse-grained lithologic end members, specific storage, recharge, pumping, and parameters needed to incorporate subsurface drains and bare-soil evaporation in the model. The values of four model parameters, however, were calibration variables: hydraulic conductivity of the fine-grained lithologic end member in the semiconfined zone, hydraulic conductivity of the Corcoran Clay Member, specific yield, and transmissivity of the confined zone. In the following subsections, data used for independently evaluating model parameters are discussed and the values used in the model are presented. Those parameters that were calibration variables also are discussed and preliminary estimates of those values are presented. In a subsequent section, the calibration methodology is discussed and the calibrated values and preliminary estimates are compared. Selected model input data are given at the end of the report.

Land-Surface Altitude and System Geometry

The ground-water flow model requires specification of the altitudes of the top and bottom of each of the five layers that constitute the semiconfined zone (including land-surface altitude). Because of aquifer compaction, land-surface altitude in the study area was remapped. This was done by digitizing 1,776 land-surface altitude data points (from section corners and along canals) from 19 U.S. Geological Survey 7.5-minute topographic maps (table 1) and by

Table 1. U.S. Geological Survey 7.5-minute topographic maps used in remapping land-surface altitude

Map name	Year
Laguna Seca	1956
Chounet Ranch	1956
Hammonds Ranch	1956
Dos Palos	1956
Monocline Ridge	1955
Chaney Ranch	1955
Broadview Farms	1955
Oxalis	1956
Lilis Ranch	1956
Levis	1956
Coit Ranch	1956
Firebaugh	1956
Poso Farm	1962
Tres Pecos Farm	1956
Cantua Creek	1956
Tranquillity	1956
Mendota Dam	1956
San Joaquin	1963
Jameson	1963

digitizing land-subsidence maps from four time periods: 1955–69 (Poland and others, 1975), 1963–66 (Bull, 1975), 1966–69 (Poland and others, 1975), and 1969–72 (Poland and others, 1975). The last releveling of the entire study area was done in 1972 (Ireland, 1986). Ireland and others (1984) and Ireland (1986) presented data indicating that since 1972 subsidence was less than 1 ft along the California Aqueduct and at 15 sites in and around the study area. Land-surface altitude at the centers of model cells was interpolated from the network of digitized data points. Given the altitude of the land surface, the altitudes of the top and bottom of each of the model layers can be specified by determining the thickness of each of the model layers.

The total thickness of deposits in the semiconfined zone was determined by taking the altitude of the top of the Corcoran Clay Member (Page, 1986) and subtracting those values from land-surface altitudes. The total thickness of the semiconfined zone was then divided into five layers. The thickness of the Corcoran Clay Member, needed for calculation of leakage between layers 5 and 6, was taken from a previously published map (Page, 1986). The thickness of the confined zone was not explicitly incorporated into the model but was implicitly incorporated in the storage coefficient and transmissivity of the confined zone.

Water Levels

Accurate water levels are needed for specification of initial conditions and for model calibration. Gronberg and others (1990) reported that there are 5,860 wells in an area about twice as large as the study area for this report, of which 1,114 were installed to monitor the water table where it is within 20 ft of land surface. Most of the shallow wells are monitored on a quarterly basis, but many are monitored on a semiannual basis. Generally, the water table is shallowest in July during the growing season and is deepest in October after the harvest. In the study area for this report, more than 400 wells were used to map the altitude of and depth to the water table. The density of the water-level data base is such that 50 percent of the model cells are within 1 mi of a well, and 95 percent of the model cells are within 3 mi of a well (fig. 5).

The depth to the water table and the altitude of the water table were mapped for the entire study area using October water levels in 1972, 1976, 1980, and 1984. Internal consistency between the depth and altitude maps was maintained first by interpolating land-surface altitude (bilinear interpolation) and water-table depth at the centers of model cells and then by calculating water-table altitude. A large number of wells are in areas of shallow ground water (depth to the water table less than 20 ft). Water levels for these wells were mapped using bilinear interpolation. There are fewer wells in areas of deep ground water; water levels for these wells were manually contoured. The depth to the water table in areas of shallow ground water also was mapped for July and October conditions from 1972 to 1988, except for July 1977. The large number of wells in areas of shallow ground water permitted automated interpolation of water-table depth for 32 time periods.

The altitude of the water table in 1972 was used as the initial condition for the five layers of the semiconfined zone, and the altitude of the water table in 1984 was used as a specified-head boundary in the steady-state phase of model calibration. The change in water-table altitude from 1972 to 1984 and the number of model cells with a water table within 7 ft of land surface from 1973 to 1988 were used to calibrate the transient model. Selected hydrographs from 1972 to 1984 were used to evaluate the accuracy of the calibrated model.

The potentiometric surface of the confined zone was taken from contour maps for 1972, 1976, 1980, and 1984 (Ireland and others, 1984; Westlands Water

District, written commun., 1987; and California Department of Water Resources, written commun., 1987). The 1972 potentiometric surface was used as the initial condition for the confined zone in the transient model, the 1984 potentiometric surface was used as a specified-head boundary for the steady-state model, and the change in altitude of the potentiometric surface from 1972 to 1984 was used in calibrating the transient model. Selected hydrographs from 1972 to 1984 were used to evaluate the accuracy of the calibrated model.

Distribution of Texture, Semiconfined Zone

Within the semiconfined zone, equivalent horizontal and vertical hydraulic conductivities depend on the distribution of texture (fraction of coarse-grained sediment) in each of the five layers that constitute the semiconfined zone, as well as the texture of the deposits present between the midplanes of adjacent layers. Lithologic and geophysical logs from 534 wells in and around the study area (fig. 6) were used to map the distribution of texture. The texture maps were made as follows: (1) each well log was examined and, from the geologic description (or geophysical log), individual horizons or beds were classified as coarse or fine grained; (2) each well log then was divided into nine discrete intervals, five intervals corresponding to the five layers of the semiconfined zone and four intervals corresponding to the deposits present between the midplanes of the five layers; (3) for each interval, the texture (fraction of coarse-grained sediment) was calculated; (4) for each interval, the texture at the center of model cells was computed using the moving average method of Sampson (1976). Laudon and Belitz (1991) provided a more complete description of the method used in mapping texture in the central part of the western San Joaquin Valley. The contact between coarse-grained sediment derived from the Coast Ranges and coarse-grained sediment derived from the Sierra Nevada was mapped using published maps of the thickness of deposits derived from the Coast Ranges and the Sierra Nevada (Miller and others, 1971).

The mean, standard deviation, and coefficient of variation of the textural values for the Coast Ranges alluvium and Sierran sand are listed in table 2 for each of the five model layers. In all five layers, the Sierran sand contains a higher fraction of coarse-grained deposits than the Coast Ranges alluvium and the coefficient of variation is smaller. These statistics are consistent with the depositional environment of the two hydrogeologic units.

Hydraulic Conductivity of Lithologic End Members

Within the semiconfined zone, three lithologic end members were identified with three distinct values of hydraulic conductivity: coarse-grained sediment de-

rived from the Coast Ranges (K_{C-cr}), coarse-grained sediment derived from the Sierra Nevada (K_{C-s}), and fine-grained sediment (K_f), independent of source area. In addition, the Corcoran Clay Member of the Tulare Formation of Pleistocene age was identified as a fourth lithologic end member, also with a distinct hydraulic

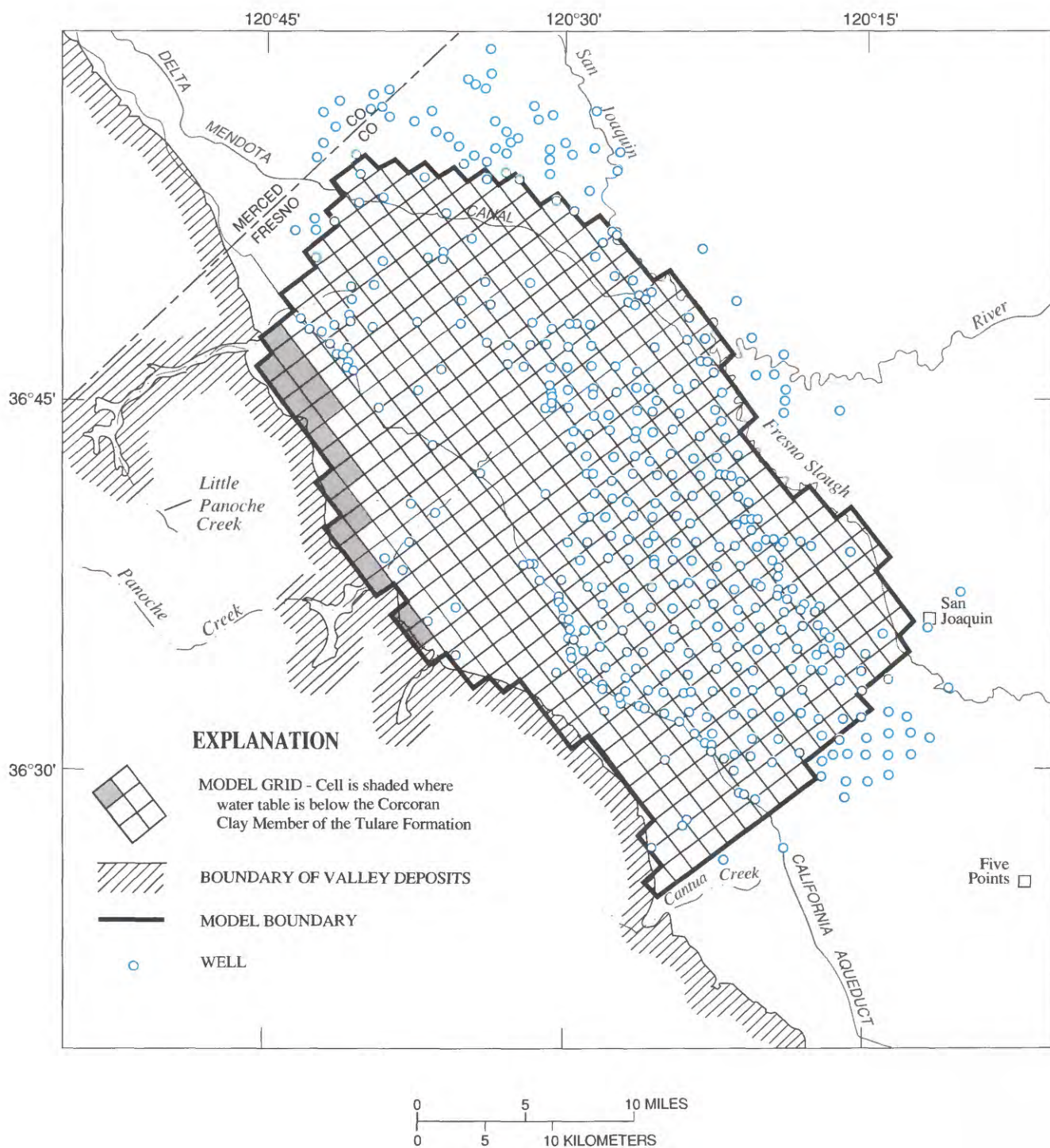


Figure 5. Location of wells used to map water table.

conductivity (K_{corc}). The hydraulic conductivities of the coarse-grained lithologic end members ($K_{\text{c-cr}}$ and $K_{\text{c-s}}$) were estimated independently of the model, and the hydraulic conductivity of the fine-grained lithologic end members (K_f and K_{corc}) were calibration variables.

Phillips and Belitz (1991), using a preliminary steady-state model of the flow system, determined that the hydraulic conductivity of a coarse-grained lithologic end member that optimized model fit was identical to the mean value obtained from interpreta-

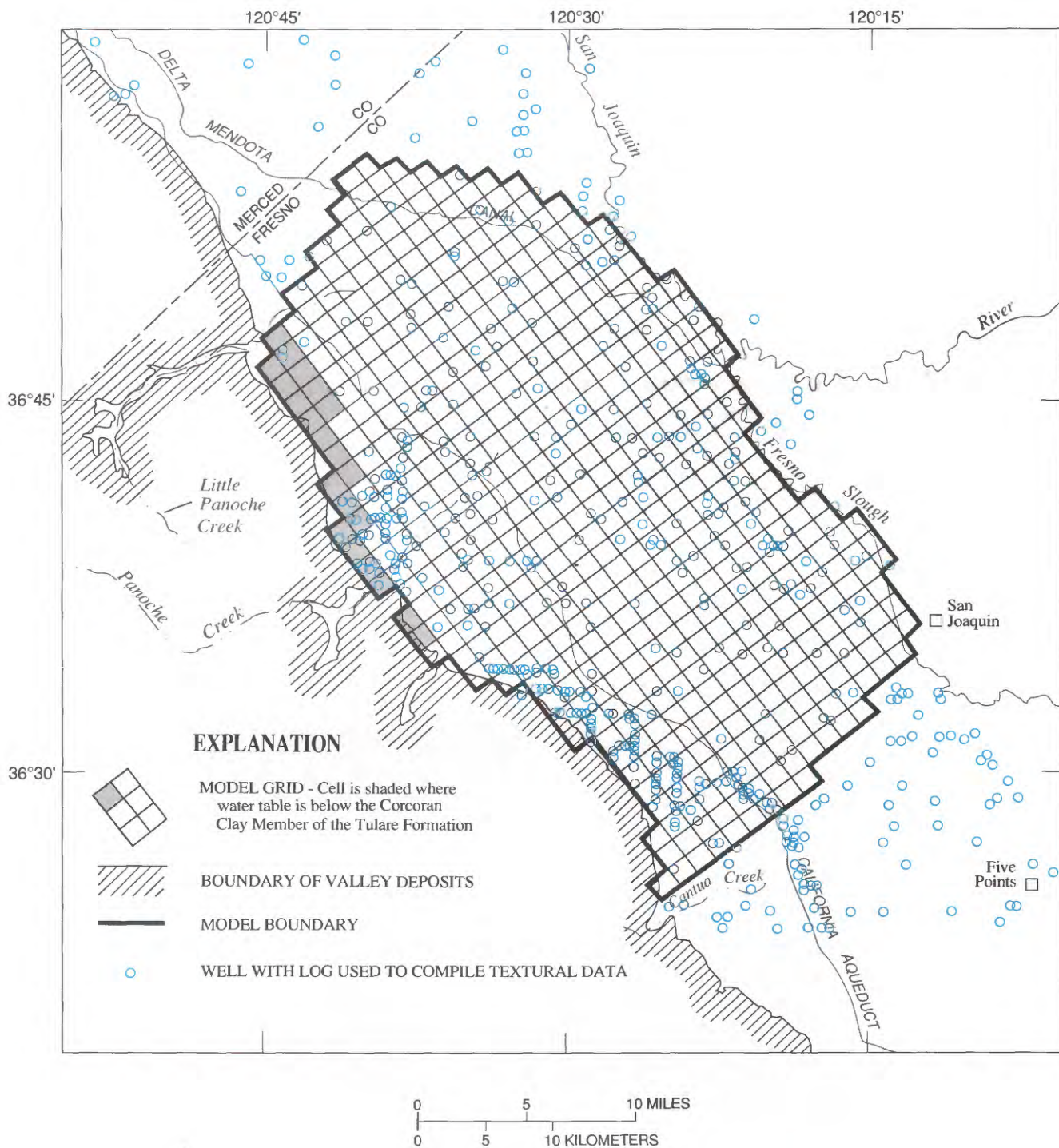


Figure 6. Location of lithologic and geophysical logs used to map distribution of texture (modified from Laudon and Belitz, 1990).

Table 2. Statistical summary of distribution of texture of Coast Ranges alluvium and Sierran sand

Model layer	Number of cells	Mean	Standard deviation	Coefficient of variation
Coast Ranges alluvium				
1	477	17.8	19.0	1.76
2	454	31.3	23.0	.73
3	429	31.7	20.9	.66
4	392	31.1	20.0	.64
5	291	21.7	12.2	.56
Sierran sand				
1	53	31.7	18.7	0.59
2	76	59.0	23.2	.39
3	101	56.7	24.5	.43
4	138	54.3	20.0	.37
5	239	48.9	20.7	.42

tion of slug-test data if arithmetic averaging was used in the horizontal direction and harmonic averaging was used in the vertical direction. Thus, the hydraulic conductivities of the two coarse-grained lithologic end members were evaluated from slug-test data obtained from 25 wells drilled at 10 well cluster sites by the U.S. Geological Survey (fig. 7, table 3). Each well has a 5- or 10-ft perforation length and sand pack, the screened interval is entirely within sandy deposits, and the holes are grouted from the sand pack to the land surface (Phillips and Belitz, 1991). Interpretation of the slug-test data (table 3), using the method of Cooper and others (1967), indicates that K_{C-cr} ranges from 1.6×10^{-6} to 1.2×10^{-3} ft/s with a mean of 3.6×10^{-4} ft/s (17 wells), and that K_{C-s} ranges from 8.9×10^{-5} to 2.9×10^{-3} ft/s with a mean of 1.2×10^{-3} ft/s (8 wells). On the basis of the results of Phillips and Belitz (1991), the mean values for K_{C-cr} and K_{C-s} were used in the transient model; the need to discriminate between K_{C-cr} and K_{C-s} is addressed in a later discussion on the sensitivity of the model.

The hydraulic conductivities of the fine-grained lithologic end members (K_f and K_{corc}) were calibration variables. For the purposes of comparison, it is useful to compile values determined in previous studies. Phillips and Belitz (1991) determined that K_f was 5.4×10^{-7} ft/s and K_{corc} was 8.3×10^{-9} ft/s if arithmetic averaging was used in the horizontal direction and harmonic averaging was used in the vertical direction. Another estimate of K_{corc} can be made from the vertical leakage of the 16 cells in the model of Williamson and others (1989) that approximately coincide with the

Table 3. Hydraulic conductivity evaluated from slug tests using method of Cooper and others (1967)

[Well: Letter and number before hyphen identifies cluster site. Number following hyphen identifies wells completed at different depths. Wells perforated either in sandy intervals of Coast Ranges alluvium or Sierran sand. Location of wells is shown in figure 7. ft, foot; in., inch; ft/s, foot per second]

Well	Well depth (ft)	Well diameter (in.)	Perforation length (ft)	Hydraulic conductivity (ft/s)
Coast Ranges alluvium (sandy intervals)				
M1-2	65	6	10	5.0×10^{-6}
M2-2	79	6	10	3.7×10^{-4}
M2-3	99	6	10	1.1×10^{-4}
M2-4	375	6	10	1.2×10^{-3}
M3-2	200	6	10	5.6×10^{-4}
M3-3	50	6	10	8.9×10^{-5}
MBS-28	20	2	10	4.6×10^{-4}
MDS-28	20	2	10	9.3×10^{-5}
P3-1	20	2	5	1.2×10^{-5}
P3-2	88	2	5	9.1×10^{-6}
P4-3	109	6	10	8.3×10^{-4}
P4-4	500	6	10	9.4×10^{-4}
P4-5	208	6	10	4.6×10^{-4}
P4-6	90	2	10	1.6×10^{-6}
P5-1	300	6	10	1.3×10^{-4}
P6-2	345	6	10	7.9×10^{-4}
P6-3	288	6	10	8.9×10^{-5}
Mean				3.6×10^{-4}
Sierran sand				
M1-1	125	6	10	1.9×10^{-4}
M1-3	262	6	10	1.7×10^{-3}
M1-4	482	6	10	1.6×10^{-3}
M2-6	570	5.75	10	8.9×10^{-5}
P1-1	65	6	10	2.9×10^{-3}
P1-3	250	6	10	2.3×10^{-3}
P1-4	410	6	10	4.2×10^{-4}
P3-3	347	6	10	4.8×10^{-4}
Mean				1.2×10^{-3}

study area. The leakance between layers 3 and 4 of the Williamson and others (1989) model incorporates the thickness of the Corcoran Clay Member with the thickness of distributed clay present between the midplanes of the layers. If the calibrated leakance values reflect the influence of the Corcoran Clay Member only, then the hydraulic conductivity of the 16 cells ranges from 2.9×10^{-10} to 2.6×10^{-8} ft/s, with a mean of 4.8×10^{-9} ft/s. If the calibrated leakance values reflect the cumulative

thickness of distributed clays as well as the influence of the Corcoran Clay Member, then the hydraulic conductivity ranges from 6.9×10^{-10} to 8.6×10^{-8} ft/s with a mean of 1.7×10^{-8} ft/s. In a subsequent section, these estimates are compared with the values determined by calibration of the transient model.

Transmissivity of the Confined Zone

Although the transmissivity of the confined zone (T_{confined}) was a calibration parameter, three preliminary estimates can be made. One estimate can be made by examining the transmissivity of the 16 cells

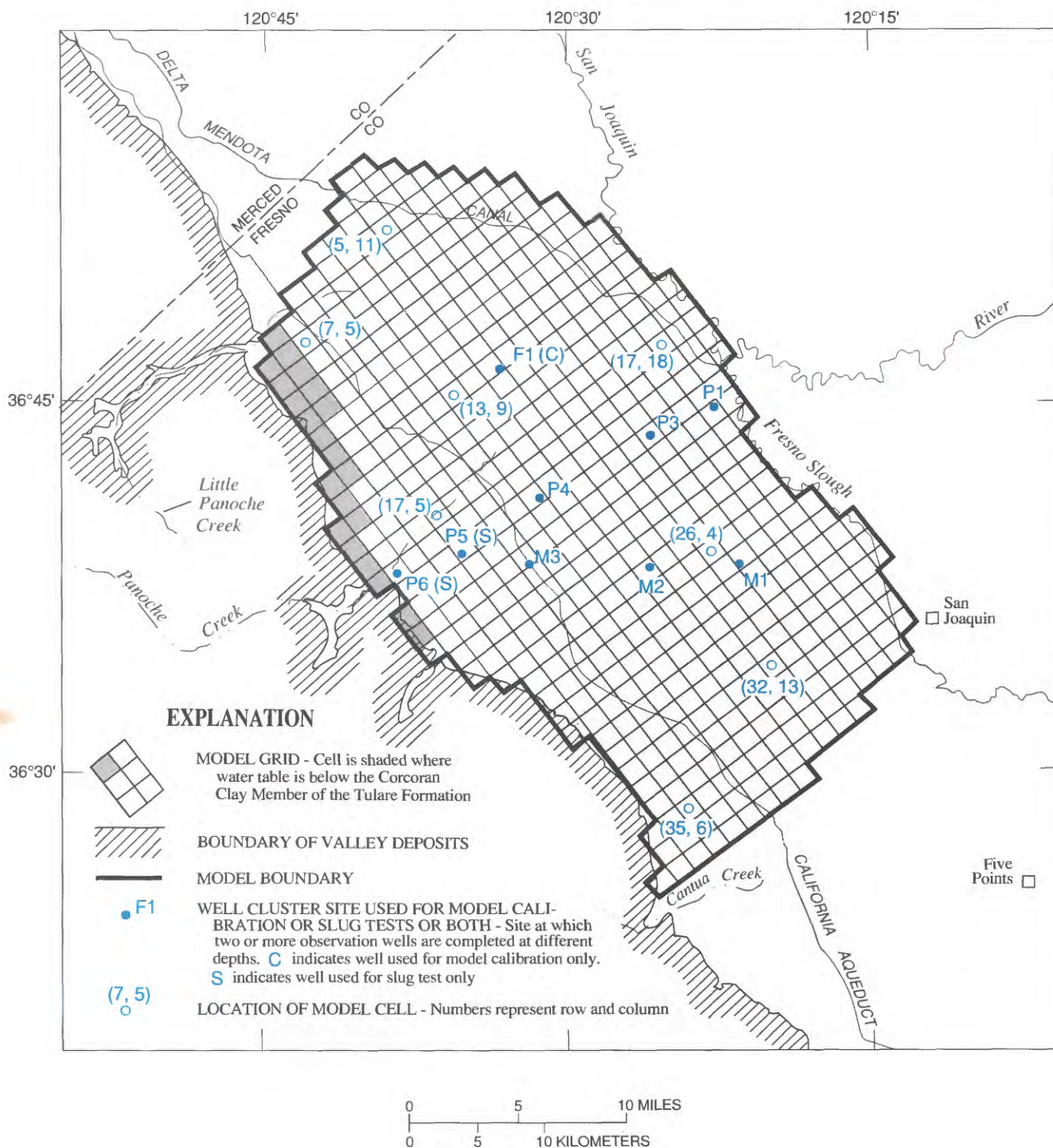


Figure 7. Location of well cluster sites used for model calibration, slug tests, and selected hydrographs.

in the model of Williamson and others (1989) that approximately coincides with the study area. The total transmissivity of layers 2 and 3 of the Williamson and others (1989) model (approximately equivalent to the confined zone) ranges from 0.02 to 0.12 ft²/s with a mean of 0.05 ft²/s.

Davis and Poland (1957, p. 429) evaluated the transmissivity of the confined zone in an area south of the study area (T. 19 S., R. 18 E., and the northern part of T. 20 S., R. 18 E.). Their estimate was based on the recovery of water levels in 54 wells during a 3-month period in 1926. Davis and Poland (1957) estimated transmissivity at 120,000 (gal/d)/ft (0.19 ft²/s).

A third estimate of the transmissivity of the confined zone can be made by using the thickness and textural data of Williamson and others (1989) and hydraulic conductivity data presented earlier. The total thickness of layers 2 and 3 in the 16 cells of the Williamson and others (1989) model ranges from 570 to 2,460 ft with an average of 1,471 ft. The texture of layers 2 and 3, where reported, ranges from 38 to 44 percent coarse grained with a mean value of 41 percent. Given these values of texture and assuming that $K = 3.6 \times 10^{-4}$ ft/s (the mean value of the sandy intervals of the Coast Ranges alluvium, table 3), the transmissivity may range from 0.09 to 0.37 ft²/s with a mean of 0.22 ft²/s. If K is assumed to be 1.2×10^{-3} ft/s (the mean value of Sierran sand, table 3), the transmissivity may range from 0.30 to 1.23 ft²/s with a mean of 0.73 ft²/s. In a subsequent section, we compare these estimates to the value determined by calibration of the model.

Specific Storage

Simulation of a transient flow system requires specification of specific storage (S_s). Williamson and others (1989) reviewed the work of Poland (1961), Riley and McClelland (1972), and Helm (1978) to evaluate the specific storage of deposits in the San Joaquin Valley. The data compiled by Williamson and others (1989) indicate a range in specific storage from 0.7×10^{-6} per foot for coarse-grained sediment to 7.5×10^{-6} per foot for fine-grained sediment. They concluded that a reasonable value of specific storage for deposits in the San Joaquin Valley is 3.0×10^{-6} per foot. Ireland and others (1984) calculated values of specific storage at seven sites ranging from 1.9×10^{-6} to 3.9×10^{-6} per foot. The mean of the seven sites is

2.7×10^{-6} per foot, a value that is consistent with the conclusions of Williamson and others (1989). Thus, a value of 3.0×10^{-6} per foot was used in all layers of the simulation model; the thickness of the confined zone was assumed to be 1,000 ft, and the storage coefficient for the confined zone was 0.003.

Specific Yield

Specific yield (S_y) was a calibration parameter; however, some data are available to make some preliminary estimates. In an area with a rising water table and in the presence of plants, a maximum value of specific yield can be defined as the difference between the total porosity and the permanent wilting point, which can be defined as the moisture content at 15 bars of tension (Hillel, 1980). Lord (1988) evaluated moisture characteristic curves for two cores of Panoche clay loam taken from the upper 5 ft of the soil profile (Panoche clay loam is a fine-grained soil present across a large percentage of the study area). The moisture content at 0.0, 0.1, and 15 bars of tension for one of the cores was 0.53, 0.37, and 0.12, respectively. The moisture content at 0.0, 0.1, and 15 bars of tension for the other core was 0.60, 0.43, and 0.17, respectively. Given these values, the specific yield in the presence of plants may be as high as 0.41 and 0.43.

In the absence of plants, specific yield can be evaluated theoretically if one knows the moisture characteristic curve and if one assumes no flow of moisture in the profile (Hillel, 1980). A theoretical analysis of Panoche clay loam (see appendix A, eq. 28) indicates a specific yield of 0.20 when the water table is 10 ft deep, 0.25 when the water table is 20 ft deep, and 0.31 when the water table is 100 ft deep. The actual specific yield will differ from the theoretical values if there is movement of water in the profile, if the porosity at depth is different from the values measured by Lord (1988), or if the moisture characteristic curve for deposits at depth differs from that of Panoche clay loam.

If there was flow of water in the profile, the calculated values of specific yield would differ from values based on an assumption of no flow. In areas of downward flow, the hydraulic head above the water table would be higher than if there were no flow. Given higher head, the tension would be lower and the moisture content would be higher. Thus in the areas of downward flow, specific yield would be

Table 4. Water-budget data for 1980

[Irrigation efficiency based on application: Computed if surface water is greater than irrigation. Irrigation requirement equals crop-water requirement divided by irrigation efficiency. Ground-water pumpage equals irrigation requirement minus surface-water delivery. Ground-water recharge equals irrigation requirement minus crop-water requirement, or surface-water delivery minus crop-water requirement, whichever is greater. ft, foot; nc, not calculated]

Subarea (fig. 8)	Crop- water require- ment (ft)	Irrigation efficiency based on depth to water table (percent)	Irrigation require- ment (ft)	Surface- water delivery (ft)	Ground- water pumpage (ft)	Ground- water recharge (ft)	Irrigation efficiency based on application (percent)
Firebaugh	1.88	80	2.35	2.63	0	0.75	71
Tranquillity	1.97	70	2.81	2.51	.30	.84	nc
Panoche	1.52	73	2.08	2.48	0	.96	61
Broadview	1.97	79	2.49	2.75	0	.78	72
San Luis	1.47	65	2.26	1.86	.40	.79	nc
Westlands							
Depth to water table							
Less than or equal to 10 ft	1.84	80	2.30	1.90	.40	.46	nc
Greater than 10 ft and less than or equal to 20 ft	1.91	72	2.65	2.19	.46	.74	nc
Greater than 20 ft							
With surface-water delivery	1.74	65	2.68	2.43	.25	.94	nc
Without surface-water delivery	1.60	65	2.46	0	2.46	.86	nc

lower than in areas of no flow; specific yield calculated under an assumption of no flow is an upper bound.

The porosity of deposits at depth was examined by Johnson and others (1968), who summarized a large number of porosity determinations for three cores from the Los Banos-Kettleman City area. Porosity for fine-grained materials (sand, silt, clay, clayey silt, sandy silt, silty clay) ranges from 31 to 56 percent with a mean of 42 percent. Porosity for coarse-grained materials (sand, clayey sand, silty sand) ranges from 28 to 50 percent with a mean of 41 percent. These mean porosities are lower than the porosity of the two cores analyzed by Lord (1988), which had porosities of 0.53 and 0.60. In the absence of plants and considering the effects of downward flow and decreased porosity with depth, specific yield of fine-grained deposits at depth should be lower than 0.25 (depth to water table 25 ft deep) to 0.30 (depth to water table 100 ft deep) and may be lower than 0.15 to 0.20. In a subsequent section, these estimates are compared to the value determined by calibration of the model.

Recharge and Pumping

Gronberg and Belitz (1992) used a crop-based approach to evaluate the components of the water

budget, including recharge and pumping, for nine subareas containing all or parts of 11 water districts (fig. 8, table 4). Three of the subareas contain all or part of a single water district (Panoche, Broadview, and San Luis), two of the subareas contain all or parts of several water districts (Firebaugh consists of all or parts of the Mercy Springs, Eagle Field, Oro Loma, Widren, and Firebaugh Water Districts, and the Tranquillity subarea consists of all or parts of the Fresno Slough and Tranquillity Water Districts), and four of the subareas are subdivisions of the Westlands Water District. The four subareas within Westlands were defined on the basis of depth to the water table and the availability of surface water. A tenth subarea, the Mendota Wildlife Refuge, was assumed to have no active recharge or pumpage. Recharge and pumping, although variable between subareas, were assumed constant within subareas.

Gronberg and Belitz (1992) compiled water budgets for the nine subareas for 1980 and 1984 water years. They noted that 1980 was a typical year with respect to crops planted, weather, and surface-water delivery and that 1984 had a higher than average crop-water requirement and higher than average surface-water delivery. Because 1980 was an average year, we used the 1980 water budget (table 4) to represent the entire simulation period (1972–88).

Gronberg and Belitz (1992) used the vertical distribution of well perforations above and below the Corcoran Clay Member to evaluate the percentage of ground-water pumpage from the semiconfined and confined zones. They identified 10 subareas for analysis (fig. 9, table 5) on the basis of water-district bound-

aries, the presence or absence of Sierran sand (Miller and others, 1971), and a map of the distribution of pumping presented by Bull and Miller (1975). The data base and the methods used to evaluate the water budget and the distribution of ground-water pumping are described by Gronberg and Belitz (1992).

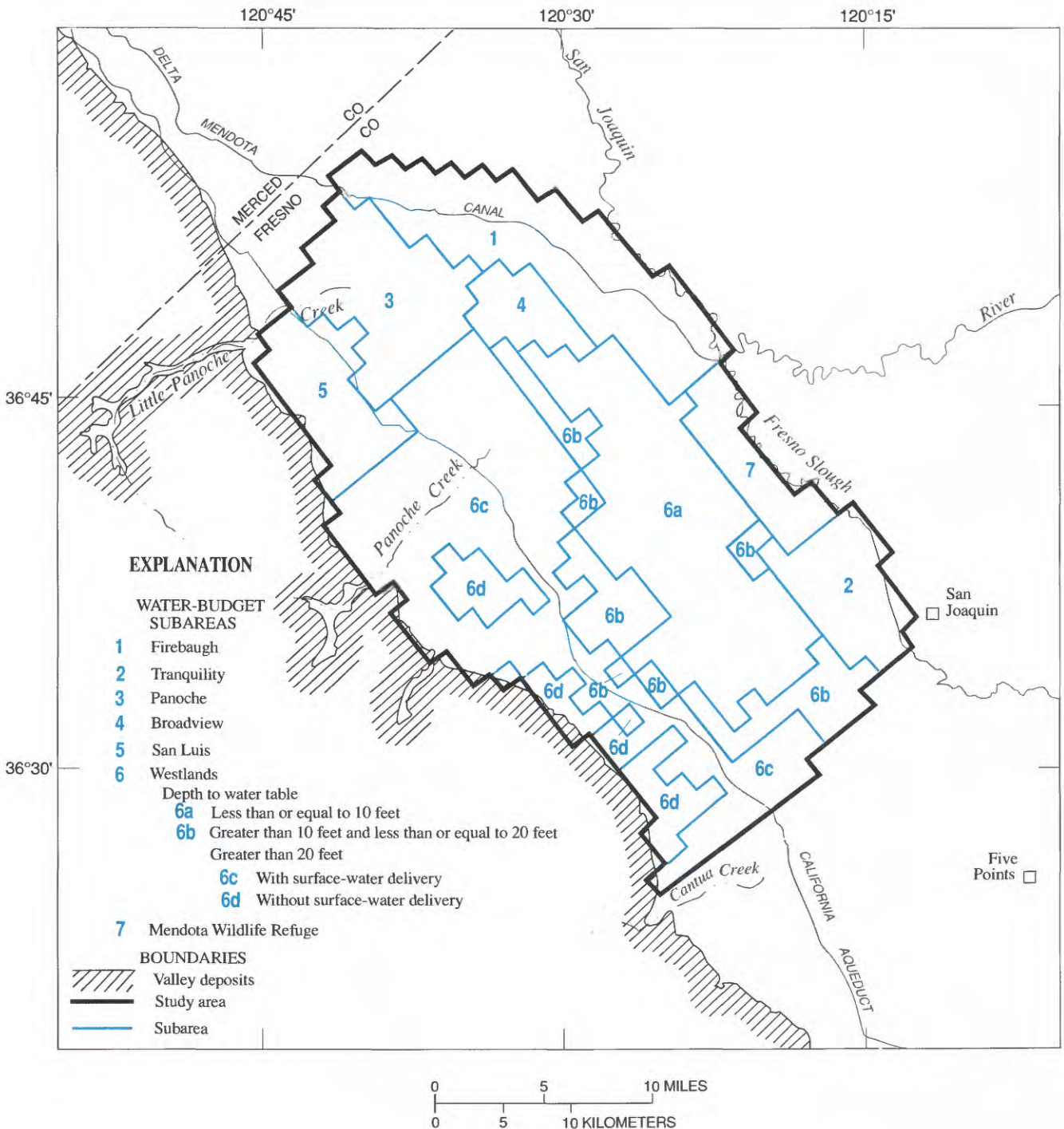


Figure 8. Water-budget subarea boundaries.

Drains

Incorporation of linear functions to represent drains (eq. 7) requires specification of the altitude and conductance of the drains. These two values can be evaluated for a given model cell, or for a set of model cells within a common drainage sys-

tem, by examining the relation between drainflow and depth to the water table. Equation 7 can be rewritten in terms of depth rather than altitude and can be generalized from a model cell to a drainage system:

$$QD = C(DT_{\text{drain}} - DTW), \quad (12)$$

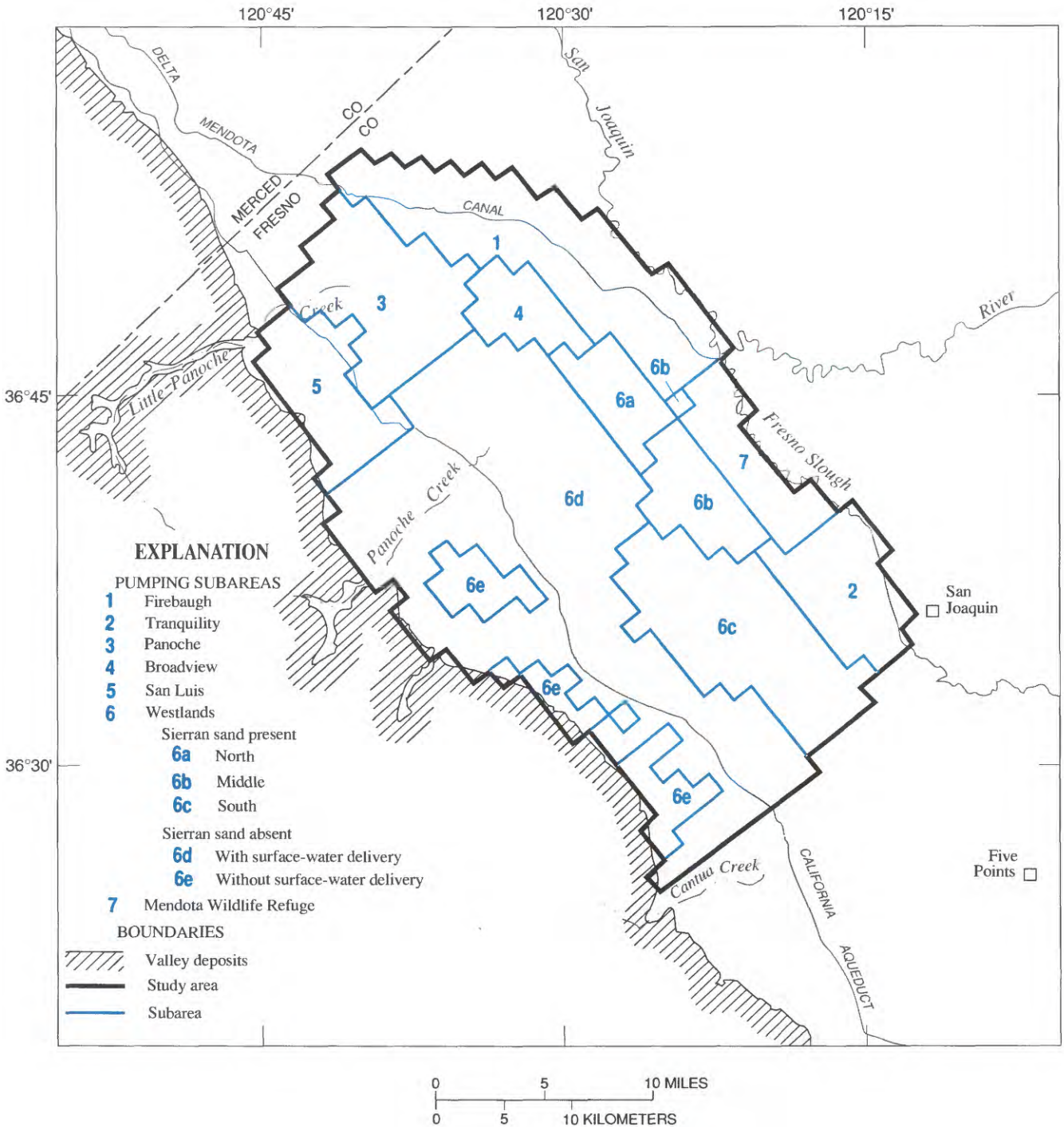


Figure 9. Subareas used for evaluating vertical distribution of ground-water pumpage.

Table 5. Summary of percentage of ground-water pumpage by subarea

Subarea (fig. 9)	Number of wells	Sierran sand	Pumpage (percent)	
			Above Corcoran Clay Member	Below Corcoran Clay Member
Firebaugh	15	Present	95	5
Tranquillity	6	Present	73	27
Panoche	39	Absent	2	98
Broadview	7	Present	18	82
San Luis	18	Absent	5	95
Westlands				
North	11	Present	35	65
Middle	20	Present	30	70
South	51	Present	63	37
With surface-water delivery	291	Absent	6	94
Without surface-water delivery	34	Absent	5	95

where

QD = total drainflow (L^3/t),

C = average or effective conductance of the drain/aquifer system (L^2/t),

DT_{drain} = average or effective depth to the drains (L), and

DTW = average or effective depth to the water table (L).

Equation 12 can be used to evaluate conductance and depth to a drain or drainage system from the slope and intercept of the relation between total drainflow (QD) and average depth to the water table (DTW). The altitude of a drain then can be evaluated given the altitude of the land surface in a model cell.

In the Westlands Water District, regional-collector drains were installed in an area of about 42,000 acres (about 67 mi^2) (fig. 10). The regional-collector system consists of concrete pipes with open connections, installed at depths ranging from 7 to 11 ft, typically running west to east and at a spacing of 0.5 mi. Within the 42,000-acre area, on-farm collectors also were installed beneath an area of about 5,000 acres (Westlands Water District, written commun., 1985). The regional-collector system was opened in 1980 but was closed in 1985 because of high concentrations of selenium in the drainwater. From 1981 to 1984, the total volumes of drainflow were 7,150; 6,327; 8,287; and 5,986 acre-ft, respectively (Westlands Water District, written commun., 1985). Drainflow per acre was 0.17; 0.15; 0.20; and 0.14 ft/yr from 1981 to 1984, respectively.

Within the area underlain by the regional-collector system, 90 wells are monitored on a quarterly basis (fig. 10). The wells are fully slotted PVC pipe (1 inch diameter) and are typically drilled to a depth of 20 ft. For the period in which the regional-collector system was fully operational, 19 months of water-level and drainflow data are available. The average depth to water was calculated for the 90 wells for each of the 19 months. The volumetric flow rate for the entire regional-collector system then was regressed against the monthly average depth to water. The resulting relation is

$$QD = 37.5 - 3.71 DTW = 3.71 (10.1 - DTW). \quad (13)$$

Equation 13 predicts an average drain depth of 10.1 ft, a value that is consistent with the actual depth of the drains (7 to 11 ft). Therefore, for the 69 model cells representing the area serviced by the regional-collector system, the altitude of the drains was specified 10.1 ft lower than land-surface altitude. Conductance (C) of the drains at a regional scale was distributed uniformly among the 69 cells, that is, $C = 3.71/69 = 0.054 \text{ ft}^2/s$ for each model cell.

North of the Westlands Water District, about 67 mi^2 is underlain by on-farm drainage systems (fig. 10). The on-farm drains are at shallower depths (6 to 8.4 ft) and at closer spacing (average spacing 260 to 530 ft) than the regional-collector drains (table 6). Lord (1988), as part of a study of irrigation management and controlled drainage, monitored daily water levels and drainflow on an irregular schedule in three fields with on-farm drains (fig. 10). Total drainflow

for each of the three fields was regressed against depth to water in wells located midway between drain laterals. The results of the regression analysis (table 6) indicate that the depth to the on-farm drains ranges from 6.5 to 7.8 ft and conductance ranges from 0.31 to 0.65 ft²/s. The average of the three sites

suggests a representative depth to drains of 7.3 ft and a representative conductance of 0.52 ft²/s. A drain depth of 7.3 ft is within the range of the measured depth to drains, and the conductance value for the on-farm drains, nearly 10 times as high as that for the regional-collector drains, is consistent with the

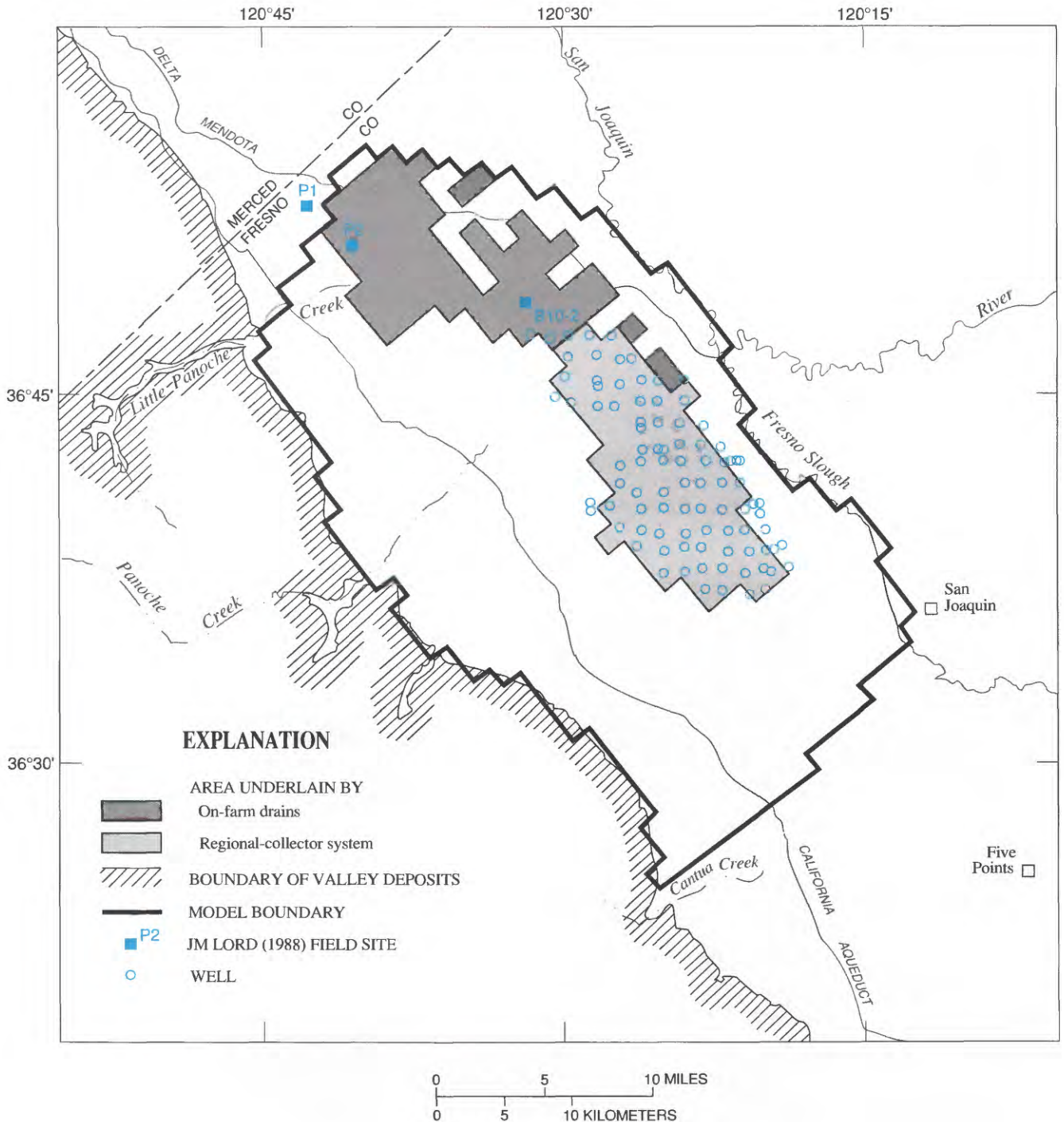


Figure 10. Location of drainage-system subareas, wells in and around area underlain by regional-collector system, and field sites used by Lord (1988).

Table 6. Drainage-system characteristics and regression parameters
[ft, foot; ft²/s, square foot per second]

Drainage system	Characteristics			Regression		
	Area (acres)	Drain spacing (ft)	Depth to drains (ft)	Conductance (ft ² /s)	Depth to drains (ft)	R ²
Regional collector	42,000	2,640	7 to 11	0.054	10.1	0.52
On-farm (Lord, 1988)						
P1	92	260 to 1,365 (average = 530)	6.8 to 8.4	.65	7.8	.66
P2	149.9	400 to 560 (average = 427)	6	.60	6.5	.67
B10	145.5	260	6.2 to 6.9	.31	7.7	.59

closer spacing of the on-farm drains. These values were specified for the 67 model cells representing the area serviced by on-farm drains.

Bare-Soil Evaporation

Using a linear function to simulate bare-soil evaporation (eq. 8) requires specification of the maximum bare-soil evaporation rate (QE_{max}), the altitude of the surface at which the maximum rate occurs (Z_{ref}), and the extinction depth (D_{ext}). These were selected on the basis of a theoretical analysis of bare-soil evaporation from Panoche clay loam, the predominant soil type in the study area (Harradine, 1950) (appendix B). For Panoche clay loam, bare-soil evaporation from the water table can be approximated with the equation

$$E = 32.0e^{-0.96L}, \quad (14)$$

where

- E = bare-soil evaporation rate (ft/yr) and
- L = depth of water table below evaporation surface (ft).

Figure 11 illustrates the bare-soil evaporation rate as a function of depth to the water table. A linear approximation of equation 14 can be accurate only for a limited depth range. Because the water table in the central part of the western San Joaquin Valley is rarely shallower than 4 ft, depths greater than 4 ft need to be approximated in equation 14. A linear approximation of equation 14 using an

extinction depth of 7 ft and a maximum bare-soil evaporation rate of 1.0 ft/yr at the land surface approximates the exponential function closely within the depth range 4 to 7 ft (fig. 11).

Head-Dependent Boundary Condition

Using a head-dependent boundary condition (eq. 10) along the northeastern and eastern boundaries of the study area requires specification of the conductance of the deposits along these boundaries and the externally specified hydraulic heads in adjacent areas. Estimating conductance of a single model cell along a boundary requires values for the area of the

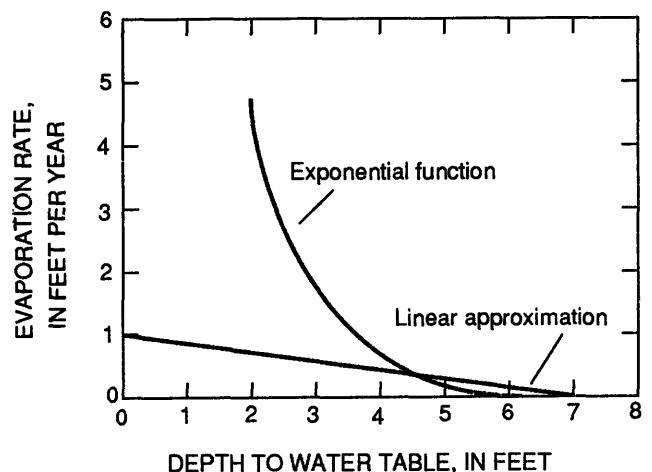


Figure 11. Bare-soil evaporation as a function of water-table depth.

cell face adjacent to the boundary, the hydraulic conductivity of the deposits between the cell and the externally specified head, and the distance between the cell and the externally specified head (eq. 11).

In the semiconfined zone, the hydraulic head in adjacent areas and the distance between the cell and the externally specified head were evaluated from the data base compiled by Gronberg and others (1990). Examination of water levels of wells along the northeastern and eastern boundaries for 1976, 1980, and 1984 indicated a typical head value of 125 ft at a distance of 2 mi. In the confined zone, the hydraulic head in adjacent areas was specified on the basis of measured lateral gradients for 1972, 1976, 1980, and 1984 (Ireland and others, 1984; Westlands Water District, written commun., 1987; and California Department of Water Resources, written commun., 1987). Inspection of the maps indicated that a head value of 125 ft at a distance of 10 mi generally would respect the measured gradients for the confined zone.

Evaluation of conductance of each cell along the boundaries was based on the geometry of the model (cell width multiplied by cell thickness) and the texture and source area of the deposits along the boundaries. The semiconfined zone was divided vertically into five layers. Along the northeastern and eastern boundaries, the uppermost layer (layer 1) consists primarily of flood-basin clays; therefore, head-dependent boundaries were not specified for layer 1. In the lower four layers of the semiconfined zone, the deposits between the boundaries and the externally specified heads are primarily Sierran sand; therefore, the hydraulic conductivity was calculated by assuming a texture of 0.65 (a value representative of Sierran sand in the valley trough) and a hydraulic conductivity of 1.2×10^{-3} ft/s (the mean value determined from slug-test data; table 3). In the confined zone, hydraulic conductivity was calculated by dividing the transmissivity of the confined zone (a calibration variable) by 1,000 ft (the assumed thickness of the confined zone).

MODEL CALIBRATION

A numerical model of the ground-water flow system in the central part of the western San Joaquin Valley requires several model parameters to be specified. Most parameters were estimated independently of the model; four parameters, however (K_f , K_{corc} , S_y , and T_{confined}), were calibration variables. The re-

lation between two of them (K_f and K_{corc}) was constrained by optimizing a steady-state model of the semiconfined zone, thus reducing the number of independent variables in the transient model from four to three. The transient model was then calibrated as a function of the remaining three variables.

Steady-State Calibration

In the steady-state phase of calibration, the known parameters were the geometry of the ground-water flow system, the distribution of texture, the location of the contact between coarse-grained deposits derived from the Coast Ranges and those derived from the Sierra Nevada, the hydraulic conductivities of coarse-grained sediment derived from the Coast Ranges and Sierra Nevada ($K_{\text{c-cr}}$ and $K_{\text{c-s}}$, respectively), the altitude of the water table and confined zone heads (specified-head boundaries), and the externally specified heads and the conductance along the northeastern and eastern boundaries (head-dependent boundary condition). The unknown parameters were the hydraulic conductivities of the two fine-grained lithologic end members (K_f and K_{corc}).

Phillips and Belitz (1991) presented a method for optimizing a steady-state model of the semiconfined flow system in the central part of the San Joaquin Valley if there were three lithologic end members: coarse-grained deposits (K_c), fine-grained deposits (K_f), and the Corcoran Clay Member (K_{corc}). The method of Phillips and Belitz (1991) can be used if the four hydraulic conductivities of the present model ($K_{\text{c-cr}}$, $K_{\text{c-s}}$, K_f , and K_{corc}) are reduced to three. This can be done if we define $K_c = K_{\text{c-cr}}$, and if we fix the ratio of $K_{\text{c-s}}/K_{\text{c-cr}}$. Slug testing of U.S. Geological Survey wells indicates that the mean value of $K_{\text{c-s}}$ is 3.2 times as large as the mean value of $K_{\text{c-cr}}$ (table 3). Thus, $K_c = K_{\text{c-cr}} = K_{\text{c-s}}/3.2$.

Following the procedure of Phillips and Belitz (1991), the remaining three parameters (K_c , K_f , and K_{corc}) can be reduced to two dimensionless parameters:

$$K' = K_c / K_f, \quad (15)$$

$$K'' = K_c / K_{\text{corc}}. \quad (16)$$

The two dimensionless parameters incorporate two known variables ($K_{\text{c-cr}}$ and $K_{\text{c-s}}$) and two unknown variables (K_f and K_{corc}). This is in contrast to Phillips and Belitz (1991) in which the two dimensionless parameters incorporated three unknown variables (K_c ,

Table 7. Location of U.S. Geological Survey well cluster sites used in calculating estimated values of head in model cells [Well cluster site: Site where two or more observation wells installed at different depths. ft, foot]

Cluster site (fig. 7)	State No.	Perforated interval		Lowermost cell penetrated by a well		
		Shallow well (ft)	Deep well (ft)	Row	Column	Layer
F1	13S/13E-28A	88-89	193-203	12	11	4
P1	13S/15E-31J	22-27	400-410	20	18	5
P3	14S/14E-10A	13-18	332-342	19	15	4
M1A	15S/15E-9D	20-25	55-65	26	15	2
M1B	15S/15E-9D	55-65	472-482	26	15	5
P4	14S/13E-24N	62-67	490-500	18	9	5
M2	15S/14E-10A	69-79	365-375	24	11	5
M3	15S/13E-11B	35-45	370-380	20	7	4

K_f , and K_{corc}). The use of the dimensionless parameters in the present investigation is for consistency with the previous work of Phillips and Belitz (1991).

The steady-state model was then run as a function of the two dimensionless parameters, K' and K'' . For each individual run of the model, two statistics were calculated:

$$RMSE = \sqrt{\sum_{i=1}^n \frac{(h_{meas} - h_{sim})^2}{n}}, \quad (17)$$

$$BIAS = \sum_{i=1}^n (h_{meas} - h_{sim})_i, \quad (18)$$

where

- $RMSE$ = root mean square error,
- h_{meas} = measured head,
- h_{sim} = simulated head,
- i = summation index, and
- n = number of measurements.

To compare simulated and measured conditions, water levels for wells were adjusted to values representative of model cells. Adjusted values of head were calculated for eight model cells at seven locations in the study area (fig. 7, table 7); each location corresponds to a U.S. Geological Survey well cluster site where several wells were drilled to different depths. At each well cluster site, an adjusted value of head was calculated for the deepest model cell (within the semiconfined zone) penetrated by a well. The adjusted value of head was calculated as follows: the vertical hydraulic-head gradient between the shallowest well (typically a water-table well) and the deepest well within the semiconfined zone was calculated,

and then the calculated gradient and the estimated altitude of the water table (1984) were used to calculate an adjusted value of head at the midpoint of the deepest cell penetrated by a well. At the M1 site, contact between the Coast Ranges alluvium and the underlying Sierran sand is at a depth of 85 ft. Two values of adjusted head were calculated for the M1 site: one at the deepest cell consisting of Coast Ranges alluvium and the other at the deepest cell consisting of Sierran sand. Optimization of the model using adjusted values of head at the deepest model cells should reproduce the overall vertical hydraulic-head gradient measured in the semiconfined zone but may not necessarily reproduce the gradients between individual wells at each of the well cluster sites (the vertical hydraulic-head gradient generally is not linear).

Given the adjusted values of head, the model was systematically run as a function of K' and K'' . Figure 12 shows contour plots of $RMSE$ and $BIAS$ for a set of model runs in which K' and K'' each range more than five orders of magnitude. Along the axis of the valley of the contoured $RMSE$ surface, the $RMSE$ ranges from 13.5 to 14.7 ft; the associated $BIAS$ ranges from -1.5 to +0.5 ft.

Phillips and Belitz (1991) reported a $RMSE$ and $BIAS$ of about 19 ft and -5 ft, respectively. The lower values in this investigation are the result of (1) a more accurate map of the altitude of the water table in 1984 and (2) a more careful selection of observation wells. The existence of a valley of minimum $RMSE$ indicates that a unique solution to the boundary value problem does not exist; many solutions optimize model fit with respect to head. However, the existence of a valley of minimum $RMSE$ can be used

in further calibration of the model. If a value of K'' is specified (that is, if K_c and K_{corc} are specified), then figure 12A can be used to select a value of K' that minimizes $RMSE$ (that is, K_f is uniquely determined). Because K_{c-cr} and K_{c-s} are specified in the transient model, one need only calibrate for either K_{corc} or K_f .

Transient Calibration

The transient model was calibrated as a function of three unknowns: specific yield (S_y), hydraulic conductivity of the Corcoran Clay Member (K_{corc}), and the transmissivity of the confined zone ($T_{confined}$). A

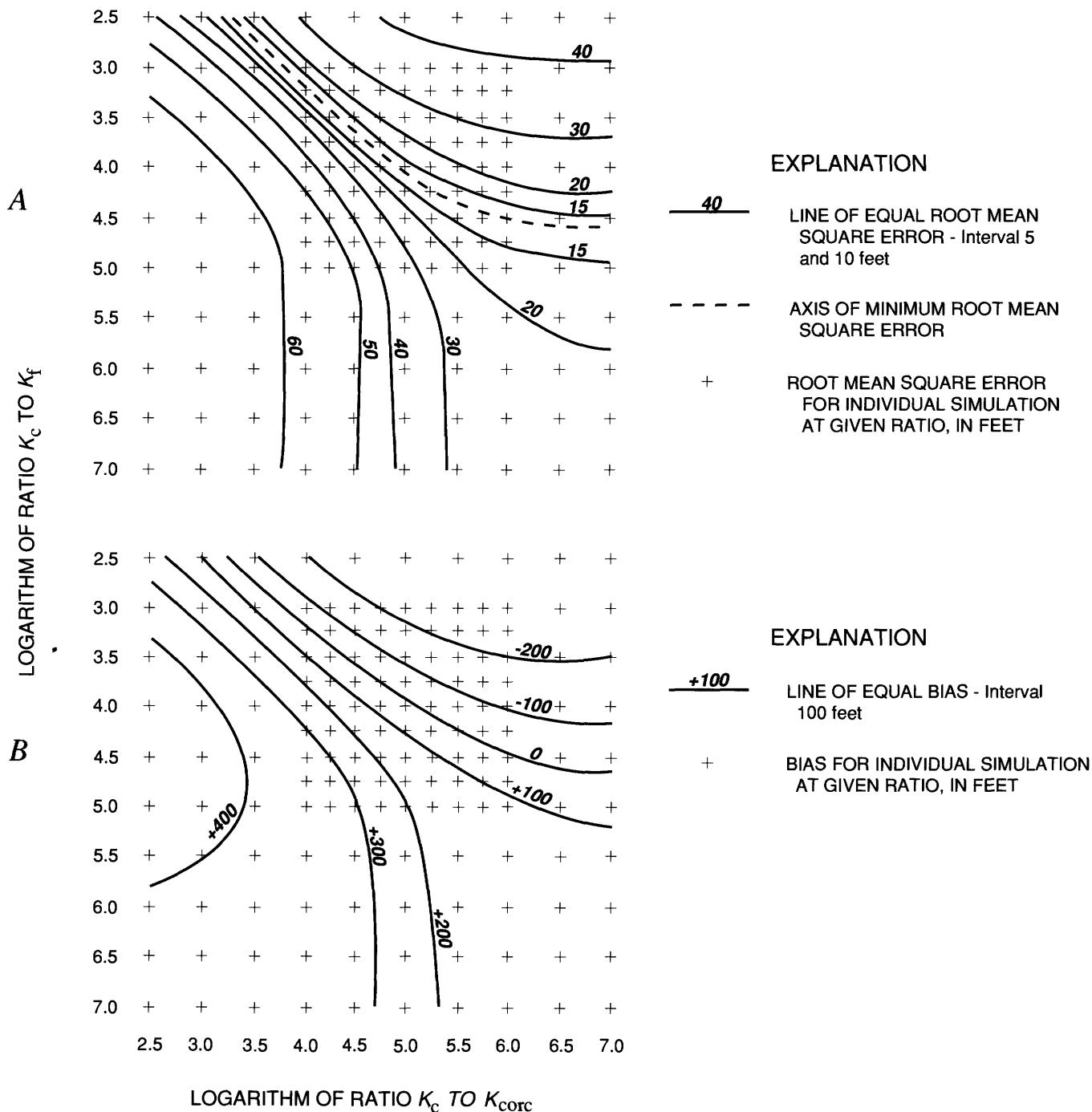


Figure 12. Root mean square error and bias mapped as a function of two dimensionless parameters, K' and K'' . A, Root mean square error. B, Bias, the sum of measured values minus simulated values. K_c is hydraulic conductivity of

coarse-grained material, K_f is hydraulic conductivity of fine-grained material, and K_{corc} is hydraulic conductivity of the Corcoran Clay Member of the Tulare Formation of Pleistocene age. Logarithms are base 10.

fourth unknown, the hydraulic conductivity of fine-grained deposits (K_f), was uniquely determined by minimizing the root mean square error for given values of K_{c-cr} and K_{corc} (fig. 12A). Three measures of the state of the ground-water flow system were used in calibrating the model: change in water-table altitude from 1972 to 1984, change in confined zone head from 1972 to 1984, and a time-series record (1972 to 1988) of the number of model cells in which the water table is within 7 ft of the land surface and therefore is subject to bare-soil evaporation. Bare-soil evaporation was evaluated for July and October conditions. These three measures of the state of the ground-water flow system were used to calibrate for the three unknown variables.

In calibrating the transient model, the following observations were made: (1) changes in S_y affected the change in water-table altitude and bare-soil evaporation; (2) changes in K_{corc} affected bare-soil evaporation but had little effect on the change in water-table altitude (note: bare-soil evaporation is sensitive to changes in water-table altitudes of less than 0.5 ft); (3) for a given value of S_y , an increase or decrease in K_{corc} resulted in a decrease or increase in bare-soil evaporation, respectively; (4) changes in $T_{confined}$ had little to no effect on the semiconfined flow system; (5) the change in confined zone head could be calibrated as a function of $T_{confined}$. Thus, the model first was calibrated for S_y (using the change in water-table altitude and bare-soil evaporation as indicators of fit), then for K_{corc} (using bare-soil evaporation as an indicator of fit), and finally for $T_{confined}$ (using the change in confined zone head as an indicator of fit).

A satisfactory match between simulated and measured conditions was obtained when S_y was 0.30 in layer 1 and 0.20 in layers 2 to 6, K_{corc} was 6.0×10^{-9} ft/s ($K_f = 4.6 \times 10^{-8}$ ft/s), and $T_{confined}$ was 0.20 ft²/s. The calibrated values of S_y are consistent with the values discussed previously: a value of 0.30 in layer 1 is consistent with S_y in the presence of plants (0.30) and a value of 0.20 in layers 2 to 6 is consistent with the values indicated by equilibrium drainage in a compacted core (0.20). The calibrated value of K_{corc} (6.0×10^{-9} ft/s) is consistent with the mean values (4.8×10^{-9} to 1.7×10^{-8} ft/s) deduced from the model results of Williamson and others (1989). The calibrated value of $T_{confined}$ (0.20 ft²/s) is higher than the upper bound (0.12 ft²/s) of the 16 cells in the model of Williamson and others (1989) but is consistent with the estimate of Davis and Poland (1957)

(0.19 ft²/s) and with the estimate of transmissivity based on the thickness and textural data of Williamson and others (1989), along with the assumption that $K = 3.6 \times 10^{-4}$ ft/s ($T_{confined} = 0.22$ ft²/s).

COMPARISON OF SIMULATED AND MEASURED CONDITIONS

The ability of the transient model to reproduce measured conditions can be evaluated by examining six measures of the state of the ground-water flow system. Three of the measures (change in water-table altitude, confined zone head, and bare-soil evaporation) were used to calibrate the transient model. Two additional measures provide a "snapshot" of the system: depth to the water table in 1984 and distribution of model cells subject to bare-soil evaporation in 1984 (cells with depth to the water table within 7 ft of land surface). The sixth measure is a set of time-series hydrographs (1972–88) of water-table altitude and confined zone head.

Limitations in both space and time should be noted when evaluating the transient model. Although the model was discretized into cells 1 mi square, many of the variables incorporated into the model were evaluated on a larger scale. For example, water-budget components (recharge and pumping) were estimated for subareas ranging in size from 16 to 155 mi². Although an annual time increment was used in the model, the specified fluxes (recharge and pumping) were constant with time. These simplifications for space and time indicate that one should be cautious in evaluating system response for short time periods (for example, yearly) and for small areas (for example, smaller than subareas).

In evaluating the transient model, it also is important to note the limitations of the data against which the model is being compared. For example, in areas where the water table is more than 20 ft below land surface, the data base is relatively sparse, and the measured altitude and depth of water table should be viewed as an estimate. The confined zone heads were mapped with a contour interval of 25 ft (Ireland and others, 1984; Westlands Water District, written commun., 1987; and California Department of Water Resources, written commun., 1987); when examining changes in confined zone head, the resulting map may have an error on the order of the contour interval. Areas subject to bare-soil evaporation are defined as those areas where the water table is within 7 ft of

land surface. This definition depends on measured altitude and depth of the water table and therefore should be viewed as an estimate. Other aspects of the data base that are relevant for comparison of simulated and measured values are included in the discussion that follows.

In maps of the changes in water-table altitude from 1972 to 1984 (fig. 13), there is a large area where the measured water-table change was less than 10 ft (generally, the distal-fan areas and interfan areas) and a relatively small area (fanhead of the Panoche Creek alluvial fan) where the water-table

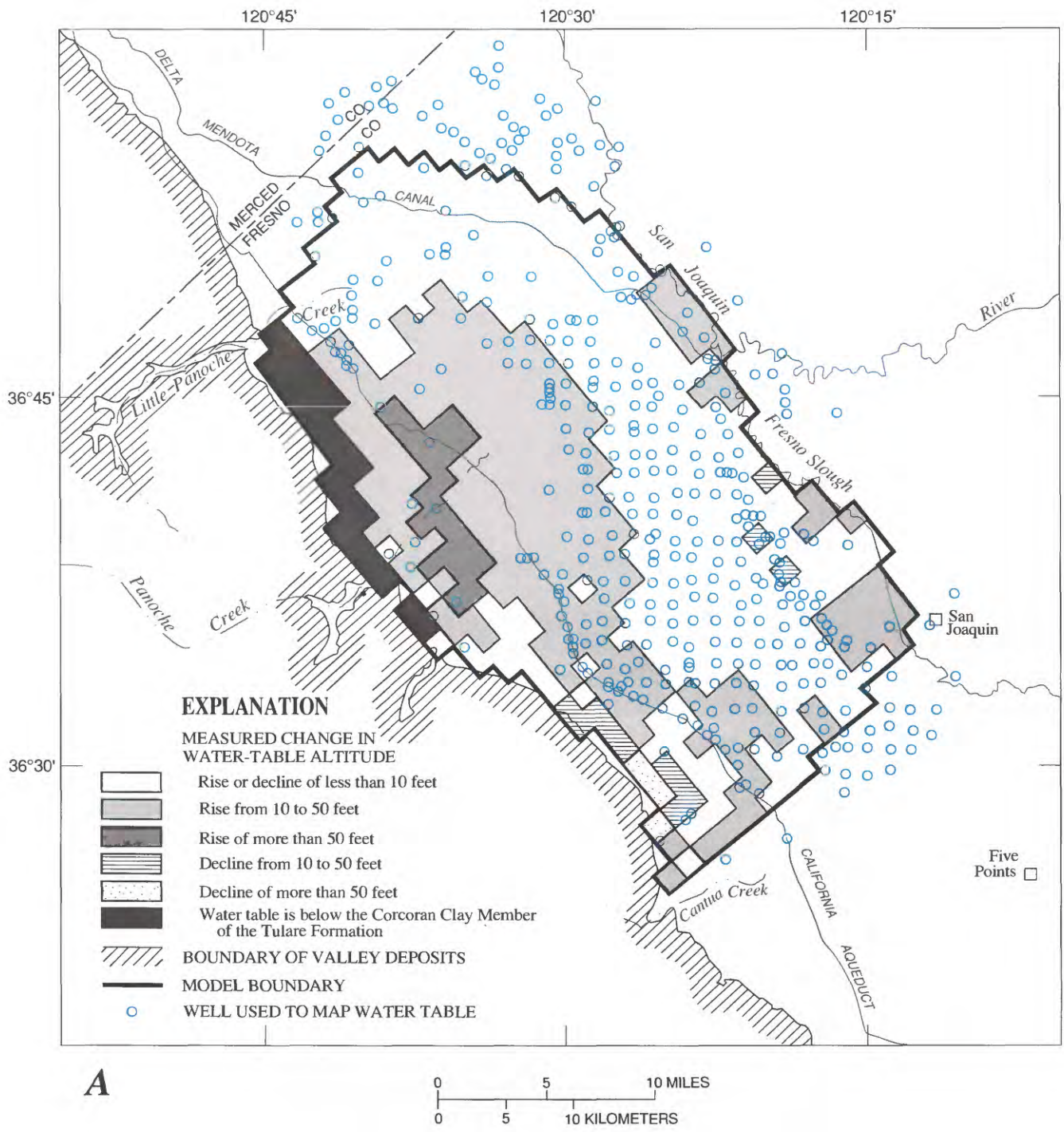


Figure 13. Change in water-table altitude, 1972–84. A, Measured. B, Simulated.

change was more than 50 ft. The relatively small change in water-table altitude in the distal and inter-fan areas is due to a water table that typically is within 10 ft of the land surface in these areas. Where the water table is shallow, evapotranspiration and drains tend to suppress additional water-table rise.

Comparison of figures 13A and 13B qualitatively demonstrates the ability of the model to reproduce the change in water-table altitude that occurred from 1972 to 1984.

The degree to which the transient model reproduces changes in water-table altitude can be assessed

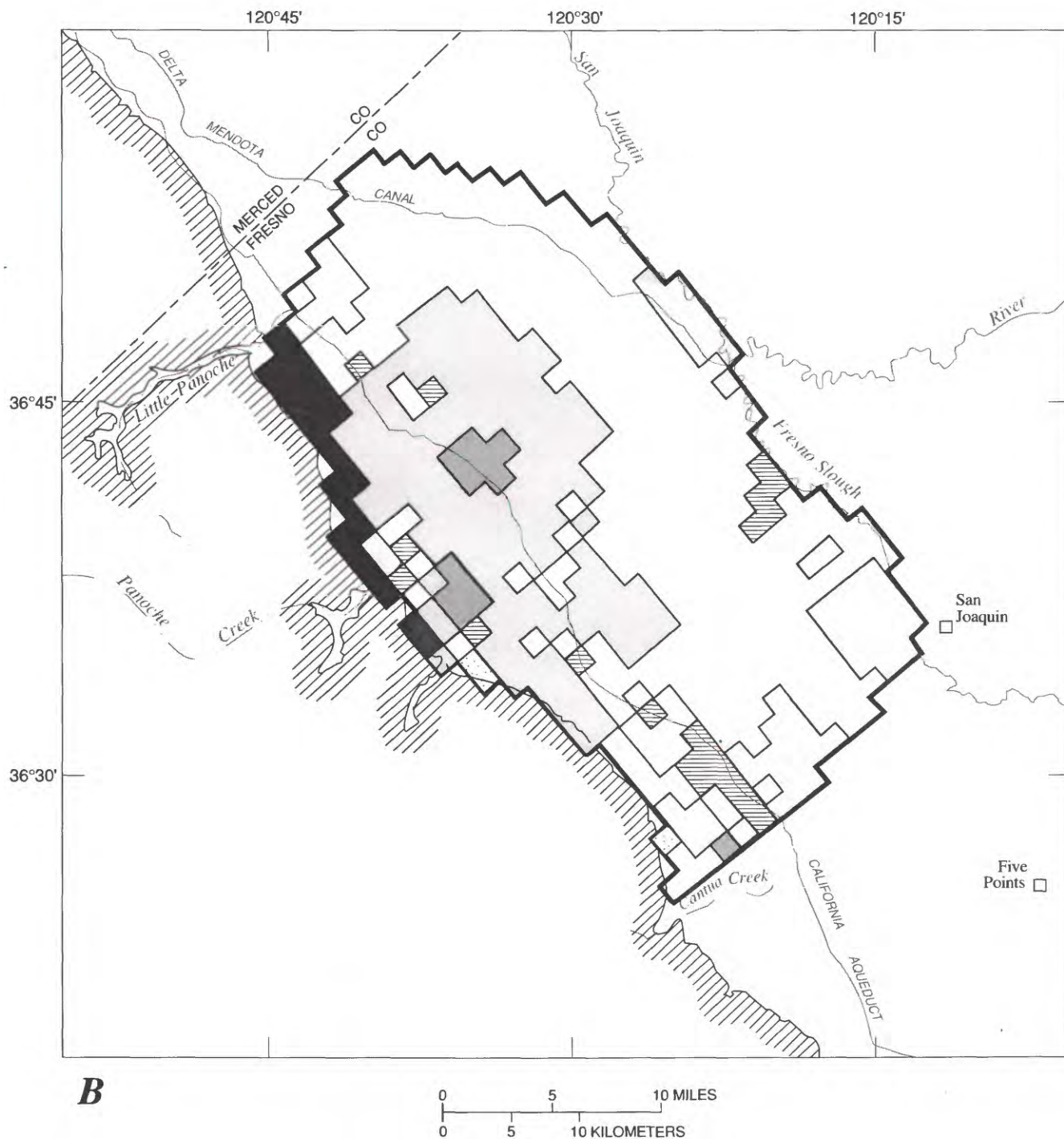


Figure 13. Continued.

Table 8. Mean and standard deviation of water-level changes, 1972 to 1984
 [Mendota Wildlife Refuge (22 model cells) not included in analysis. ft, foot]

Subarea (fig. 8)	Number of water- table cells	Measured		Simulated		Difference (measured minus simulated)	
		Mean (ft)	Standard deviation (ft)	Mean (ft)	Standard deviation (ft)	Mean (ft)	Standard deviation (ft)
Firebaugh	73	3.7	9.0	3.6	8.3	0.1	4.1
Tranquillity	30	9.2	9.8	21.3	13.3	-12.1	8.4
Panoche	48	6.8	13.4	10.7	11.1	-3.9	10.2
Broadview	16	4.2	5.8	4.4	7.2	-.2	2.4
San Luis	17	28.0	20.2	12.1	14.6	15.9	17.8
Westlands Water District							
Depth to water table							
Less than or equal to 20 ft, drained	69	2.2	5.4	.5	4.2	1.7	3.6
Less than or equal to 20 ft, undrained	70	7.8	8.9	5.5	7.4	2.3	9.3
Greater than or equal to 20 ft . . .	185	20.9	26.4	21.1	23.1	-.2	24.9
Model	530	11.5	19.3	11.1	17.7	.4	16.7
Change in confined zone							
head, 1972-84	530	119.7	58.2	101.2	52.4	18.6	25.0

by examining relevant summary statistics (table 8). For the model as a whole, the mean change in estimated water-table altitude was 11.5 ft; the mean simulated change was 11.1 ft. A cell-by-cell comparison of water-level change indicates a mean error of 0.4 ft with a standard deviation of 16.7 ft. These statistics indicate that the model is accurate at the regional scale but not at the cell-by-cell scale. The inaccuracy of the model at the cell-by-cell scale (standard deviation of 16.7 ft) is the same order of magnitude as the deviations of the estimated cell-by-cell changes from the mean change (standard deviation of 19.3 ft).

The ability of the transient model to reproduce water-level changes varies from subarea to subarea. The model generally does well in the Firebaugh, Broadview, and Westlands subareas, but does not do as well in the Panoche, San Luis, and Tranquillity subareas. In the Panoche subarea, considerable recycling of water in this subarea made it difficult to accurately estimate recharge and pumpage for the water budget (Gronberg and Belitz, 1992). In the San Luis subarea, altitudes of the water table, the confined zone heads, and the Corcoran Clay Member are sparse and poorly constrained. In the Tranquillity subarea, errors may originate in estimated water-

table altitudes rather than the simulation as many wells are perforated in Sierran sand and may not accurately reflect water-table altitudes in the overlying flood-basin deposits. Generally, the model is better able to reproduce changes in water-table altitude for large areas than for small areas.

The transient model was able to reproduce the large variation (10, 20, 50, 100, 200, and 400 ft) in depth to the water table for October 1984 (fig. 14). The eastern part of the study area is underlain by a water table within 20 ft of land surface, and the western part is underlain by a water table more than 50 ft below land surface. The ability of the transient model to reproduce the depth to the water table for 1984 is a result of the model's ability to reproduce the change in water-table altitude from 1972 to 1984 (fig. 13).

Generally, the water table is shallowest in July during the irrigation season and deepest in October after the harvest. The 122 filled circles in figure 15 indicate areas where the water table is within 7 ft of land surface in both July and October; these areas can be interpreted as areas with year-round bare-soil evaporation. The 76 open circles indicate areas where the water table is within 7 ft of land surface in

July only; these areas can be interpreted as having seasonal bare-soil evaporation. The 10 open squares indicate areas where the water table is within 7 ft of land surface in October only. These cells reflect water levels of wells that were measured in October but not in July. The water table may be within 7 ft of land surface in July at these locations.

A perfectly calibrated model should, at minimum, reproduce areas with year-round bare-soil evaporation and should not indicate bare-soil evaporation where it does not occur. The ability of the transient model to reproduce areas with seasonal bare-soil evaporation can be considered neutral (fig. 16). If the model reproduced only those areas with

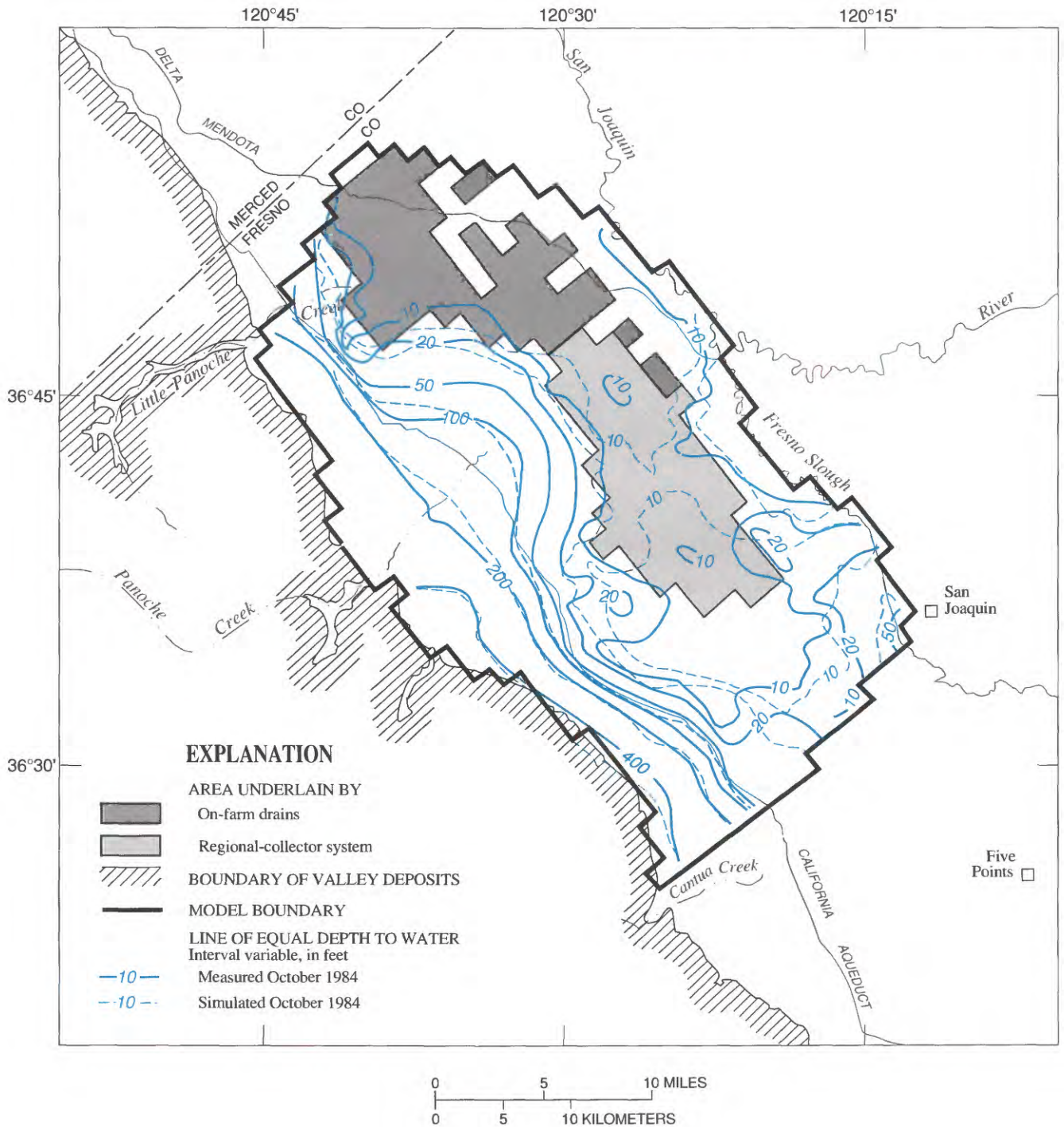


Figure 14. Measured and simulated depth to water, October 1984.

year-round bare-soil evaporation, then one could interpret the model as representative of fallow conditions. If the model also reproduced those areas with seasonal bare-soil evaporation, then one could interpret the model as representative of cropped conditions. The model reproduces 95 of the 122 cells estimated to be subject to bare-soil evaporation year

round (78 percent), 31 of the 86 cells estimated to be subject to bare-soil evaporation seasonally (36 percent), and predicts 36 cells subject to bare-soil evaporation that were not subject to bare-soil evaporation.

Accuracy of the model can be evaluated by comparing the locations of measured and simulated bare-soil evaporation. Overall, 78 percent of the sim-

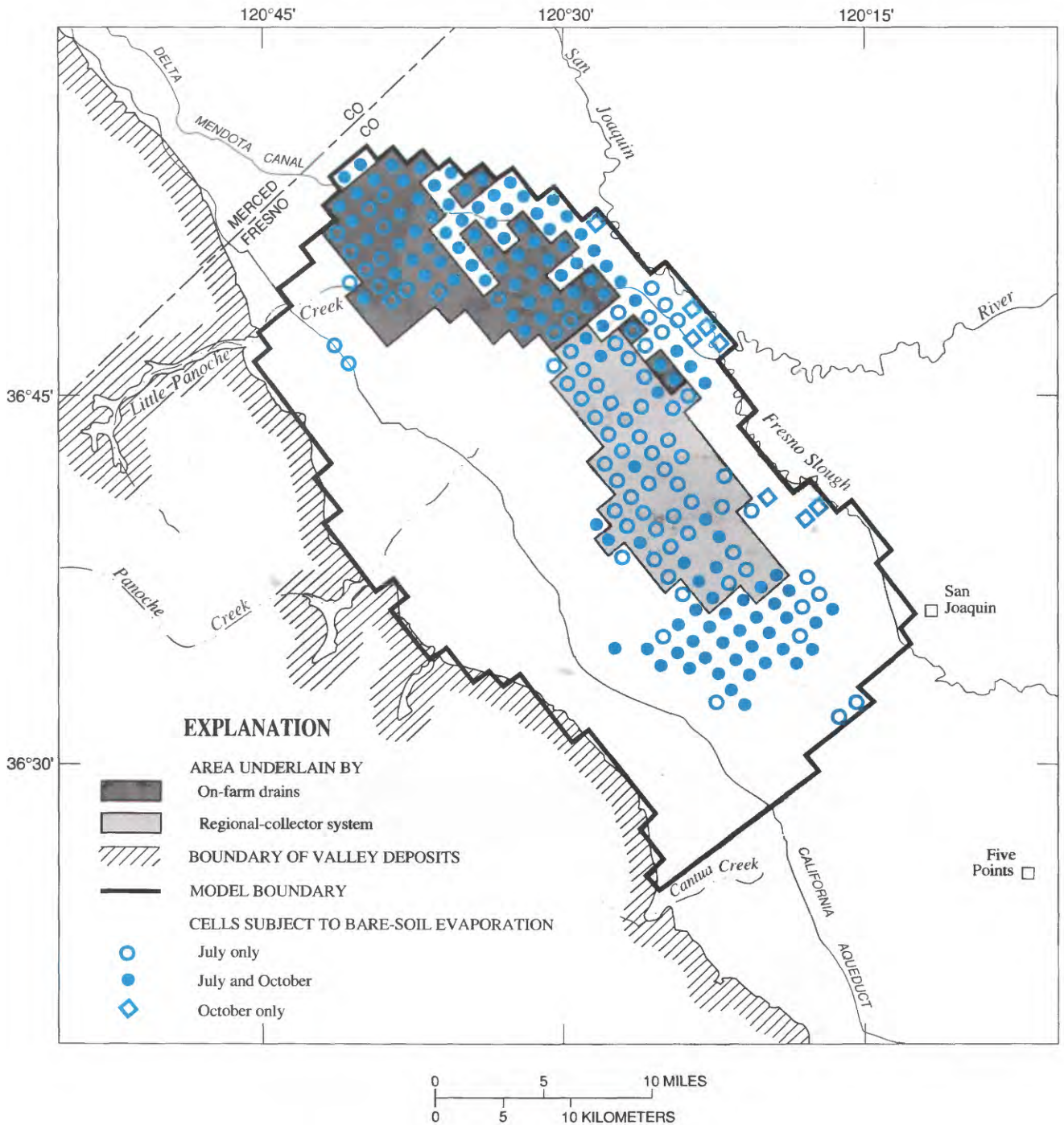


Figure 15. Measured areas subject to bare-soil evaporation, 1984.

ulated areas of bare-soil evaporation occur in areas where evaporation is estimated as occurring (in July or October, or both). Conversely, only 61 percent of the areas with bare-soil evaporation are predicted by the model as subject to evaporation.

A time-series record (1972–88) of the number of model cells subject to bare-soil evaporation was

drawn to compare measured and simulated conditions (fig. 17). Data for cells that were subject to bare-soil evaporation were generated from measured areas and used for comparison with simulation results and are shown at the back of the report. The measured values of bare-soil evaporation are a synthesis of more than 6,000 data points. Bare-soil evaporation is sensitive

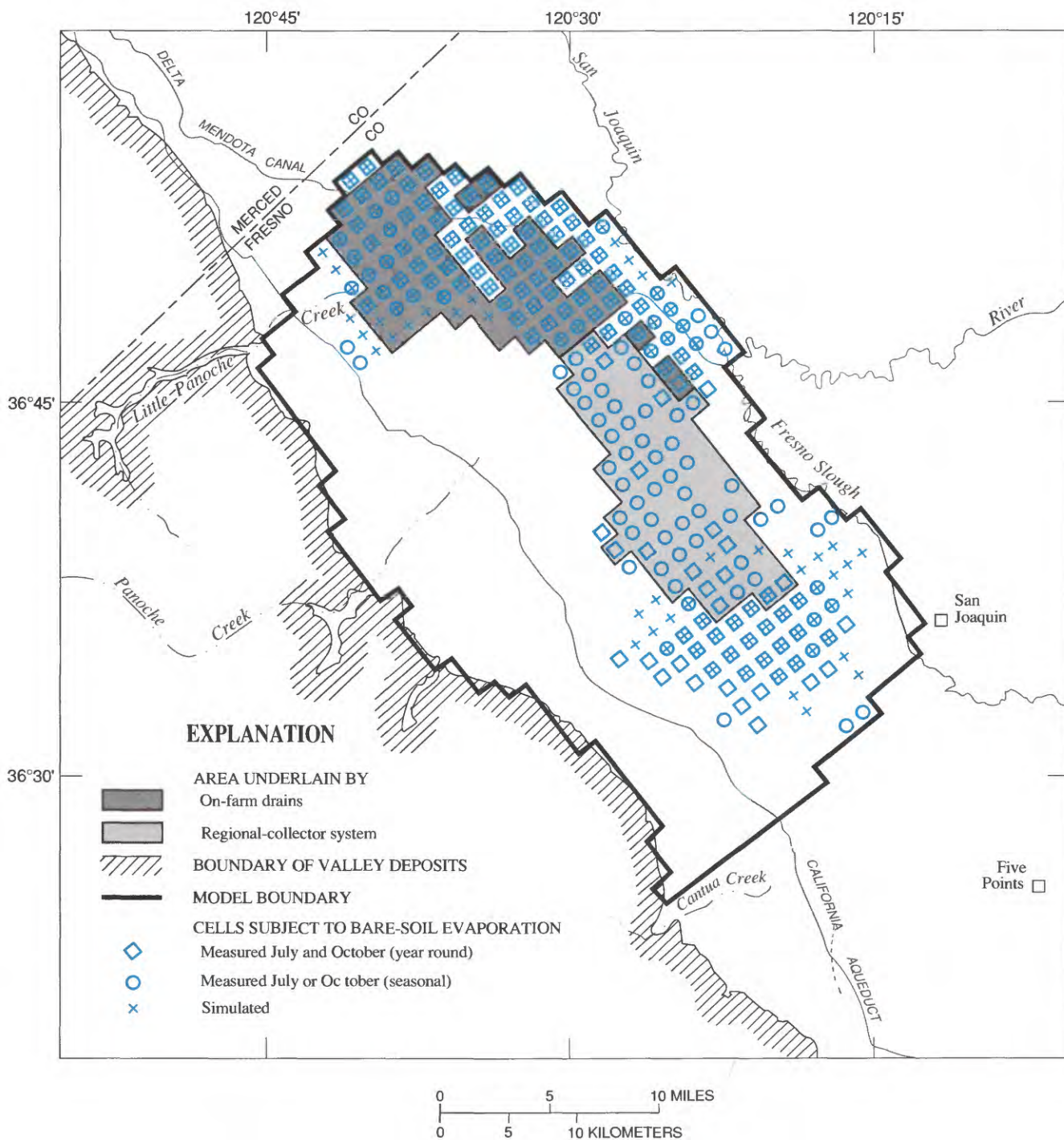


Figure 16. Measured and simulated areas subject to bare-soil evaporation, 1984.

to extinction depth: if the extinction depth is 6.5 ft (rather than 7.0 ft), bare-soil evaporation decreases by 10 to 20 model cells for July and by as many as 25 model cells for October. A change in extinction depth to 7.5 ft similarly increases bare-soil evaporation. The simulated values of bare-soil evaporation are most consistent with the measured values from 1972 to 1985 and are least consistent with the measured values from 1986 to 1988. On the whole, the simulated values are within the bounds of the measured values during the period of simulation.

A map of the measured change of head in the confined zone from 1972 to 1984 (fig. 18A) documents an increase in head of more than 100 ft for more than half the study area and as much as 275 ft locally. This substantial rise in water levels is due to the decrease in ground-water pumpage that began in 1967. For most of the study area, the simulated changes over the same period (fig. 18B) are within 25 ft of the measured changes, but differ by as much as 50 ft in the southwestern part of the study area. On average (table 8), the model reproduces the change in confined zone head within 19 ft of the measured change. The overall agreement between the measured and simulated changes indicates that an assumption of spatially constant transmissivity in the confined zone is reasonable.

Time-series hydrographs were used to compare measured and simulated water-table altitudes and confined zone head. Figure 19 shows hydrographs for four model cells with a relatively shallow water table (depth to the water table less than 20 ft), and figure 20 shows hydrographs for four cells with a relatively deep water table (depth to the water table more than 50 ft). These cells were selected because they contain wells that represent a range of conditions in the study area, and are not intended to illustrate the best or worst

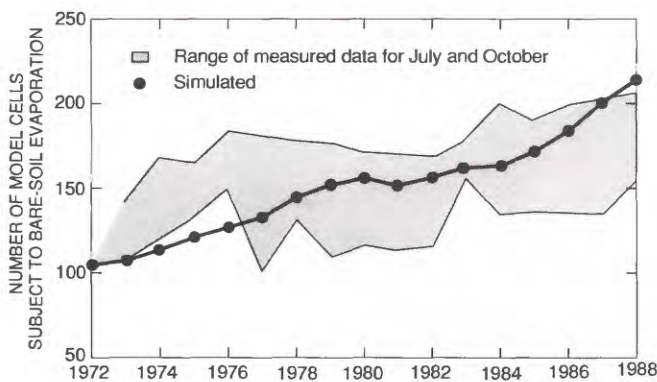


Figure 17. Measured and simulated number of model cells subject to bare-soil evaporation, 1972–88.

matches between simulated and measured conditions. The model reproduces changes in the water table and the confined zone heads fairly well. The time-series hydrographs indicate that the model is better able to reproduce the long-term changes in the ground-water flow system (for example, 1972 to 1984) as compared to the short-term changes (for example, 1980 to 1984). This aspect of the model, especially pronounced for the confined zone heads, is partly due to the specification of constant values of recharge and pumping on the basis of the 1980 water budget rather than values computed on an annual basis.

WATER BUDGET

A representative water budget is shown in figure 21 for the study area for 1981 to 1984, a period when the regional-collector drainage system within the Westlands Water District was operational. Of the 10 water-budget components demarcated in the figure, 3 were specified as input to the model: recharge to the water table (deep percolation), ground-water pumpage from the semiconfined zone (shallow wells), and ground-water pumpage from the confined zone (deep wells). Recharge to the water table (260,000 acre-ft/yr) is significantly less than the total quantity of irrigation water applied (830,000 acre-ft/yr).

The other seven components were calculated by the model: evapotranspiration of water from the shallow water table, drainflow, outflow to the east from the semiconfined zone across the valley trough, inflow from the east to the confined zone across the valley trough, leakage from the semiconfined zone to the confined zone, input to storage (ΔS) in the semiconfined zone, and input to storage (ΔS) in the confined zone.

One of the water-budget components calculated by the model—drainflow—can be compared to measured values. In the area underlain by the regional-collector system (42,000 acres represented by 69 model cells), average drainflow volume from 1981 to 1984 was 6,900 acre-ft; the average simulated value was 4,800 acre-ft, or 70 percent of the measured volume. In the area underlain by on-farm drains, average drainflow volume per unit area at the three field sites investigated by Lord (1988) was 0.64 ft/yr; the simulated value in 1988 was 0.58 ft/yr, or 91 percent of the measured value. The difference between measured and simulated drainflow provides some perspective on the accuracy of the model.

DISCUSSION OF MODEL ASSUMPTIONS

Our model incorporated several assumptions and simplifications. These include (1) use of a steady-state model to constrain the relation between the hydraulic conductivities of lithologic end members, (2) specification of the initial head distribution in 1972,

and (3) evaluation of model parameters using data averaged for long time periods and for large areas.

A steady-state model of the semiconfined zone was used to develop a relation between hydraulic conductivity of the fine-grained sediment in the semiconfined zone (K_f) and hydraulic conductivity of the Corcoran Clay Member (K_{corc}). That relation

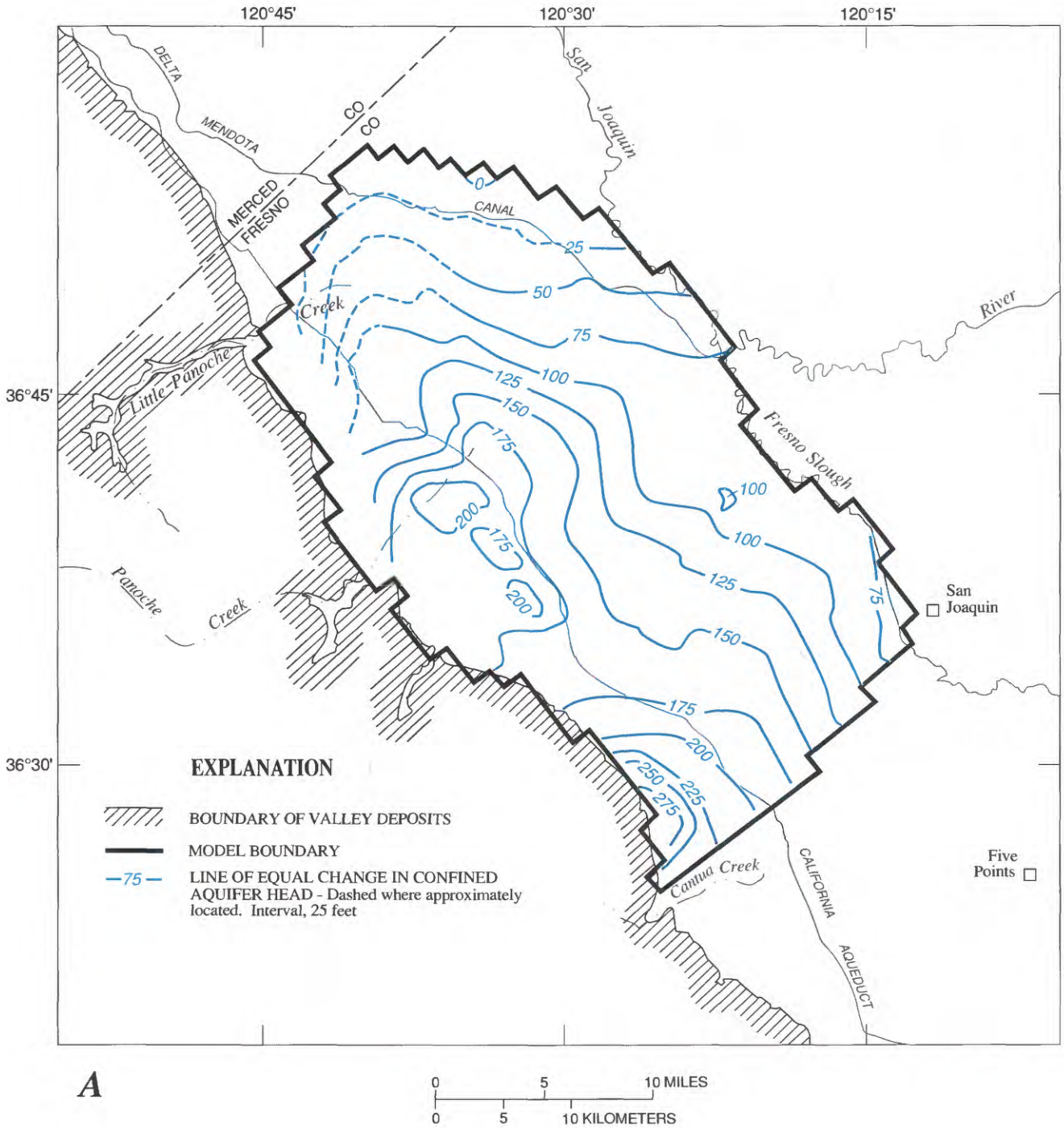


Figure 18. Change of head in confined zone, 1972–84. A, Measured. B, Simulated.

then was used in the calibration of the transient model. Two important questions arise: (1) what is the sensitivity of the coupling between K_f and K_{CORC} and (2) is it appropriate to use the relation derived by steady-state modeling in a transient model?

The relation between K_f and K_{CORC} was derived by optimizing the steady-state model as a function of two

dimensionless parameters ($K' = K_{\text{C-cr}}/K_f$ and $K'' = K_{\text{C-cr}}/K_{\text{CORC}}$, where $K_{\text{C-cr}}$ and $K_{\text{C-s}}$ are the hydraulic conductivities of coarse-grained sediment derived from the Coast Ranges and Sierra Nevada, respectively). Implicit in the optimization was an assumption that the ratio of $K_{\text{C-s}}/K_{\text{C-cr}}$ is 3.2. The sensitivity of the relation between K_f and K_{CORC} (K' and K'' when expressed as

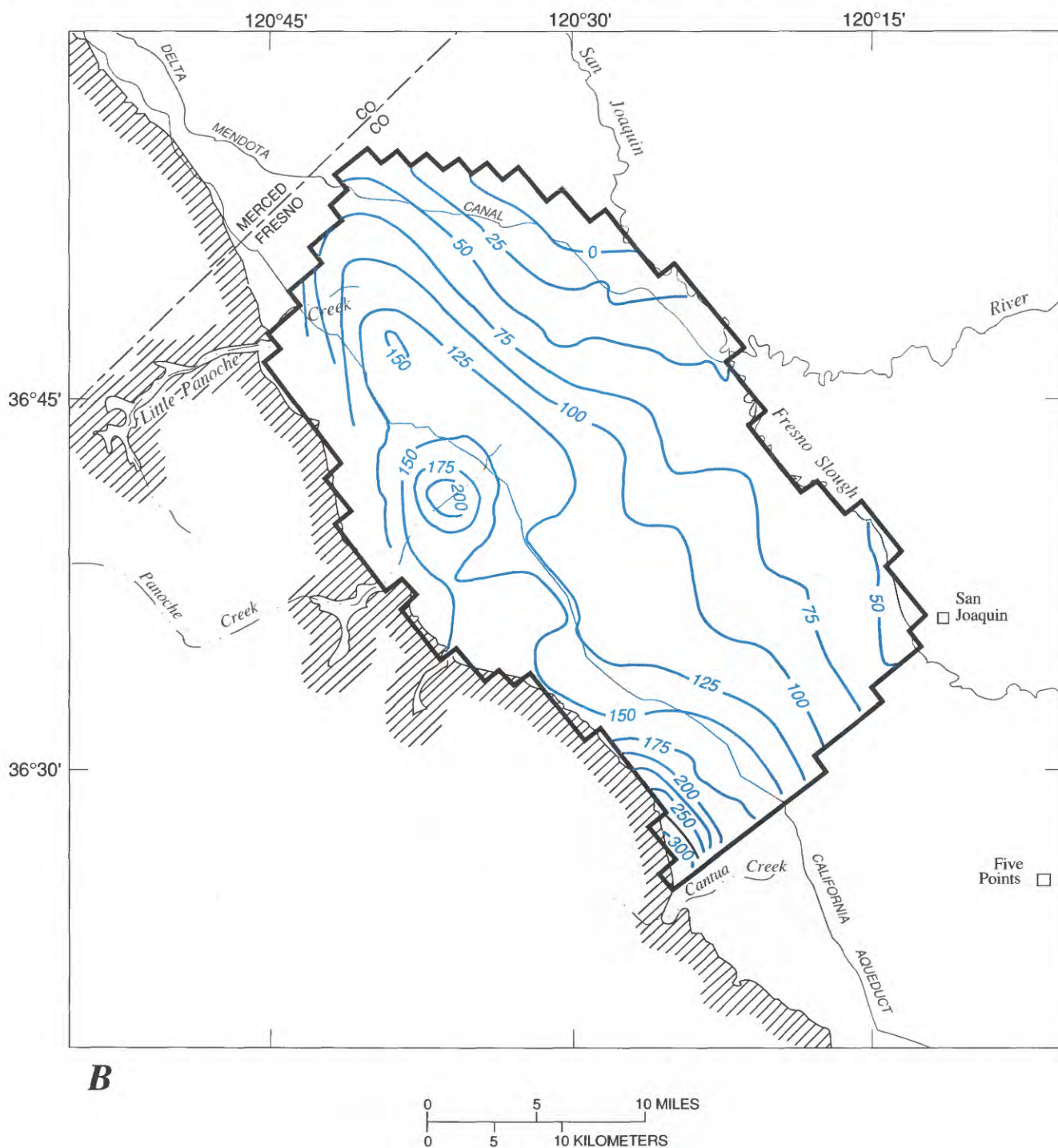
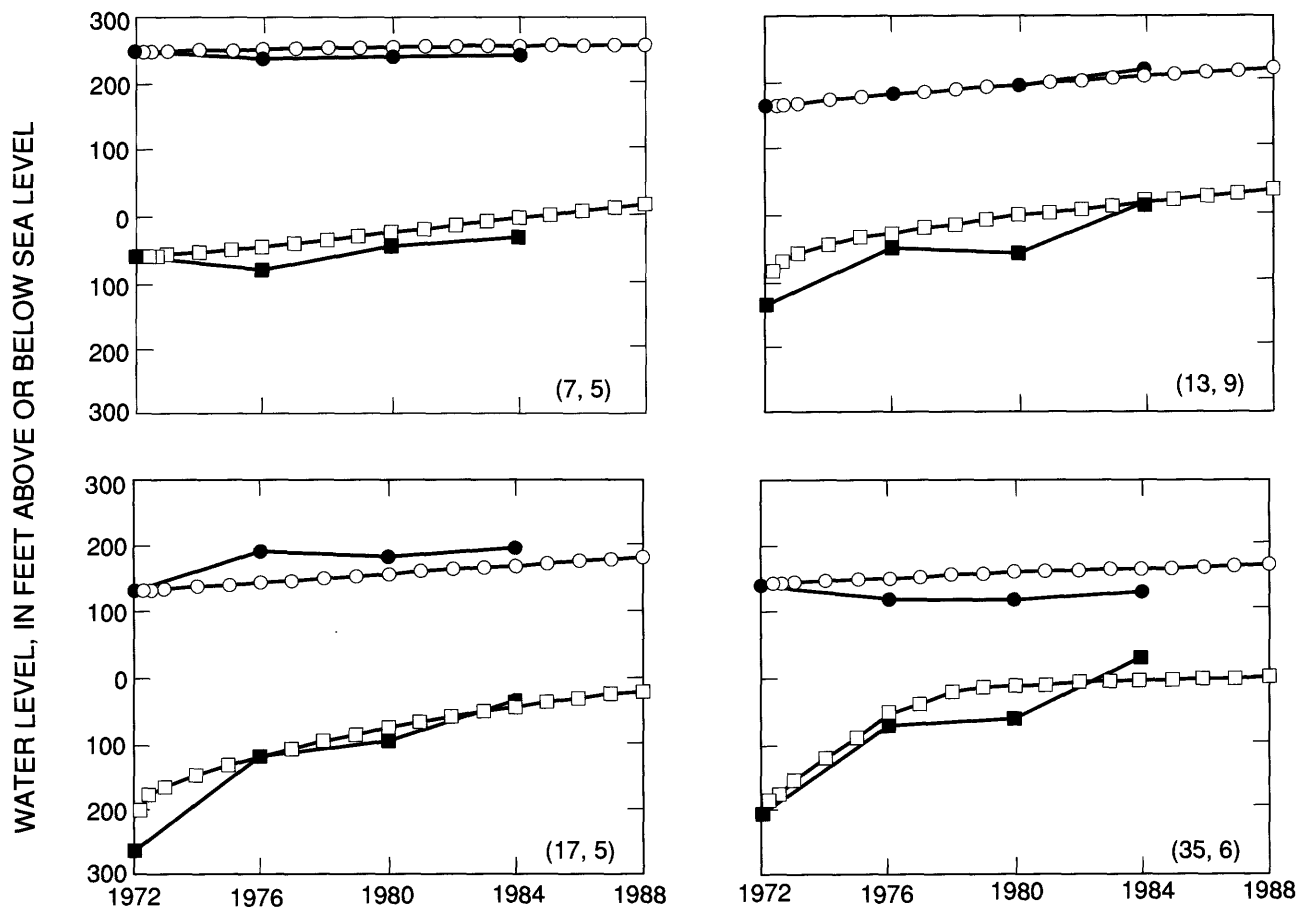


Figure 18. Continued.

dimensionless parameters) was evaluated by repeating the steady-state modeling for two additional values of K_{c-s}/K_{c-cr} (1.0 and 10.0). Figure 22 shows that the axes of minimum *RMSE* for the three ratios of K_{c-s}/K_{c-cr} are coincident where $\log K''$ is less than 5.0 and divergent where $\log K''$ is 5.0 or greater. Because $\log K''$ was 4.78 in the calibrated transient model, one can conclude that the coupling between K_f and K_{corc} (K' and K'' when expressed as dimensionless parameters) was not affected by the ratio of K_{c-s}/K_{c-cr} .

The applicability of using a relation derived from the steady-state model in the transient model

can be partly addressed by using the steady-state model to obtain an estimate of K_{corc} and then by comparing that estimate to the value obtained by calibrating the transient model. Toward that end, the steady-state model was used to map the flux across the Corcoran Clay Member as a function of K_c and K_{corc} (fig. 23); for each run of the steady-state model, K_f was selected to minimize *RMSE*. Figure 23 indicates that the flux across the Corcoran Clay Member is sensitive to K_{corc} and relatively insensitive to K_c . Thus, figure 23 can be used to obtain an estimate of K_{corc} if one can independently estimate



EXPLANATION

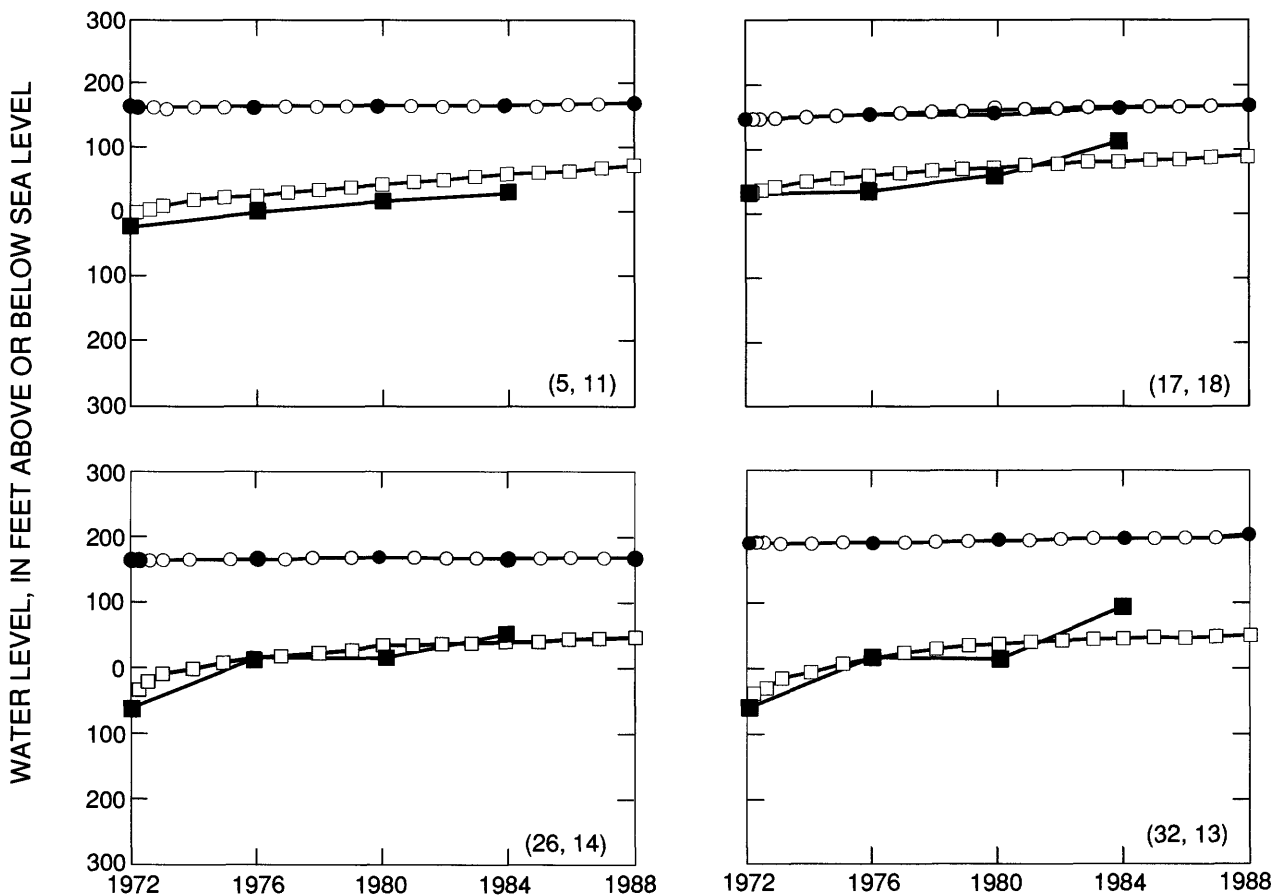
- MEASURED WATER TABLE
- MEASURED HEAD IN CONFINED ZONE
- SIMULATED WATER TABLE
- SIMULATED HEAD IN CONFINED ZONE

Figure 19. Measured and simulated altitude of water table and head in confined zone for selected model cells in areas where water table is within 20 feet of land surface, 1972–88. Numbers in parentheses represent row and columns of model cell.

the flux across the Corcoran Clay Member. Because the steady-state model implicitly incorporated pumping, the estimated flux across the Corcoran Clay Member must account for all ground water removed from the deep parts of the ground-water flow system—this would include ground-water pumpage from the semiconfined and confined zones. Ideally, independently estimated flux across the Corcoran Clay Member also would include the change in storage in the confined zone and would account for the influx to the confined zone from surrounding areas. Gronberg and Belitz (1992) estimated ground-water pumpage per unit area at 0.26 ft/yr in 1984 (the year

for which the steady-state model was developed). The value of K_{corc} that allows that flux across the lower boundary of the model is about 5.0×10^{-9} ft/s, which, considering the assumptions incorporated into the steady-state calibration, is reasonably consistent with the value determined from the transient calibration (6.0×10^{-9} ft/s).

Accurate solution of an initial value problem requires accurate specification of initial conditions. The water-table altitude and the distribution of hydraulic head in the confined zone for 1972 were evaluated using extensive well data and previously prepared maps. The initial head distribution below the water



EXPLANATION

- MEASURED WATER TABLE
- SIMULATED WATER TABLE
- MEASURED HEAD IN CONFINED ZONE
- SIMULATED HEAD IN CONFINED ZONE

Figure 20. Measured and simulated altitude of water table and head in confined zone for selected model cells in areas where water table is more than 50 feet below land surface, 1972–88. Numbers in parentheses represent row and columns of model cell.

table and above the Corcoran Clay Member, however, is not as well known. The initial head distribution in the semiconfined zone below the water table was

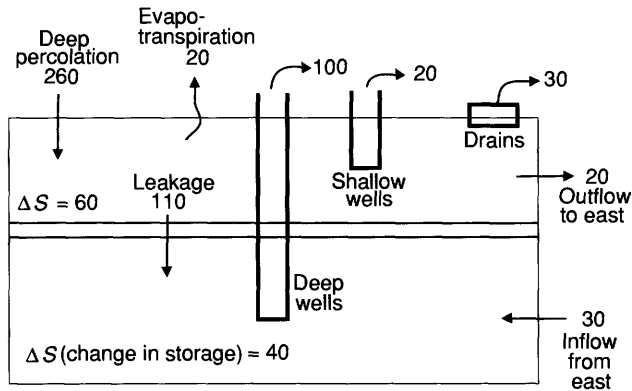


Figure 21. Water budget for study area, 1981–84 (values are in thousands of acre-feet, rounded to the nearest 10,000).

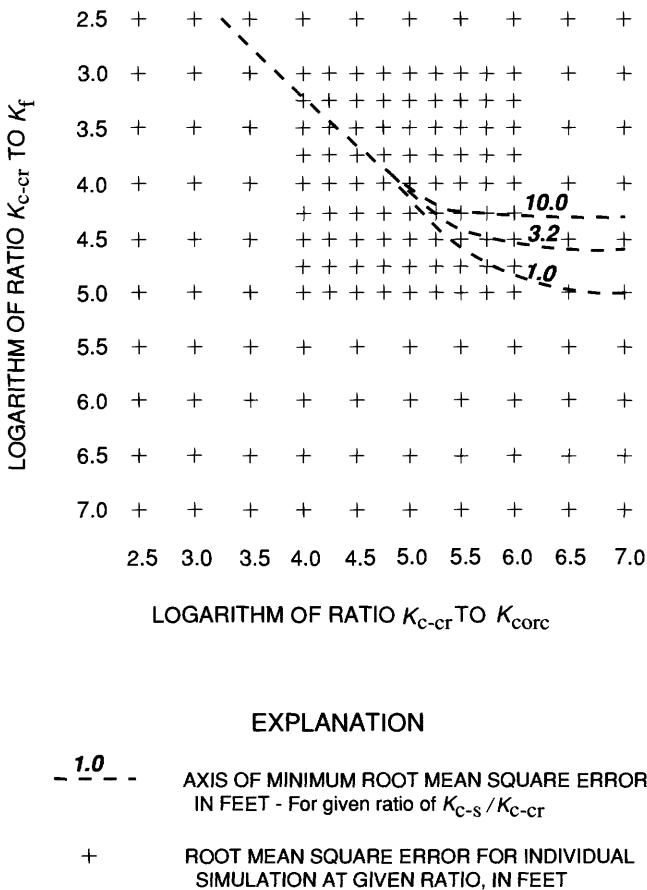


Figure 22. Axes of minimum root mean square error for different values of ratio of hydraulic conductivities of coarse-grained material derived from Sierra Nevada (K_{C-S}) to that from Coast Ranges (K_{C-CR}). K_f is hydraulic conductivity of fine-grained material and K_{C-CR} is hydraulic conductivity of the Corcoran Clay Member of the Tulare Formation of Pleistocene age. Logarithms are base 10.

specified as equal to the altitude of the overlying water table. Although this hydrostatic initial condition is incorrect, we can show that the model is not significantly affected by the error.

Let us examine hydrographs for model cells located where the thickness of the semiconfined zone is large and the misspecification of a hydrostatic initial condition would be expected to be most significant (fig. 24). In these hydrographs, the altitude of the water table and confined zone heads increased throughout the period of simulation, but heads at depth in the semiconfined zone decreased in the first 0.2 year and then increased. The increases in water-table altitude and confined zone head are consistent with measured change (figs. 13, 18, 19, and 20). The initial decrease in head at depth in the semiconfined zone is due to misspecification of the initial condition; however, the briefness of this decrease indicates that the assumed initial condition in the semiconfined zone is not critical to model performance in later years. Transient decreases in head in the semiconfined zone

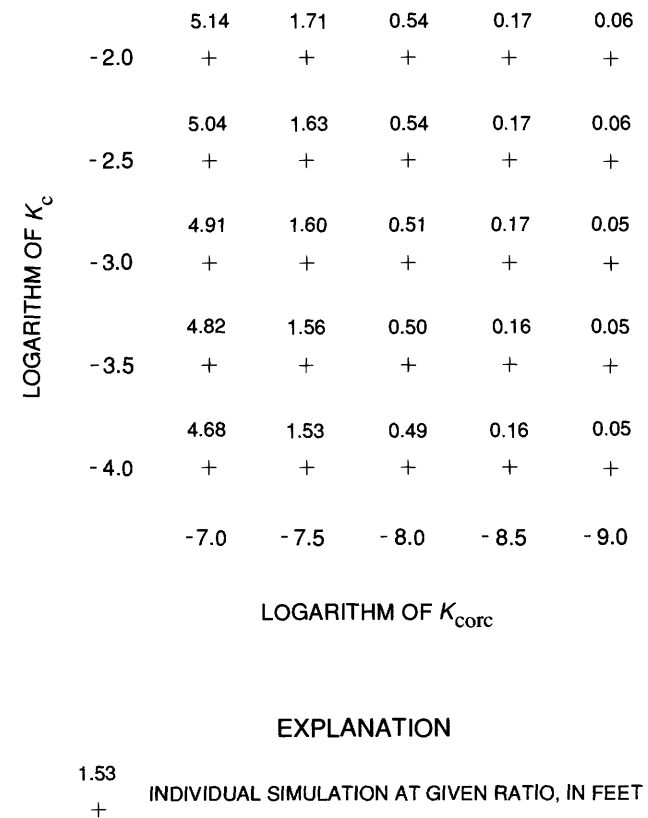


Figure 23. Flux across the Corcoran Clay Member in 1984 mapped as a function of hydraulic conductivity of coarse-grained material (K_c) and that of the Corcoran Clay Member of the Tulare Formation of Pleistocene age (K_{C-CR}). Logarithms are base 10.

have little effect on the overlying water table and underlying confined zone because the volume of water represented by the initial decrease in heads is small relative to other fluxes in the ground-water flow system (for example, recharge and pumping). In general, the confined zone heads at depth in the semiconfined zone can be interpreted as being in dynamic equilibrium with the overlying water table and underlying confined zone.

The transient model was developed using data sets averaged for relatively long time periods and for relatively large areas. For example, two of the calibration variables, specific yield (S_y) and confined

zone (T_{confined}) transmissivity, were evaluated using changes in water levels for a 12-year period; the third calibration variable, hydraulic conductivity of the Corcoran Clay Member (K_{corc}), was evaluated using a 16-year period for the total area subject to bare-soil evaporation. In addition, many of the data sets input to the model as known were averaged for relatively long time periods and for relatively large areas. For example, rates of recharge and pumping were evaluated on an annual basis (1980 was selected as representative) for subareas ranging in size from 16 to 155 mi^2 and were assumed to be temporally constant during the period of simulation. If the model was calibrated using seasonal or monthly data or if the water-budget subareas were subdivided, it might be necessary to recalibrate the model. In addition, refinement (spatial or temporal) of any of the other model parameters (for example, parameters representing drains) might necessitate a recalibration of the model.

SUMMARY

A three-dimensional, finite-difference numerical model was developed to simulate the regional ground-water flow system in the central part of the western San Joaquin Valley. The modeled area is 550 mi^2 and includes the Panoche Creek alluvial fan and parts of the Little Panoche Creek and Cantua Creek alluvial fans. Areally, the model grid is 36 rows by 20 columns with each model cell 1 mi on a side. Vertically, the semiconfined zone was divided into five layers, and the confined zone beneath the Corcoran Clay Member was represented by a sixth layer. The model incorporates distributed recharge and pumping, regional-collector drains in the Westlands Water District subarea (operative from 1980 to 1985), on-farm drains in parts of the Panoche, Broadview, and Firebaugh subareas, and bare-soil evaporation from the water table. The transient model was calibrated using hydrologic data from 1972 to 1988.

An extensive data base was assembled to develop and calibrate the model. Land subsidence in the study area necessitated a remapping of land-surface altitude (land-surface altitude at 1,776 points and four land-subsidence maps were digitized). Previously published maps were used to map the thickness of Coast Ranges alluvium, Sierran sand, and the Corcoran Clay Member of the Tulare Formation of Pleisto-

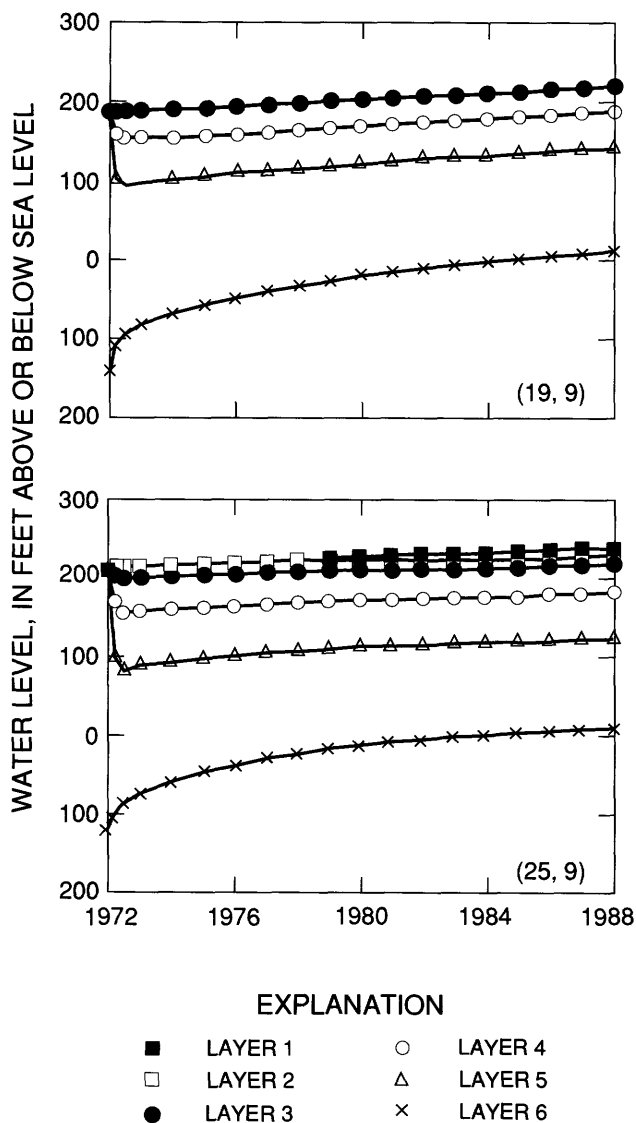


Figure 24. Simulated semiconfined and confined zone heads for selected locations where thickness of semiconfined zone is large. Numbers in parentheses represent row and columns of model cell.

cene age. Lithologic and geophysical logs from 534 wells were used to map the fraction of coarse-grained deposits in the semiconfined zone.

Specification of an initial condition and calibration of the model required delineation of water levels. The altitude of the water table and the depth to the water table in 1972, 1976, 1980, and 1984 were mapped using October water-level measurements from more than 400 wells. The depth to the water table in July and October 1973 to 1988 was mapped in areas where the water table is within 20 ft of land surface. Confined zone heads were discretized from existing contour maps for 1972, 1976, 1980, and 1984.

Recharge and pumping in the model were areally distributed but temporally constant in the transient model. The rates of recharge and pumping were based on an analysis of 1980 water budgets of nine subareas ranging in size from 16 to 155 mi². The vertical distribution of pumping (semiconfined zone compared with confined zone) was based on an analysis of the length of well perforations above and below the Corcoran Clay Member.

The model uses linear head-dependent functions to represent the subsurface drains and bare-soil evaporation. Regional-collector drains were parameterized by regression of measured monthly drainflow volume for the entire drainage system compared with average depth to the water table in the drained area. On-farm drains were parameterized by regression of measured daily drainflow volume compared with depth to the water table in three agricultural fields. Bare-soil evaporation was parameterized by a theoretical analysis of bare-soil evaporation from Panoche clay loam.

Some of the hydraulic properties of the deposits in the central part of the western San Joaquin Valley were evaluated independently of the model and others were calibration parameters. The hydraulic conductivities of coarse-grained deposits derived from the Coast Ranges and from the Sierra Nevada were evaluated from slug tests done for 25 wells drilled by the U.S. Geological Survey. Specific storage was based on previously published values. The hydraulic conductivity of fine-grained deposits in the semiconfined zone and of the Corcoran Clay Member, the transmissivity of the confined zone, and specific yield were calibration parameters. Two of the parameters (hydraulic conductivity of the fine-grained deposits and of the Corcoran Clay Member) were coupled in the first phase of model calibration, thus reducing independent parameters from four to three.

Three measures of the state of the ground-water flow system were used to calibrate the transient model: (1) the change in water-table altitude from 1972 to 1984 was used to calibrate for specific yield; (2) a time-series record (1972 to 1988) of the number of model cells susceptible to bare-soil evaporation (defined as number of model cells with a water table within 7 ft of land surface) was used to calibrate for the hydraulic conductivity of the Corcoran Clay Member; and (3) the change in confined zone head from 1972 to 1984 was used to calibrate for confined zone transmissivity. Three additional measures of the state of the ground-water flow system were used to help evaluate the fit of the model: depth to the water table in 1984, distribution of model cells susceptible to bare-soil evaporation in 1984, and time-series hydrographs (1972–88) of water-table altitude and confined zone head. Overall, the model reproduces long-term changes more accurately than short-term changes (for example, decade compared with yearly changes) and large-scale features more accurately than small-scale features.

The transient model described in this report can be used to evaluate the response of the water table to changes in management practices that affect recharge to or discharge from the ground-water flow system. Such activities include land retirement (cessation of recharge and pumping), improved irrigation efficiency and consequent reduction in recharge, installation or shutting down of drainage systems, and increased ground-water pumping. The response of the ground-water flow system can be quantified in terms of changes in one or more of the following: water-table altitude, confined zone head, number (and distribution) of model cells subject to bare-soil evaporation, and changes in the water budget, including drainflow and bare-soil evaporation. Because the model was calibrated with data that were averaged for relatively large areas (16 to 155 mi²), the model is best suited for evaluating changes that occur across relatively large areas. Because the model was calibrated on an annual basis for a 16-year period (1972–88) using a representative water budget, the model is best suited for evaluating changes for relatively long time periods (years to decades).

REFERENCES CITED

Belitz, Kenneth, and Heimes, F.J., 1990, Character and evolution of the ground-water flow system in the central

- part of the western San Joaquin Valley, California: U.S. Geological Survey Water-Supply Paper 2348, 28 p.
- Belitz, Kenneth, and Phillips, S.P., 1992, Simulation of water-table response to management alternatives, central part of the western San Joaquin Valley, California: U.S. Geological Survey Water-Resources Investigations Report 91-4193, 41 p.
- Bull, W.B., 1975, Land subsidence due to ground-water withdrawal in the Los Banos-Kettleman City area, California, Part 2: Subsidence and compaction of deposits: U.S. Geological Survey Professional Paper 437-F, 90 p.
- Bull, W.B., and Miller, R.E., 1975, Land subsidence due to ground-water withdrawal in the Los Banos-Kettleman City area, California, Part 1: Changes in the hydrologic environment conducive to subsidence: U.S. Geological Survey Professional Paper 437-E, 71 p.
- Cooper, H.H., Bredehoeft, J.D., and Papadopoulos, I.S., 1967, Response of a finite diameter well to an instantaneous charge of water: *Water Resources Research*, v. 3, no. 1, p. 263-269.
- Davis, S.N., and De Wiest, R.J.M., 1966, *Hydrogeology*: New York, Wiley, 463 p.
- Davis, G.H., and Poland, J.F., 1957, Ground-water conditions in the Mendota-Huron area, Fresno and Kings Counties, California, in *Contributions to the hydrology of the United States*: U.S. Geological Survey Water-Supply Paper 1360-G, p. 409-588.
- Deverel, S.J., Gilliom, R.J., Fujii, Roger, Izbicki, J.A., and Fields, J.C., 1984, Areal distribution of selenium and other inorganic constituents in shallow ground water of the San Luis Drain service area, San Joaquin Valley, California—A preliminary study: U.S. Geological Survey Water-Resources Investigations Report 84-4319, 67 p.
- Gilliom, R.J., and others, 1989, Preliminary assessment of sources, distribution, and mobility of selenium in the San Joaquin Valley, California: U.S. Geological Survey Water-Resources Investigations Report 88-4186, 129 p.
- Gronberg, J.M., and Belitz, Kenneth, 1992, Estimation of a water budget for the central part of the western San Joaquin Valley, California: U.S. Geological Survey Water-Resources Investigations Report 91-4192, 22 p.
- Gronberg, J.M., Belitz, Kenneth, and Phillips, S.P., 1990, Distribution of wells in the central part of the western San Joaquin Valley, California: U.S. Geological Survey Water-Resources Investigations Report 89-4158, 51 p.
- Harradine, F.F., 1950, *Soils of western Fresno County*: Berkeley, University of California Press, 86 p.
- Helm, D.C., 1978, Field verification of a one-dimensional mathematical model for transient compaction and expansion of a confined aquifer system, in *Specialty conference on verification of mathematical and physical models in hydraulic engineering*: College Park, Maryland, American Society of Civil Engineers, p. 189-196.
- Hillel, D., 1980, *Applications of soil physics*: New York, Academic Press, 385 p.
- Ireland, R.L., 1986, Land subsidence in the San Joaquin Valley, California, as of 1983: U.S. Geological Survey Water-Resources Investigations Report 85-4196, 50 p.
- Ireland, R.L., Poland, J.F., and Riley, F.S., 1984, Land subsidence in the San Joaquin Valley, California, as of 1980: U.S. Geological Survey Professional Paper 437-I, 93 p.
- Johnson, A.I., Moston, R.P., and Morris, D.A., 1968, Physical and hydrologic properties of water-bearing materials in subsiding areas in central California: U.S. Geological Survey Professional Paper 497-A, 71 p.
- Laudon, Julie, and Belitz, Kenneth, 1991, Texture and depositional history of Late Pleistocene-Holocene alluvium in the central part of the western San Joaquin Valley, California: *Bulletin of the Association of Engineering Geologists*, v. 28, no. 1, p. 73-88.
- Lord, J.M. Incorporated, 1988, Innovative techniques to reduce subsurface drainage flows: Report prepared for the San Joaquin Valley Drainage Program, Sacramento, Calif., 27 p.
- McDonald, M.G., and Harbaugh, A.W., 1988, A modular three-dimensional finite-difference ground-water flow model: U.S. Geological Survey Techniques of Water-Resources Investigations, Book 6, Chapter A1, 586 p.
- McDonald, M.G., Harbaugh, A.W., Orr, B.R., and Ackerman, D.J., [1992], A method of converting no-flow cells to variable-head cells for the U.S. Geological Survey modular finite-difference ground-water flow model: U.S. Geological Survey Open-File Report 91-536, 99 p.
- Miller, R.E., Green, J.H., and Davis, G.H., 1971, Geology of the compacting deposits in the Los Banos-Kettleman City subsidence area, California: U.S. Geological Survey Professional Paper 497-E, 46 p.
- Nielson, D.R., Biggar, J.W., and Erh, K.T., 1973, Spatial variability of field-measured soil-water properties: *Hilgardia*, v. 42, no. 7, p. 215-259.
- Ohlendorf, H.M., Hothem, R.L., Bunck, C.M., Aldrich, T.W., and Moore, J.F., 1986, Relationships between selenium concentrations and avian reproduction: North American Wildlife and Natural Resources Conference, 51st, Reno, Nev., Transactions, p. 330-442.
- Page, R.W., 1986, Geology of the fresh ground-water basin of the Central Valley, California, with texture maps and sections: U.S. Geological Survey Professional Paper 1401-C, 54 p.
- Phillips, S.P., and Belitz, Kenneth, 1991, Calibration of a texture-based model of a ground-water flow system, western San Joaquin Valley, California: *Ground Water*, v. 29, no. 5, p. 702-715.

- Poland, J.F., 1961, The coefficient of storage in a region of major subsidence caused by compaction of an aquifer system, *in* Geological Survey Research, 1961: U.S. Geological Survey Professional Paper 424-B, p. 52-54.
- Poland, J.F., Lofgren, B.E., Ireland, R.L., and Pugh, R.G., 1975, Land subsidence in the San Joaquin Valley, California, as of 1972: U.S. Geological Survey Professional Paper 437-H, 78 p.
- Presser, T.S., and Barnes, Ivan, 1985, Dissolved constituents including selenium in waters in the vicinity of Kesterson National Wildlife Refuge and the West Grassland, Fresno and Merced Counties, California: U.S. Geological Survey Water-Resources Investigations Report 85-4220, 73 p.
- Rantz, S.E., compiler, 1969, Mean annual precipitation in the California Region: U.S. Geological Survey open-file report, scale 1:1,000,000, 2 sheets. (Reprinted 1972 and 1975.)
- Riley, F.S., and McClelland, E.J., 1972, Application of the modified theory of leaky aquifers to a compressible multiple-aquifer system: U.S. Geological Survey Open-File Report, 96 p.
- Sampson, R.J., 1976, Surface II graphics system (revision 1): Kansas Geological Survey, Number One Series on Spatial Analysis, 240 p.
- San Joaquin Valley Drainage Program, 1989, Preliminary planning alternatives for solving agricultural drainage and drainage-related problems in the San Joaquin Valley: San Joaquin Valley Drainage Program, 337 p.
- Williamson, A.K., Prudic, D.E., and Swain, L.A., 1989, Ground-water flow in the Central Valley, California: U.S. Geological Survey Professional Paper 1401-D, 127 p.

APPENDIXES A–D

APPENDIX A: SPECIFIC YIELD

Specific yield (S_y) can be defined as the change in moisture content for a unit change in the altitude of the water table. Given a mathematical function describing moisture content as a function of tension and assuming equilibrium drainage, specific yield can be calculated as a function of water-table depth. If the moisture characteristic curve is described by the equation

$$\theta = A + B1n\psi, \quad (19)$$

where

θ = moisture content = volume of water per unit volume of soil (dimensionless) and
 ψ = tension (L),

then at time t_1 ,

$$\theta_T = \int_0^{L_1} (A + B1n\psi) d\psi, \quad (20)$$

where

θ_T = moisture stored in the profile from the land surface to depth L_1 (L) and
 L_1 = depth of the water table at time t_1 (L),

and at time t_2 ,

$$\theta_T = \phi(L_1 - L_2) + \int_0^{L_2} (A + B1n\psi) d\psi, \quad (21)$$

where

θ = porosity (dimensionless) and
 L_2 = depth of the water table at time t_2 (L).

The change in moisture content ($\Delta\theta_T$) therefore is

$$\Delta\theta_T = \phi(L_1 - L_2) + \int_0^{L_2} (A + B1n\psi) d\psi - \int_0^{L_1} (A + B1n\psi) d\psi. \quad (22)$$

The specific yield thus can be calculated:

$$S_y = \frac{\Delta\theta_T}{L_1 - L_2} = \phi + \frac{\int_0^{L_2} (A + B1n\psi) d\psi - \int_0^{L_1} (A + B1n\psi) d\psi}{L_1 - L_2}. \quad (23)$$

Equation 23 can be integrated:

$$S_y = \phi - A + \frac{B}{L_1 - L_2} (\psi 1n\psi - \psi) \Big|_{L_1}^{L_2}. \quad (24)$$

Equation 24 can be expanded and simplified:

$$S_y = \phi - A + B + \frac{B}{L_1 - L_2} (L_2 1nL_2 - L_1 1nL_1) \quad (25)$$

Equation 25 provides an estimate for specific yield for a change in depth to the water table from L_1 to L_2 . Equation 25 can be applied to Panoche clay loam using data from Lord (1988), who presented moisture content and tension data for a core taken from a field site in the Panoche Water District (P1-1). The porosity of the core is

$$\phi = 0.526. \quad (26)$$

Regression of moisture content against tension (in meters) indicates

$$\phi = 0.367 - 0.0471 1n\psi, \quad (27)$$

with R^2 -adj = 99.6 percent.

Substitution of 26 and 27 into 25 leads to

$$S_y = 0.11 - \frac{0.471}{L_1 - L_2} (L_2 1nL_2 - L_1 1nL_1). \quad (28)$$

Equation 28 can be used to estimate specific yield for Panoche clay loam. If depth to the water table changes from $L_1=30$ meters to $L_2=29$ meters, then $S_y=0.31$; if depth to the water table changes from $L_1=7$ m to $L_2=6$ m, then $S_y=0.25$; and if depth to the water table changes from $L_1=3$ m to $L_2=2$ m, then $S_y=0.20$.

APPENDIX B: BARE-SOIL EVAPORATION

Evaporation from bare soil can be evaluated as a function of the depth to the water table by solving the appropriate boundary-value problem (Hillel, 1980). The governing equation is

$$E = K(\psi) (d\psi/dz - 1). \quad (29)$$

Boundary conditions are

$$\psi = 0 \quad \text{at } z = -L, \quad (30a)$$

$$\psi = \psi_{\max} \quad \text{at } z = 0, \quad (30b)$$

where

E = evaporation rate (L/t),

ψ = soil-moisture tension (L),

$K(\psi)$ = hydraulic conductivity, a function of tension (L/t),

z = vertical distance, positive upward (L), and

L = water-table depth (L).

If $K(\psi) = ae^{-b\psi}$, equation 29 can be solved by separation of variables:

$$E = a(1 - e^{bL - b\psi_{\max}})/(e^{bL} - 1). \quad (31)$$

If $\psi_{\max} \rightarrow \infty$ then $e^{bL - b\psi_{\max}} \rightarrow 0$, and if $bL > 1$ then $e^{bL} \gg 1$ and

$$E = ae^{-bL}. \quad (32)$$

Thus, the bare-soil evaporation rate can be calculated as a function of water-table depth if one can estimate the parameters a and b .

Nielson and others (1973) compiled a large amount of data on soil moisture, soil tension, and hydraulic conductivity data for Panoche clay loam. Synthesis of data from Nielson and others (1973, their tables 2 and 4) provides an estimate of hydraulic conductivity as a function of tension: at 0.0, 0.33, 1.0, 2.0, and 3.0 ft of tension, the hydraulic conductivity was 243.0, 85.0, 30.0, 4.9, and 0.73 ft/yr, respectively. Regression of $\ln K$ compared to soil tension for the three data points at largest tension indicates

$$K = 32.0e^{-0.96\psi}, \quad (33)$$

where

K = hydraulic conductivity (ft/yr).

Application of equation 33 to Panoche clay loam indicates

$$E = 32.0e^{-0.96L}, \quad (34)$$

where

E = evaporation rate (ft/yr) and

L = depth of water table below evaporation surface (ft).

APPENDIX C: SELECTED MODEL INPUT DATA

The following data were used directly as model input or used in combination with other data presented in this report to generate model input:

Altitude of land surface, in feet above sea level;

Model layer containing interface between Coast Ranges and Sierran deposits;

Thickness of the semiconfined zone and of the Corcoran Clay Member of the Tulare Formation of Pleistocene age, in feet;

Altitude of the water table, October 1972 and 1984, in feet above sea level;

Altitude of the piezometric surface in the confined zone, 1972, 1976, and 1984, in feet above and below (-) sea level;

Texture of materials in layers 1, 2, 3, 4, and 5 is in percentage of coarse-grained materials;

Texture of materials between midpoint of layers 1 and 2, 2 and 3, 3 and 4, and 4 and 5 is in percentage of coarse-grained materials; and

Matrix (modflow ibound array) indicating distribution of potentially active cells for layers 1 to 5 and distribution of active cells for layer 6.

These are presented below in tabular form.

Altitude of the land surface

[--, null value]

Row	Column																			
	1	2	3	4	5	6	7	8	9	10	11	12	13	14	15	16	17	18	19	20
1	--	--	--	--	--	--	--	--	--	--	150	138	--	--	--	--	--	--	--	--
2	--	--	--	--	--	--	--	--	--	174	158	149	137	--	--	--	--	--	--	--
3	--	--	--	--	--	--	--	232	203	179	166	157	149	139	--	--	--	--	--	--
4	--	--	--	--	--	309	272	239	208	183	171	161	152	146	140	--	--	--	--	--
5	--	--	413	351	301	265	235	207	189	178	171	163	155	141	142	--	--	--	--	--
6	--	--	552	437	373	307	259	224	206	191	184	179	171	164	156	149	142	--	--	--
7	--	--	564	488	406	325	260	228	214	202	193	189	179	170	164	155	146	--	--	--
8	--	--	619	520	418	330	262	238	227	217	207	197	187	181	174	164	153	145	--	--
9	--	--	568	492	407	314	270	255	244	230	217	207	197	190	182	171	156	149	--	--
10	--	--	547	449	367	310	285	274	255	239	226	215	205	196	183	172	160	149	140	--
11	--	--	536	439	358	319	300	283	261	245	234	221	212	200	186	174	160	152	146	--
12	--	618	535	427	358	331	315	289	268	252	239	226	215	203	189	175	160	152	147	--
13	--	606	512	421	366	341	325	303	282	261	245	230	218	205	193	181	168	156	146	--
14	699	601	489	402	374	351	328	309	288	268	252	237	223	210	197	184	169	158	151	144
15	634	552	461	414	382	357	338	316	296	276	254	242	225	212	200	186	171	160	148	150
16	582	489	444	416	389	365	343	321	302	276	260	242	227	215	201	187	173	159	152	153
17	497	481	449	417	388	366	344	323	302	277	256	239	228	212	199	186	173	164	155	155
18	--	534	464	423	393	364	342	318	298	278	257	242	227	212	198	186	174	164	157	158
19	698	592	500	443	400	359	330	306	291	278	256	241	227	212	197	185	174	165	157	--
20	738	615	536	477	424	371	326	297	282	266	249	235	221	207	194	181	171	163	157	--
21	741	641	564	498	439	376	326	290	274	258	241	227	215	201	189	175	165	157	154	--
22	--	667	559	496	438	382	325	282	262	248	233	220	207	195	182	173	161	155	--	--
23	--	680	566	482	422	366	320	276	252	237	229	212	200	188	177	167	155	153	--	--
24	--	--	579	480	400	351	302	263	241	228	215	202	192	181	172	162	155	153	--	--
25	--	--	--	473	375	326	286	250	225	215	206	195	183	176	166	161	154	157	--	--
26	--	--	--	485	389	318	272	237	218	203	195	188	178	173	164	157	156	155	160	--
27	--	--	--	529	434	340	272	237	220	203	192	184	174	167	161	158	157	154	158	--
28	--	--	--	533	447	368	296	260	236	212	194	183	174	167	162	160	158	156	158	162
29	--	--	--	--	498	401	325	288	253	221	199	186	176	169	164	160	159	161	159	160
30	--	--	--	--	497	406	355	313	269	235	210	194	184	174	165	162	161	164	161	161
31	--	--	--	--	494	430	377	331	284	248	223	206	195	182	169	168	164	164	163	--
32	--	--	--	--	503	455	392	338	296	260	234	218	204	192	176	172	166	166	165	--
33	--	--	--	--	496	443	397	346	297	267	246	231	212	197	181	174	170	168	166	--
34	--	--	--	511	466	413	366	329	298	275	254	238	222	203	188	175	171	169	--	--
35	--	--	--	463	425	391	357	330	305	281	262	243	226	207	192	--	--	--	--	--
36	--	--	534	450	421	394	365	336	312	290	270	--	--	--	--	--	--	--	--	--

Model layer containing interface between Coast Ranges and Sierran deposits

Row	Column																			
	1	2	3	4	5	6	7	8	9	10	11	12	13	14	15	16	17	18	19	20
1	--	--	--	--	--	5	4	--	--	--	--	--	--	--	--	--	--	--	--	--
2	--	--	--	--	--	5	5	5	--	--	--	--	--	--	--	--	--	--	--	--
3	--	--	--	--	--	5	5	4	--	--	--	--	--	--	--	--	--	--	--	--
4	--	--	--	--	--	5	5	5	4	--	--	--	--	--	--	--	--	--	--	--
5	--	--	--	--	--	5	5	4	3	--	--	--	--	--	--	--	--	--	--	--
6	--	--	--	--	--	5	5	4	3	1	--	--	--	--	--	--	--	--	--	--
7	--	--	--	--	--	5	5	5	4	2	--	--	--	--	--	--	--	--	--	--
8	--	--	--	--	--	5	5	5	4	3	1	--	--	--	--	--	--	--	--	--
9	--	--	--	--	--	5	5	5	4	3	1	--	--	--	--	--	--	--	--	--
10	--	--	--	--	--	5	5	5	4	3	1	1	--	--	--	--	--	--	--	--
11	--	--	--	--	--	5	5	5	4	3	1	1	--	--	--	--	--	--	--	--
12	--	--	--	--	--	5	5	4	3	2	1	--	--	--	--	--	--	--	--	--
13	--	--	--	--	--	5	5	4	3	2	1	--	--	--	--	--	--	--	--	--
14	--	--	--	--	--	5	5	4	4	2	1	1	--	--	--	--	--	--	--	--
15	--	--	--	--	--	5	5	5	4	2	1	1	--	--	--	--	--	--	--	--
16	--	--	--	--	--	5	5	5	4	2	1	1	--	--	--	--	--	--	--	--
17	--	--	--	--	--	5	5	5	4	2	1	1	--	--	--	--	--	--	--	--
18	--	--	--	--	--	5	5	4	4	2	1	1	--	--	--	--	--	--	--	--
19	--	--	--	--	--	5	5	4	3	2	1	--	--	--	--	--	--	--	--	--
20	--	--	--	--	--	5	5	4	3	2	1	--	--	--	--	--	--	--	--	--
21	--	--	--	--	--	5	5	4	3	2	1	--	--	--	--	--	--	--	--	--
22	--	--	--	--	--	5	5	5	4	3	2	--	--	--	--	--	--	--	--	--
23	--	--	--	--	--	5	5	5	4	4	3	1	--	--	--	--	--	--	--	--
24	--	--	--	--	--	5	5	5	5	4	3	2	1	--	--	--	--	--	--	--
25	--	--	--	--	--	5	5	5	5	4	3	2	1	--	--	--	--	--	--	--
26	--	--	--	--	--	5	5	5	5	4	3	3	2	1	1	--	--	--	--	--
27	--	--	--	--	--	5	5	5	5	4	3	2	1	1	1	--	--	--	--	--
28	--	--	--	--	--	5	5	5	5	4	3	2	1	1	1	1	--	--	--	--
29	--	--	--	--	--	5	5	5	5	4	3	2	1	1	1	1	--	--	--	--
30	--	--	--	--	--	5	5	5	5	4	3	2	1	1	1	1	--	--	--	--
31	--	--	--	--	--	5	5	5	4	3	2	1	1	1	1	--	--	--	--	--
32	--	--	--	--	--	5	5	4	3	2	1	1	1	1	--	--	--	--	--	--
33	--	--	--	--	--	5	5	4	3	2	1	1	1	1	--	--	--	--	--	--
34	--	--	--	--	--	5	5	4	3	2	1	1	--	--	--	--	--	--	--	--
35	--	--	--	--	--	5	5	5	4	--	--	--	--	--	--	--	--	--	--	--
36	--	--	--	--	--	--	--	--	--	--	--	--	--	--	--	--	--	--	--	--

Thickness of the semiconfined zone

[--, null value]

Row	Column																			
	1	2	3	4	5	6	7	8	9	10	11	12	13	14	15	16	17	18	19	20
1	--	--	--	--	--	--	--	--	--	--	359	349	--	--	--	--	--	--	--	--
2	--	--	--	--	--	--	--	--	--	364	370	354	339	--	--	--	--	--	--	--
3	--	--	--	--	--	--	--	293	349	379	373	359	349	323	--	--	--	--	--	--
4	--	--	--	--	--	219	259	303	359	399	383	370	354	334	319	--	--	--	--	--
5	--	--	--	124	149	249	279	323	389	409	399	379	370	349	329	313	--	--	--	--
6	--	--	149	199	223	279	313	349	399	419	409	399	379	370	349	329	319	--	--	--
7	--	--	199	249	299	319	339	370	403	429	424	419	403	383	364	344	334	--	--	--
8	--	--	249	299	323	344	359	379	414	439	450	439	424	409	389	364	349	334	--	--
9	--	--	274	299	349	359	373	393	439	453	459	453	444	424	409	389	370	349	--	--
10	--	--	299	323	349	373	387	424	459	463	469	469	453	439	424	403	379	370	349	--
11	--	--	299	323	349	399	439	463	473	479	483	479	473	459	439	414	383	373	349	--
12	--	299	323	349	373	424	499	499	494	494	499	499	489	469	450	419	389	373	359	--
13	--	323	349	373	424	499	589	589	539	524	519	519	504	483	450	419	389	373	361	--
14	299	323	349	399	473	549	649	649	599	559	549	539	524	499	459	419	389	379	364	349
15	323	349	399	450	524	623	699	699	649	599	574	553	530	514	469	424	393	379	364	349
16	349	399	450	499	574	649	699	713	674	610	579	563	539	519	473	429	399	383	370	349
17	349	399	473	549	649	699	723	719	674	610	610	569	530	514	473	434	399	383	373	359
18	--	424	524	599	699	723	749	739	699	669	623	574	549	509	473	450	419	393	379	370
19	399	500	599	649	723	749	773	749	719	690	659	599	574	524	479	463	429	409	393	--
20	450	599	699	749	773	799	783	759	723	699	664	623	574	530	499	469	444	424	414	--
21	623	723	773	824	850	824	779	749	723	690	599	599	559	524	499	473	450	434	419	--
22	--	799	824	850	850	824	773	723	690	679	654	599	559	524	494	473	450	434	--	--
23	--	--	824	850	850	824	759	713	684	669	649	599	559	524	499	473	450	439	--	--
24	--	--	850	850	824	773	699	684	674	664	649	589	549	524	504	479	459	450	--	--
25	--	--	--	824	749	699	674	649	649	649	623	579	543	524	504	483	473	473	--	--
26	--	--	--	799	723	674	649	629	623	623	613	574	539	524	514	499	499	499	499	--
27	--	--	--	773	723	679	633	610	599	599	579	549	539	524	514	514	519	519	514	--
28	--	--	--	799	799	749	674	633	589	574	553	543	533	524	524	533	539	549	530	509
29	--	--	--	--	799	799	773	719	649	589	569	549	539	533	533	549	552	552	549	524
30	--	--	--	--	799	799	799	759	674	599	569	549	549	543	539	549	559	549	539	524
31	--	--	--	--	799	799	799	759	664	589	559	549	553	551	549	549	563	549	549	--
32	--	--	--	--	799	799	799	739	649	584	569	563	563	563	563	563	569	559	559	--
33	--	--	--	--	799	799	773	699	649	599	584	579	579	574	579	579	579	569	553	--
34	--	--	--	699	723	723	699	623	610	649	649	599	584	579	594	594	483	569	--	--
35	--	--	--	599	623	623	599	599	594	623	659	639	594	579	594	--	--	--	--	--
36	--	--	599	599	599	599	599	599	584	610	664	--	--	--	--	--	--	--	--	--

Thickness of the Corcoran Clay Member ---- modified from Page (1986)

Row	Column																			
	1	2	3	4	5	6	7	8	9	10	11	12	13	14	15	16	17	18	19	20
1	--	--	--	--	--	--	--	--	--	--	95	95	--	--	--	--	--	--	--	--
2	--	--	--	--	--	--	--	--	--	130	97	95	95	--	--	--	--	--	--	--
3	--	--	--	--	--	--	--	100	115	140	120	99	96	95	--	--	--	--	--	--
4	--	--	--	--	--	60	80	100	115	135	145	125	100	97	95	--	--	--	--	--
5	--	--	--	38	40	60	80	90	110	120	130	130	110	100	97	90	--	--	--	--
6	--	--	40	60	75	60	58	70	90	105	105	110	110	105	99	85	84	--	--	--
7	--	--	52	70	81	82	70	55	60	65	75	85	105	100	88	79	79	0	--	--
8	--	--	55	70	80	88	84	70	59	56	55	60	80	92	82	77	77	80	--	--
9	--	--	55	70	76	86	88	86	80	70	65	70	75	85	83	77	75	80	--	--
10	--	--	58	70	76	82	92	94	90	90	90	90	89	87	84	78	75	78	82	--
11	--	--	56	65	100	115	79	78	87	90	90	90	89	87	87	80	75	74	80	--
12	--	45	55	70	90	100	110	100	75	80	80	79	79	82	87	83	75	70	68	--
13	--	50	60	80	90	90	92	105	90	75	75	75	75	75	82	86	78	65	58	--
14	50	55	80	105	100	94	80	94	100	76	73	67	70	75	78	86	80	60	58	57
15	50	60	110	110	110	100	90	80	103	80	70	60	65	69	72	80	80	58	58	57
16	50	80	120	140	130	110	100	85	85	103	75	75	60	65	60	75	75	65	59	57
17	50	90	115	120	115	100	90	90	90	80	60	70	74	65	65	65	75	65	61	57
18	--	100	120	110	100	78	75	75	82	59	58	56	62	65	69	69	69	65	60	56
19	50	80	100	102	102	80	78	80	80	60	58	58	55	60	60	63	64	62	58	--
20	40	60	80	80	80	75	70	80	85	78	57	57	55	52	52	58	60	60	57	--
21	35	40	50	55	56	55	55	65	80	60	56	56	60	60	60	58	56	56	56	--
22	--	35	45	48	45	45	55	80	85	82	60	52	53	53	53	52	52	53	--	--
23	--	35	40	45	45	45	50	58	60	85	80	57	52	53	59	56	52	50	--	--
24	--	--	45	62	62	70	75	60	60	83	80	82	60	60	76	62	54	50	--	--
25	--	--	--	62	66	82	105	75	60	70	70	80	59	55	55	70	58	50	--	--
26	--	--	--	42	52	70	100	95	55	56	55	50	50	50	50	56	55	50	40	--
27	--	--	--	20	40	55	84	65	55	58	60	60	50	50	55	59	58	50	47	--
28	--	--	--	15	20	45	85	86	60	58	65	58	45	52	68	72	59	54	50	60
29	--	--	--	--	20	40	80	85	82	59	62	60	45	54	81	80	60	55	50	55
30	--	--	--	--	20	34	50	65	70	58	62	57	45	60	82	80	55	46	45	46
31	--	--	--	--	24	30	34	52	70	60	59	62	59	66	81	80	58	38	40	--
32	--	--	--	--	10	26	34	60	70	78	59	65	70	70	70	70	60	39	36	--
33	--	--	--	--	10	30	32	60	70	62	59	61	62	62	64	70	70	50	39	--
34	--	--	--	10	30	42	30	40	60	58	61	58	56	56	56	68	82	74	--	--
35	--	--	--	22	38	40	30	30	40	64	64	58	70	60	50	--	--	--	--	--
36	--	--	15	25	30	30	25	20	30	40	61	--	--	--	--	--	--	--	--	--

Altitude of the water table, October 1972

[--, null value]

Row	Column																			
	1	2	3	4	5	6	7	8	9	10	11	12	13	14	15	16	17	18	19	20
1	--	--	--	--	--	--	--	--	--	--	146.8	135.2	--	--	--	--	--	--	--	--
2	--	--	--	--	--	--	--	--	--	172.0	156.8	145.8	133.3	--	--	--	--	--	--	--
3	--	--	--	--	--	--	--	212.0	190.4	173.4	161.7	152.3	144.5	134.2	--	--	--	--	--	--
4	--	--	--	--	--	289.0	252.0	219.0	197.5	176.3	164.8	155.4	148.0	141.9	137.0	--	--	--	--	--
5	--	--	--	--	331.0	281.0	245.0	217.1	201.0	182.0	171.9	165.7	158.9	151.0	136.5	135.2	--	--	--	--
6	--	--	--	--	353.0	287.0	241.5	217.1	197.0	182.1	175.9	172.7	166.8	161.8	152.5	143.8	135.4	--	--	--
7	--	--	--	--	386.0	305.0	255.1	221.4	203.6	190.9	181.5	177.1	172.3	168.4	161.5	152.1	142.7	--	--	--
8	--	--	--	--	398.0	310.0	252.9	223.6	207.0	199.1	188.7	183.7	180.3	178.1	169.7	160.6	149.5	141.6	--	--
9	--	--	--	--	387.0	294.0	250.0	235.0	224.0	210.0	197.0	189.5	189.5	185.0	174.9	165.0	151.8	144.8	--	--
10	--	--	--	429.0	347.0	290.0	265.0	254.0	235.0	219.0	206.0	195.0	196.2	189.9	175.0	165.9	157.7	144.9	134.6	--
11	--	--	--	419.0	338.0	299.0	280.0	263.0	241.0	225.0	214.0	201.0	198.3	194.6	180.6	169.2	156.4	149.1	138.1	--
12	--	--	--	407.0	338.0	311.0	295.0	269.0	248.0	232.0	219.0	206.0	196.4	196.6	183.3	170.6	154.6	144.2	134.1	--
13	--	--	492.0	401.0	346.0	321.0	305.0	283.0	262.0	241.0	225.0	210.0	198.0	192.9	186.6	173.8	157.1	143.0	126.0	--
14	--	--	469.0	382.0	354.0	331.0	308.0	289.0	268.0	248.0	232.0	217.0	203.0	196.3	188.2	174.1	157.1	143.2	131.0	124.0
15	--	532.0	441.0	394.0	362.0	337.0	318.0	296.0	276.0	256.0	234.0	222.0	205.0	201.6	192.0	177.1	160.5	148.5	128.0	130.0
16	--	469.0	424.0	396.0	369.0	345.0	323.0	301.0	282.0	256.0	240.0	222.0	207.0	207.2	193.9	179.0	163.7	144.9	132.0	133.0
17	--	461.0	429.0	397.0	368.0	346.0	324.0	303.0	282.0	257.0	236.0	219.0	208.0	201.2	189.6	178.7	164.8	155.2	135.0	135.0
18	--	514.0	444.0	403.0	373.0	344.0	322.0	298.0	278.0	258.0	237.0	222.0	209.2	204.9	189.4	179.1	167.9	158.7	149.0	138.0
19	--	572.0	480.0	423.0	380.0	339.0	310.0	286.0	271.0	258.0	236.0	221.0	217.3	202.2	187.6	180.3	166.0	145.6	137.0	--
20	--	595.0	516.0	457.0	404.0	351.0	306.0	277.0	262.0	246.0	229.0	217.1	211.0	198.8	183.6	175.3	160.6	143.3	137.0	--
21	721.0	621.0	544.0	478.0	419.0	356.0	306.0	270.0	254.0	238.0	221.0	213.1	207.2	194.5	178.7	166.7	151.6	139.9	137.8	--
22	--	647.0	539.0	476.0	418.0	362.0	305.0	262.0	242.0	228.0	213.0	209.2	200.3	187.7	171.5	161.7	148.7	143.1	--	--
23	--	660.0	546.0	462.0	402.0	346.0	300.0	256.0	232.0	217.0	213.3	202.9	193.9	181.0	167.3	155.3	143.8	146.5	--	--
24	--	--	559.0	460.0	380.0	331.0	282.0	243.0	221.0	208.0	201.4	195.4	185.2	175.6	163.4	152.5	147.0	148.9	--	--
25	--	--	--	453.0	355.0	306.0	266.0	230.0	205.0	195.6	193.1	185.6	176.1	169.6	160.1	154.9	146.7	146.6	--	--
26	--	--	--	465.0	369.0	298.0	252.0	218.0	202.3	187.4	181.1	175.8	170.2	167.1	157.4	148.9	145.4	137.4	140.0	--
27	--	--	--	509.0	414.0	320.0	252.0	220.0	208.6	191.3	179.9	173.0	166.3	160.9	154.0	146.0	139.9	134.0	138.0	--
28	--	--	--	513.0	427.0	348.0	276.0	240.0	227.6	206.0	188.1	175.4	167.7	160.5	157.8	151.7	140.9	136.0	138.4	142.1
29	--	--	--	--	478.0	381.0	305.0	268.0	237.7	213.8	192.6	180.5	171.3	164.3	159.7	148.9	143.0	143.7	143.7	148.3
30	--	--	--	--	477.0	386.0	335.0	293.0	249.0	222.4	202.2	188.4	179.5	167.7	156.4	143.1	141.0	144.0	141.0	141.2
31	--	--	--	--	474.0	410.0	357.0	311.0	264.0	228.0	205.2	194.0	188.8	173.7	156.1	148.0	144.0	144.0	143.0	--
32	--	--	--	--	483.0	435.0	372.0	318.0	276.0	240.0	214.0	198.8	192.9	185.3	161.4	152.0	146.0	146.0	145.0	--
33	--	--	--	--	476.0	423.0	377.0	326.0	277.0	247.0	226.0	211.0	194.2	185.5	166.2	154.0	150.0	148.0	146.0	--
34	--	--	--	--	491.0	446.0	393.0	346.0	309.0	278.0	255.0	234.0	218.0	202.0	188.8	179.9	155.0	151.0	149.0	--
35	--	--	--	--	443.0	405.0	371.0	337.0	310.0	285.0	261.0	242.0	223.0	206.0	188.4	184.3	--	--	--	--
36	--	--	514.0	430.0	401.0	374.0	345.0	316.0	292.0	270.0	250.0	--	--	--	--	--	--	--	--	--

Altitude of the water table, October 1984

Row	Column																			
	1	2	3	4	5	6	7	8	9	10	11	12	13	14	15	16	17	18	19	20
1	--	--	--	--	--	--	--	--	--	--	145.2	134.2	--	--	--	--	--	--	--	--
2	--	--	--	--	--	--	--	--	--	171.4	151.9	142.7	131.2	--	--	--	--	--	--	--
3	--	--	--	--	--	--	--	206.0	192.8	172.9	158.5	149.9	142.8	134.5	--	--	--	--	--	--
4	--	--	--	--	--	220.9	217.7	204.5	191.6	176.3	163.7	154.1	145.9	141.4	136.8	--	--	--	--	--
5	--	--	--	212.2	231.5	226.8	224.9	213.1	193.8	181.7	171.5	164.7	157.2	150.3	137.2	139.9	--	--	--	--
6	--	--	219.1	212.9	238.7	258.9	241.1	218.5	198.9	184.5	177.7	173.1	165.4	159.1	152.2	145.8	138.8	--	--	--
7	--	--	202.8	215.3	238.2	317.8	252.0	219.5	207.8	194.3	187.5	183.1	173.4	165.0	159.6	151.2	142.8	--	--	--
8	--	--	208.5	215.0	239.6	320.8	247.0	227.6	218.2	208.5	200.5	190.8	181.5	176.1	169.8	160.6	150.1	142.2	--	--
9	--	--	187.9	209.7	237.0	277.7	238.9	226.7	228.2	216.1	206.5	199.5	190.7	185.1	178.2	168.4	154.2	147.1	--	--
10	--	--	184.3	207.2	224.1	250.0	247.5	237.4	230.6	219.1	210.3	203.6	197.3	190.8	179.1	169.7	158.2	147.2	133.2	--
11	--	--	--	176.5	210.6	211.6	235.1	238.8	235.6	224.7	215.8	210.7	208.7	205.0	194.5	181.7	171.0	158.2	150.3	131.6
12	--	180.2	188.8	186.6	207.4	219.9	224.4	216.8	211.6	210.7	209.9	213.7	208.6	196.0	186.6	173.2	155.3	147.5	133.5	--
13	--	182.4	187.9	184.5	196.9	207.0	212.9	204.6	201.0	202.9	206.9	210.4	210.1	197.4	185.4	174.5	162.0	149.9	134.7	--
14	188.1	189.2	186.0	176.0	194.0	192.5	190.9	184.5	182.6	190.3	203.6	215.9	214.8	202.5	190.6	177.2	161.9	151.2	141.0	130.4
15	214.6	219.8	211.5	196.4	191.1	184.7	167.5	160.0	169.7	189.4	204.9	231.1	216.8	203.9	193.0	178.6	163.5	152.7	138.4	134.3
16	271.0	266.9	228.0	213.1	194.6	175.0	147.7	147.2	171.3	188.4	210.6	227.4	217.7	206.3	191.1	179.2	165.5	151.8	142.6	153.7
17	213.2	217.4	191.4	174.7	189.9	187.3	181.6	183.1	192.5	201.3	214.6	227.1	218.4	204.4	188.6	178.0	166.5	157.3	151.2	155.7
18	--	183.4	153.0	144.7	185.7	192.3	198.9	212.3	214.0	222.9	228.2	229.2	217.5	204.3	189.6	179.1	167.3	157.5	148.4	158.7
19	188.8	147.7	103.9	120.9	173.7	198.6	224.6	229.7	237.7	241.4	236.5	231.9	218.6	203.9	187.3	177.9	165.0	158.3	145.5	--
20	165.7	127.0	81.0	118.5	177.8	224.8	261.2	250.5	249.1	244.9	238.6	227.0	214.0	199.5	185.2	173.0	160.6	151.7	144.7	--
21	157.3	152.8	139.5	153.2	185.7	235.3	281.7	267.7	257.9	251.4	232.8	218.8	206.6	192.5	180.7	164.8	153.9	145.8	141.4	--
22	--	184.6	167.4	163.4	188.3	248.0	285.3	269.1	249.5	242.5	225.1	211.1	197.7	186.4	174.1	165.7	151.3	143.8	--	--
23	--	169.5	159.1	158.8	197.5	266.3	299.2	249.7	232.8	229.6	222.1	203.8	191.4	179.5	167.9	158.8	145.4	141.5	--	--
24	--	--	160.4	158.8	196.4	283.1	285.7	250.6	231.2	217.3	206.1	194.0	183.7	174.4	164.8	154.0	147.7	135.8	--	--
25	--	--	--	157.9	169.4	291.5	273.5	238.2	201.6	197.5	198.7	189.1	172.4	169.2	158.4	153.4	148.4	143.8	--	--
26	--	--	--	157.8	162.5	256.1	266.8	225.5	204.3	190.0	186.3	183.6	171.1	165.6	153.0	133.9	140.8	147.6	148.9	--
27	--	--	--	127.7	158.3	253.0	260.5	231.4	211.6	196.1	186.2	177.0	165.1	159.2	149.2	136.9	143.3	148.9</		

Altitude of the piezometric surface in the confined zone, 1972

[--, null value]

Row	Column																			
1	--	--	--	--	--	--	--	--	--	--	18	34	--	--	--	--	--	--	--	--
2	--	--	--	--	--	--	--	--	--	-10	3	23	44	--	--	--	--	--	--	--
3	--	--	--	--	--	--	--	-39	-39	-26	-8	12	38	60	--	--	--	--	--	--
4	--	--	--	--	--	-45	-56	-60	-50	-43	-18	2	28	54	71	--	--	--	--	--
5	--	--	-35	-47	-59	-69	-72	-64	-48	-28	-3	23	50	66	91	--	--	--	--	--
6	--	--	-45	-57	-74	-95	-117	-105	-86	-65	-38	-8	13	40	61	81	98	--	--	--
7	--	--	-60	-72	-94	-130	-135	-132	-99	-72	-44	-8	8	30	51	67	88	98	--	--
8	--	--	-75	-97	-129	-137	-139	-135	-109	-79	-49	-13	8	30	46	66	83	93	--	--
9	--	--	-120	-132	-139	-145	-143	-137	-119	-86	-58	-21	3	24	41	56	72	88	98	--
10	--	--	-145	-148	-149	-151	-147	-140	-130	-99	-66	-31	-3	13	30	51	66	78	88	--
11	--	-165	-176	-173	-167	-155	-151	-143	-136	-108	-78	-37	-10	7	24	36	46	67	78	--
12	--	-185	-186	-190	-190	-177	-157	-150	-138	-116	-88	-48	-18	7	13	30	46	56	67	--
13	-190	-191	-196	-209	-221	-199	-173	-156	-142	-121	-95	-59	-28	-9	2	16	30	46	56	67
14	-195	-201	-217	-234	-257	-235	-187	-159	-144	-125	-101	-70	-39	-21	-5	8	24	35	46	56
15	-205	-216	-227	-235	-258	-236	-186	-159	-144	-125	-105	-78	-53	-29	-15	0	14	30	36	51
16	-216	-226	-229	-231	-235	-212	-176	-155	-142	-125	-110	-84	-64	-41	-22	-7	9	25	31	41
17	--	-227	-230	-222	-209	-183	-159	-149	-136	-123	-109	-88	-70	-52	-29	-12	5	16	26	31
18	-226	-227	-230	-219	-203	-178	-155	-142	-134	-121	-108	-89	-71	-51	-29	-12	3	15	26	--
19	-226	-227	-230	-225	-211	-182	-153	-137	-124	-113	-98	-81	-62	-43	-25	-10	3	12	22	--
20	-226	-227	-229	-230	-213	-215	-154	-135	-120	-104	-91	-74	-54	-39	-24	-11	-1	8	19	--
21	--	-226	-229	-222	-205	-213	-153	-135	-121	-107	-91	-75	-57	-43	-33	-21	-8	4	--	--
22	--	-226	-222	-205	-195	-201	-148	-131	-119	-105	-95	-85	-67	-53	-42	-32	-14	2	--	--
23	--	--	-212	-195	-182	-158	-139	-126	-113	-105	-95	-87	-69	-61	-47	-32	-11	2	--	--
24	--	--	-189	-171	-154	-136	-124	-111	-101	-91	-79	-68	-57	-41	-23	-4	5	--	--	--
25	--	--	-189	-170	-154	-136	-125	-113	-99	-86	-72	-58	-45	-32	-14	-1	7	15	--	--
26	--	--	-192	-172	-158	-141	-127	-114	-97	-82	-68	-52	-42	-27	-12	0	9	17	--	--
27	--	--	-196	-175	-157	-148	-132	-116	-97	-79	-66	-52	-41	-28	-13	-2	8	18	27	--
28	--	--	--	-183	-169	-157	-140	-119	-99	-81	-70	-56	-44	-32	-17	-2	9	20	31	--
29	--	--	--	-202	-181	-166	-148	-129	-107	-89	-74	-60	-45	-30	-15	-3	12	22	35	--
30	--	--	--	-242	-194	-178	-158	-136	-111	-97	-78	-61	-44	-24	-6	5	16	27	--	--
31	--	--	--	-262	-204	-179	-164	-141	-120	-98	-77	-57	-40	-19	-1	10	21	30	--	--
32	--	--	--	-274	-205	-170	-167	-145	-124	-97	-75	-54	-37	-17	1	13	23	32	--	--
33	--	--	--	-317	-265	-205	-177	-164	-145	-120	-96	-73	-52	-35	-16	2	16	26	--	--
34	--	--	--	-319	-256	-197	-178	-162	-142	-118	-92	-70	-49	-32	-15	--	--	--	--	--
35	--	--	-352	-314	-227	-188	-177	-158	-136	-116	-90	--	--	--	--	--	--	--	--	--
36	--	--	--	--	--	--	--	--	--	--	--	--	--	--	--	--	--	--	--	--

Altitude of the piezometric surface in the confined zone, 1976

Row	Column																			
1	--	--	--	--	--	--	--	--	--	--	17	24	--	--	--	--	--	--	--	--
2	--	--	--	--	--	--	--	--	--	7	13	18	24	--	--	--	--	--	--	--
3	--	--	--	--	--	--	--	-10	-4	1	13	13	23	30	--	--	--	--	--	--
4	--	--	--	--	--	-42	-32	-22	-12	-4	3	10	18	24	31	--	--	--	--	--
5	--	--	-72	-62	-54	-43	-33	-21	-10	-2	6	14	25	31	41	--	--	--	--	--
6	--	--	-84	-82	-79	-65	-57	-41	-29	-18	-6	2	11	20	26	31	43	--	--	--
7	--	--	-90	-88	-84	-77	-58	-46	-37	-25	-11	-1	8	18	26	31	38	--	--	--
8	--	--	-96	-94	-90	-82	-66	-51	-42	-30	-18	-4	5	15	21	32	38	43	--	--
9	--	--	-101	-99	-96	-86	-71	-54	-44	-35	-22	-6	3	13	21	26	38	43	--	--
10	--	--	-105	-104	-102	-90	-74	-65	-48	-39	-25	-9	1	12	21	26	32	43	43	--
11	--	--	-108	-108	-106	-97	-83	-63	-50	-42	-29	-13	-2	8	18	26	31	38	43	--
12	--	-115	-113	-111	-108	-102	-91	-63	-51	-44	-31	-16	-4	6	16	26	31	37	43	--
13	--	-119	-116	-113	-110	-104	-89	-65	-53	-37	-25	-17	-5	6	15	25	31	36	42	--
14	-126	-123	-119	-117	-111	-101	-87	-65	-43	-36	-24	-17	-6	4	14	24	30	36	41	47
15	-137	-127	-124	-120	-114	-105	-87	-63	-36	-29	-23	-15	-6	4	13	23	29	35	41	46
16	-148	-138	-129	-125	-118	-107	-84	-58	-34	-28	-22	-13	-4	5	14	22	29	35	41	46
17	-151	-151	-142	-132	-118	-98	-78	-53	-35	-29	-21	-12	0	8	17	23	29	35	41	46
18	--	-152	-155	-142	-109	-86	-75	-58	-37	-33	-24	-11	1	11	18	23	30	36	41	46
19	-151	-152	-155	-138	-102	-85	-74	-67	-52	-41	-27	-11	1	13	23	24	30	36	41	--
20	-151	-152	-155	-131	-101	-83	-75	-65	-55	-45	-29	-12	0	12	23	29	35	35	41	--
21	-151	-152	-154	-126	-101	-82	-73	-64	-53	-41	-27	-12	1	10	23	28	34	35	41	--
22	--	-151	-154	-119	-100	-79	-70	-61	-49	-35	-21	-8	1	11	22	28	34	40	--	--
23	--	-151	-147	-120	-95	-78	-67	-54	-38	-30	-14	-5	3	11	23	28	34	40	--	--
24	--	--	-134	-111	-87	-74	-62	-47	-32	-22	-13	-4	5	12	23	29	35	40	--	--
25	--	--	--	-102	-80	-70	-59	-46	-33	-23	-13	-3	5	14	23	29	35	40	--	--
26	--	--	--	-101	-78	-68	-56	-44	-30	-21	-10	-2	5	13	20	27	34	40	46	--
27	--	--	--	-107	-81	-66	-52	-40	-27	-15	-6	0	6	13	19	27	34	42	46	--
28	--	--	--	-113	-82	-60	-45	-32	-21	-7	-2	3	7	12	19	27	34	43	51	51
29	--	--	--	--	-82	-54	-39	-26	-17	-7	-1	4	8	14	20	28	36	44	51	51
30	--	--	--	--	-85	-52	-36	-26	-16	-3	0	6	12	17	23	31	37	44	51	52
31	--	--	--	--	-87	-56	-40	-27	-17	-4	1	8	15	21	31	36	40	45	52	--
32	--	--	--	--	-92	-59	-46	-31	-19	-4	3	10	17	28	39	43	44	46	52	--
33	--	--	--	--	-99	-72	-54	-40	-22	-8	4	13	24	37	46	56	53	46	47	--
34	--	--	--	-202	-103	-75	-62	-44	-26	-7	6	13	35	44	58	68	46	--	--	--
35	--	--	--	-204	-101	-75	-65	-47	-28	-9	5	17	40	54	70	--	--	--	--	--
36	--	--	-222	-207	-97	-76	-63	-46	-29	-14	2	--	--	--	--	--	--	--	--	--

Altitude of the piezometric surface in the confined zone, 1984

[--, null value]

	Column																			
Row	1	2	3	4	5	6	7	8	9	10	11	12	13	14	15	16	17	18	19	20
1	--	--	--	--	--	--	--	--	--	--	18	39	--	--	--	--	--	--	--	--
2	--	--	--	--	--	--	--	--	--	8	23	38	49	--	--	--	--	--	--	--
3	--	--	--	--	--	--	--	-11	-2	7	22	42	53	65	--	--	--	--	--	--
4	--	--	--	--	--	-29	-25	-12	-2	7	27	42	53	64	76	--	--	--	--	--
5	--	--	--	-30	-27	-29	-25	-12	-3	7	27	42	53	65	76	86	--	--	--	--
6	--	--	-35	-37	-34	-30	-26	-12	-3	6	32	42	53	70	81	91	98	--	--	--
7	--	--	-40	-37	-34	-30	-26	-12	-4	5	31	42	53	70	81	91	103	--	--	--
8	--	--	-40	-37	-34	-30	-26	-17	-5	5	35	47	53	70	81	92	103	103	--	--
9	--	--	-40	-42	-39	-35	-26	-17	-4	10	35	47	53	75	81	91	103	103	--	--
10	--	--	-45	-42	-39	-35	-26	-15	-4	14	40	51	63	74	81	91	102	103	108	--
11	--	--	-45	-43	-44	-36	-27	-15	0	28	39	49	62	73	85	91	101	103	108	--
12	--	-45	-46	-43	-45	-36	-27	-13	10	31	42	48	65	72	84	96	101	102	108	--
13	--	-45	-46	-43	-45	-36	-31	-10	30	35	44	57	64	77	83	90	101	101	107	--
14	-45	-46	-46	-44	-43	-33	-19	23	35	40	45	61	67	75	82	89	100	101	106	107
15	-45	-46	-42	-44	-37	-30	-7	30	37	45	54	60	66	74	81	88	94	100	101	106
16	-45	-46	-42	-44	-34	-21	17	33	40	46	54	60	67	74	81	82	94	100	101	106
17	-46	-46	-44	-43	-28	-17	28	34	40	46	56	61	63	70	77	78	89	100	101	106
18	--	-47	-45	-37	-25	-15	28	33	39	44	51	52	54	60	68	78	90	101	101	106
19	-46	-47	-45	-35	-22	-14	27	29	33	39	42	44	47	51	53	74	85	101	101	--
20	-46	-47	-45	-33	-22	-14	25	27	31	33	38	40	44	50	53	69	85	95	101	--
21	-46	-47	-44	-38	-21	-14	26	28	30	34	36	39	45	50	58	68	84	95	101	--
22	--	-46	-44	-42	-23	-11	25	28	30	34	38	42	46	50	57	68	84	95	--	--
23	--	-46	-42	-40	-18	-1	27	29	31	36	38	42	46	49	53	68	84	95	--	--
24	--	--	-42	-39	-17	1	18	29	33	37	41	49	47	49	52	69	85	100	--	--
25	--	--	--	-32	-12	10	20	29	35	41	45	49	50	52	53	69	90	100	--	--
26	--	--	--	-21	-5	12	20	29	37	45	52	57	67	73	73	81	90	100	101	--
27	--	--	--	-16	2	16	20	27	37	49	62	72	78	80	84	90	95	101	106	--
28	--	--	--	-16	8	19	22	27	36	53	73	78	80	85	89	92	95	101	106	106
29	--	--	--	--	13	20	23	28	37	53	74	78	83	89	92	95	101	101	106	106
30	--	--	--	--	15	21	24	29	37	53	75	81	85	90	94	96	101	101	106	107
31	--	--	--	--	18	22	26	30	39	52	75	81	87	92	96	96	101	101	102	--
32	--	--	--	--	18	23	29	33	41	57	75	80	86	91	96	96	96	96	97	--
33	--	--	--	--	16	25	30	33	44	57	74	78	85	90	94	95	95	95	97	--
34	--	--	--	-27	13	24	31	37	47	59	72	77	83	87	90	89	89	89	--	--
35	--	--	--	-44	14	29	33	39	48	60	72	77	80	85	90	--	--	--	--	--
36	--	--	-127	-79	14	30	36	42	53	60	69	--	--	--	--	--	--	--	--	--

Texture of materials in layer 1 -- percentage coarse-grained

[--, null value]

Row	Column																			
1	--	--	26	32	50	43	19	13	10	9	6	4	5	5	21	52	55	40	39	
2	--	--	20	17	1	7	21	8	3	2	1	2	5	5	6	8	17	28	38	43
3	--	13	14	13	12	24	31	15	3	0	0	1	5	8	9	10	18	21	24	34
4	--	7	6	9	18	28	28	19	5	0	0	1	4	7	9	10	17	18	45	17
5	--	6	5	5	11	21	21	20	8	0	1	2	2	2	1	6	18	16	28	25
6	--	5	5	5	11	19	20	16	5	2	2	2	1	0	0	5	31	32	27	26
7	6	5	5	6	8	16	17	6	2	1	1	3	2	1	0	1	23	31	29	29
8	10	6	5	5	5	7	8	3	5	1	0	1	2	1	0	0	3	22	25	29
9	24	10	4	5	5	6	7	5	3	3	2	7	5	0	0	0	4	15	25	32
10	38	21	2	2	7	7	8	9	3	12	16	14	9	5	2	2	2	0	49	21
11	46	33	1	0	14	9	7	5	0	9	19	14	10	8	5	3	1	25	0	1
12	50	43	0	1	18	18	21	1	1	6	11	7	6	7	10	9	6	2	1	4
13	32	48	0	0	33	27	49	14	2	4	5	5	5	6	18	23	15	0	1	11
14	5	0	0	0	11	44	41	1	1	11	6	9	7	7	15	23	22	0	0	15
15	1	0	0	35	47	27	24	3	10	37	36	23	8	5	3	3	15	12	16	39
16	0	1	2	13	35	26	33	5	19	40	43	26	0	4	1	0	19	25	34	39
17	39	38	34	18	59	47	43	31	39	40	40	28	12	9	11	2	8	3	21	39
18	74	80	57	1	29	40	41	39	43	41	41	17	10	10	27	17	2	5	26	27
19	72	74	62	5	2	0	4	11	40	40	24	7	11	15	61	16	0	2	9	17
20	70	69	5	46	24	4	4	7	28	20	12	2	4	4	21	8	0	14	24	16
21	68	56	84	67	45	17	9	15	29	21	11	2	9	15	57	11	13	43	4	28
22	75	75	75	77	35	1	28	37	30	17	4	0	14	34	60	13	8	21	73	34
23	74	79	66	42	9	19	50	35	21	10	6	12	23	31	67	29	20	21	34	20
24	52	27	24	5	1	3	1	5	14	14	15	26	6	10	18	20	20	22	25	20
25	10	4	16	67	4	9	2	4	13	14	16	18	3	9	11	30	35	56	20	9
26	32	46	79	62	27	10	8	3	1	4	5	5	4	1	9	22	66	70	7	3
27	66	85	88	89	51	6	5	5	0	4	5	5	7	9	6	14	30	44	16	6
28	72	77	71	62	17	1	13	14	7	5	7	10	14	9	6	48	69	54	44	29
29	57	66	71	72	89	22	15	13	10	10	10	10	14	2	22	49	32	33	22	36
30	55	52	40	12	41	21	28	13	11	10	10	11	19	7	9	49	56	32	32	58
31	55	55	62	93	84	12	15	25	24	21	15	14	13	10	1	40	63	26	42	57
32	56	60	63	53	95	71	47	26	25	25	24	21	13	3	3	25	58	56	47	52
33	66	84	83	40	51	62	63	32	37	25	23	31	37	8	6	22	38	53	50	51
34	71	85	98	79	61	32	32	22	28	11	9	35	53	19	0	20	24	24	26	32
35	45	50	40	34	32	21	22	23	1	5	5	28	50	30	16	25	23	23	29	31
36	31	28	22	17	19	7	7	38	34	21	11	11	29	36	21	26	19	31	32	33

Texture of materials in layer 2 -- percentage coarse-grained

Row	Column																			
1	--	--	--	--	--	--	--	23	25	22	14	8	6	14	20	19	16	32	56	--
2	--	--	--	--	--	--	21	23	25	24	11	3	3	4	10	6	0	21	66	79
3	--	--	--	--	--	22	22	25	29	32	12	0	4	6	12	15	21	67	87	88
4	--	--	--	--	--	22	23	26	30	30	20	8	11	14	15	36	65	87	92	89
5	--	--	--	21	22	23	24	27	28	26	22	21	22	17	14	27	66	76	82	86
6	--	20	20	21	22	23	25	27	26	24	23	24	27	18	14	26	42	69	78	83
7	--	20	19	18	16	20	25	26	25	25	24	21	23	22	31	30	12	27	66	77
8	24	21	14	7	10	17	24	26	25	25	25	23	17	13	16	2	2	26	77	76
9	25	22	16	7	7	15	24	26	25	25	25	20	13	5	5	4	6	64	84	73
10	26	24	17	6	6	11	26	28	23	22	23	18	13	7	7	3	8	52	82	83
11	28	26	16	7	5	6	26	30	21	21	22	22	24	24	17	6	1	57	53	54
12	29	30	16	8	7	7	16	43	38	27	23	23	25	25	22	15	23	68	59	50
13	10	29	13	9	21	10	3	11	23	25	21	20	21	22	21	20	26	21	8	36
14	6	0	0	1	15	21	18	1	8	25	22	20	19	21	20	20	27	31	25	16
15	8	0	3	43	58	64	74	39	30	36	33	20	15	19	28	31	27	26	42	82
16	3	29	56	56	69	62	68	42	36	33	25	17	13	16	32	35	30	28	53	55
17	63	70	79	41	48	58	65	57	54	24	2	22	16	17	29	31	17	25	46	59
18	95	59	4	22	26	24	13	58	83	78	68	57	41	33	23	9	10	6	44	47
19	79	43	21	22	3	0	3	18	81	81	71	69	68	61	39	8	6	25	35	46
20	88	76	36	75	43	5	5	6	57	79	79	66	71	69	63	21	1	85	90	70
21	64	35	28	64	30	21	10	5	35	64	56	41	74	68	72	61	40	72	60	54
22	51	20	55	56	33	29	5	2	16	25	20	1	29	54	69	47	15	34	63	66
23	80	96	79	82	37	27	20	17	18	23	26	42	37	38	65	63	37	41	71	75
24	76	54	55	46	7	16	32	31	27	25	27	18	34	37	76	97	96	81	74	77
25	32	26	32	85	7	19	32	29	13	11	23	23	34	33	70	97	99	93	75	72
26	51	63	98	63	63	27	24	6	1	5	21	23	23	10	27	99	99	87	69	67
27	81	98	99	99	98	25	12	5	0	3	20	22	21	10	24	80	91	90	80	69
28	79	93	90	80	60	22	7	15	8	7	18	21	17	20	43	47	63	83	91	74
29	46	71	82	86	94	18	7	15	14	16	19	13	7	2	26	41	59	68	62	59
30	40	41	34	15	70	45	49	36	54	67	45	11	2	1	12	43	62	78	58	44
31	40	42	61	93	80	32	50	66	97	94	84	31	13	10	17	53	83	89	66	44
32	42	56	95	96	94	71	55	90	99	90	71	46	39	40	43	56	82	84	70	53
33	60	89	96	89	40	34	60	44	42	53	43	44	45	44	46	52	61	73	69	59
34	70	86	98	84	71	69	61	12	40	36	36	42	46	45	46	59	59	62	64	62
35	40	48	43	38	27	16	21	28	20	33	35	41	45	48	55	62	60	61	64	66
36	21	18	19	20	15	6	12	34	28	27	33	39	46	50	55	59	61	66	71	74

Texture of materials in layer 3 -- percentage coarse-grained

Row	Column																				
1	3	3	2	2	2	4	11	17	19	18	21	21	21	34	68	82	83	79	72	65	
2	2	1	1	1	0	0	0	3	10	7	4	4	2	6	23	76	86	88	84	72	61
3	1	1	1	0	0	0	1	3	0	0	0	0	1	13	55	83	86	83	69	53	
4	1	1	1	0	1	1	4	7	4	1	1	1	1	7	19	57	83	88	80	54	
5	2	1	0	0	0	4	11	14	14	15	10	3	2	5	7	22	78	99	90	71	
6	4	1	0	0	0	7	17	17	18	20	15	1	0	4	6	5	37	83	88	79	
7	9	4	1	1	4	12	17	18	19	19	13	1	0	3	1	1	4	27	66	65	
8	19	15	10	7	15	21	22	23	24	21	13	7	10	9	4	0	2	32	59	60	
9	26	27	27	31	44	52	55	53	49	39	26	15	14	6	5	19	57	74	62	60	
10	28	29	33	42	55	64	66	63	50	41	29	25	14	6	11	52	75	74	88	55	
11	27	28	33	39	49	60	70	66	46	36	26	30	19	17	20	49	44	66	46	81	
12	25	27	33	37	47	48	66	76	69	28	22	29	21	18	23	45	54	71	64	55	
13	27	30	34	37	48	51	57	64	68	40	40	50	42	30	34	38	62	70	49	22	
14	39	39	49	76	78	49	38	34	43	49	54	57	53	37	36	37	56	72	71	12	
15	81	90	92	90	87	50	20	20	25	37	46	48	39	31	29	29	48	53	72	50	
16	98	99	99	94	93	49	43	30	31	32	31	36	38	17	18	25	34	45	74	72	
17	92	92	91	76	82	74	50	34	35	34	30	33	24	2	5	6	30	40	60	72	
18	53	34	31	67	64	66	44	33	34	45	41	39	24	14	6	4	42	47	73	73	
19	38	55	55	54	59	49	41	37	42	41	39	39	33	31	24	6	16	73	77	78	
20	31	40	32	24	26	41	42	38	34	28	34	38	41	33	33	13	2	89	94	81	
21	37	39	30	24	24	28	31	26	30	34	34	33	45	38	37	36	66	96	73	70	
22	39	40	38	27	19	17	19	20	23	27	26	20	28	23	24	37	86	93	77	74	
23	38	38	37	34	19	19	21	22	22	25	23	18	12	4	2	30	78	85	78	78	
24	36	35	36	34	26	24	26	24	23	18	9	5	5	5	11	74	91	88	80	80	
25	35	34	34	27	24	27	26	25	21	15	10	5	6	16	45	88	92	89	83	84	
26	34	33	30	19	28	33	29	20	17	17	18	21	20	43	51	68	79	77	83	85	
27	38	38	37	34	35	30	29	27	17	18	20	20	23	44	50	54	56	63	73	81	
28	53	57	56	56	30	27	27	46	33	24	21	20	20	24	38	53	41	50	59	54	
29	68	69	68	65	28	18	25	45	43	36	24	15	9	6	20	62	44	38	20	25	
30	71	76	84	93	29	18	20	38	58	51	30	14	6	5	16	54	60	69	40	67	
31	73	76	78	75	44	22	21	54	72	54	26	19	11	8	18	54	81	87	72	73	
32	71	72	72	73	68	27	24	62	79	53	19	19	14	10	13	36	77	81	75	70	
33	73	73	73	74	72	56	41	36	50	46	23	19	14	8	11	21	41	68	71	71	
34	71	70	70	70	68	67	49	38	43	47	45	22	19	9	28	23	26	44	62	67	
35	65	65	65	65	66	66	57	52	50	49	47	23	10	9	19	21	23	33	53	61	
36	61	60	58	56	54	53	58	65	73	58	50	26	12	12	16	21	31	48	58	62	

Texture of materials in layer 4 -- percentage coarse-grained

Row	Column																			
1	42	41	41	41	41	37	24	19	21	35	49	48	44	50	62	66	67	68	70	71
2	45	46	45	46	47	47	41	26	21	20	14	8	14	26	60	67	68	70	76	77
3	46	47	47	47	47	47	44	29	19	19	8	1	3	11	42	65	69	75	80	83
4	48	48	49	50	49	46	38	23	19	18	13	5	2	3	12	44	69	76	78	83
5	47	49	50	52	51	42	25	18	18	18	14	6	1	1	1	16	63	74	76	79
6	46	49	50	52	52	36	16	14	17	24	12	2	0	1	1	6	39	69	75	77
7	42	46	48	48	44	27	15	14	14	9	9	1	0	3	3	8	40	53	70	75
8	31	36	39	36	31	27	21	18	15	11	9	5	5	7	15	51	53	58	71	75
9	25	26	29	28	27	27	32	42	44	25	20	12	8	4	8	44	57	63	71	77
10	21	22	25	28	29	30	44	59	54	30	27	25	10	4	10	47	57	63	92	66
11	21	21	23	28	34	39	43	67	54	21	26	33	12	9	13	48	48	76	65	78
12	21	20	24	26	34	35	41	51	44	18	18	27	14	9	13	42	59	84	74	59
13	21	15	24	28	36	32	28	35	36	25	28	34	28	16	15	17	49	61	46	34
14	30	29	41	73	74	43	39	43	42	34	36	38	35	21	14	15	47	46	77	39
15	65	71	85	88	85	54	50	49	45	39	38	37	34	24	17	20	50	54	69	58
16	74	75	97	93	91	49	49	47	40	39	39	39	31	27	24	24	55	68	67	65
17	69	62	80	76	82	73	52	35	35	40	39	42	30	27	21	16	66	80	88	80
18	54	61	62	51	69	67	45	31	32	43	55	51	33	26	17	15	67	84	92	91
19	36	34	36	40	50	55	34	33	39	44	52	50	30	28	27	23	35	78	85	88
20	35	31	12	23	27	22	8	23	40	44	44	40	31	30	40	29	22	88	93	77
21	31	28	19	24	22	8	3	5	25	36	33	34	35	41	50	46	40	70	67	62
22	32	33	31	23	11	6	2	2	12	28	28	34	35	39	38	39	44	64	61	59
23	28	30	26	18	7	5	2	2	6	24	28	29	30	38	38	36	41	60	62	62
24	16	9	7	6	4	3	2	2	4	16	17	16	26	34	40	40	42	62	65	67
25	9	6	6	4	3	2	3	2	5	14	14	11	24	36	52	54	62	83	84	83
26	12	9	7	3	2	3	7	7	7	13	16	18	32	65	72	71	74	83	92	93
27	21	23	23	18	4	13	16	15	13	16	22	30	48	67	72	69	71	76	83	91
28	41	44	47	51	31	25	23	22	29	29	29	35	42	47	56	63	66	71	73	71
29	65	66	65	63	42	25	28	36	45	39	29	30	32	31	40	61	65	65	54	55
30	68	75	83	97	27	19	39	51	55	42	23	21	29	30	36	58	63	62	56	60
31	67	69	72	71	47	51	55	63	66	44	13	10	23	32	39	55	62	63	61	61
32	61	59	55	49	48	54	57	67	71	42	1	4	24	39	43	48	60	62	61	60
33	58	55	51	48	49	56	59	65	66	36	5	12	35	43	43	42	48	57	60	60
34	56	55	54	54	60	61	61	62	56	34	20	31	42	43	39	40	43	49	56	58
35	58	58	58	60	62	62	62	62	55	36	32	38	42	42	41	41	42	46	51	54
36	60	60	62	64	66	67	65	64	58	43	37	39	41	42	41	42	44	48	50	52

Texture of materials in layer 5 -- percentage coarse-grained

[--, null value]

	Column																			
Row	1	2	3	4	5	6	7	8	9	10	11	12	13	14	15	16	17	18	19	20
1	21	22	22	22	23	25	28	31	35	38	40	38	38	44	53	56	56	56	57	58
2	22	22	23	23	25	27	30	34	36	35	24	16	20	30	51	56	56	56	57	59
3	22	22	23	23	24	26	29	33	38	42	22	10	14	29	52	57	56	58	59	60
4	22	22	22	22	22	22	24	28	33	38	28	16	20	44	58	60	61	61	61	61
5	21	22	22	21	21	20	20	20	20	19	19	16	23	54	62	64	63	62	62	61
6	20	21	22	22	21	19	19	18	16	15	14	7	8	51	62	71	66	62	61	60
7	21	21	22	23	22	20	19	18	16	14	12	8	8	42	77	77	60	60	58	54
8	20	21	22	24	25	24	20	17	10	8	9	15	24	33	56	53	53	58	53	50
9	19	19	21	23	26	26	24	15	6	5	8	22	27	35	39	55	65	63	51	49
10	18	17	17	20	24	25	22	17	7	6	14	21	25	33	36	61	70	66	47	48
11	19	16	13	14	15	17	20	19	13	13	18	22	12	10	19	59	68	66	33	43
12	23	17	10	11	11	11	18	18	15	13	15	20	13	10	16	45	67	68	58	51
13	27	27	12	12	14	13	13	16	18	18	24	30	26	22	34	41	59	63	57	56
14	28	30	31	55	60	24	22	25	25	27	33	35	33	34	38	38	57	66	61	53
15	18	24	47	73	67	25	31	31	29	27	30	33	33	34	37	41	58	60	50	37
16	8	4	66	46	33	19	21	27	30	26	24	26	30	31	31	35	53	54	35	31
17	11	15	44	32	27	18	20	30	34	28	23	26	29	31	27	24	29	45	36	38
18	23	38	44	39	27	24	26	32	34	42	30	29	25	25	24	24	36	71	72	63
19	18	18	22	31	33	29	30	35	41	42	34	30	18	17	25	38	67	96	98	89
20	11	6	7	15	20	17	15	28	41	42	41	36	24	23	57	69	85	99	99	81
21	11	10	13	14	13	12	11	15	34	46	46	35	35	58	79	78	83	92	81	68
22	12	12	12	13	12	12	11	13	26	50	53	31	34	62	68	70	73	74	69	69
23	12	12	12	12	13	13	16	19	23	45	46	41	50	59	62	66	67	68	67	66
24	12	12	12	13	14	15	18	19	22	39	45	46	60	59	59	62	64	67	67	66
25	12	12	13	13	14	16	18	19	24	39	44	42	56	59	60	61	61	66	71	72
26	11	12	12	13	15	16	18	20	25	33	39	44	52	61	61	61	56	58	75	78
27	8	9	10	11	12	14	16	17	17	17	18	27	44	59	61	62	53	39	54	74
28	5	5	5	6	7	10	12	12	12	11	8	10	26	40	54	71	67	39	32	53
29	3	2	2	3	3	5	9	13	12	10	7	8	21	26	39	79	78	61	57	58
30	2	1	1	1	2	3	9	16	19	17	15	15	23	25	34	72	79	80	64	60
31	2	1	1	1	1	2	7	19	28	32	34	34	30	30	42	68	82	86	79	68
32	2	2	1	1	1	1	7	22	33	38	38	39	44	46	49	59	78	83	81	73
33	3	2	1	1	1	2	8	24	35	37	38	42	53	48	47	52	62	74	77	74
34	4	4	3	2	2	4	12	26	35	35	33	42	68	58	52	52	55	62	68	71
35	--	6	5	5	5	8	15	28	35	35	34	43	69	67	55	53	54	57	59	60
36	--	8	8	8	8	11	16	27	35	37	40	48	60	62	57	55	54	53	53	54

Texture of materials between midpoint of layers 1 and 2 -- percentage coarse-grained

[--, null value]

Row	Column																			
1	--	--	--	26	42	34	21	32	33	23	9	4	5	6	6	23	59	71	68	--
2	--	--	--	15	1	6	6	19	18	7	1	0	2	5	7	18	45	56	60	61
3	--	--	--	--	8	7	8	18	13	0	0	0	0	3	7	24	45	53	60	66
4	--	--	--	--	11	9	10	12	6	0	0	0	0	0	1	19	39	48	55	65
5	--	--	--	10	11	10	10	9	4	1	1	1	1	0	0	6	30	32	41	54
6	--	--	10	9	8	8	7	5	2	1	1	1	1	0	0	1	13	30	38	48
7	--	--	10	6	2	3	4	3	1	1	1	2	2	1	0	0	1	10	41	56
8	--	--	10	2	2	3	4	5	3	1	0	2	2	0	0	0	0	21	57	59
9	51	41	20	2	2	2	4	6	7	7	3	8	4	0	0	1	11	28	67	58
10	56	45	21	3	2	1	4	7	6	19	26	19	6	4	3	4	10	20	98	62
11	66	53	13	3	3	0	3	0	4	17	31	20	15	17	12	4	1	27	4	17
12	70	62	6	4	7	6	5	18	16	15	25	20	18	18	16	7	11	33	25	22
13	46	67	9	10	13	10	0	4	9	12	21	20	17	17	14	4	5	4	5	25
14	12	0	0	1	13	15	12	0	3	11	17	14	8	7	7	5	2	1	2	12
15	11	0	0	43	57	49	58	11	10	16	18	15	3	3	7	7	5	3	30	83
16	0	18	35	38	52	47	43	13	14	18	27	20	0	2	7	7	7	12	62	68
17	19	28	50	38	51	50	43	32	47	37	28	22	5	3	5	7	9	5	43	70
18	73	52	3	17	24	28	12	46	70	64	24	24	12	3	5	3	9	9	52	56
19	72	42	20	15	3	0	0	12	63	62	31	22	9	6	11	5	3	20	31	41
20	80	68	2	38	26	1	0	3	28	54	60	16	1	6	17	23	0	34	59	37
21	63	36	54	56	85	32	2	7	26	41	42	21	64	37	96	91	44	73	14	29
22	63	42	65	73	70	35	9	6	17	6	0	1	25	56	87	64	61	43	42	48
23	84	95	91	69	24	30	28	17	11	9	19	32	29	21	58	57	59	52	48	48
24	72	47	43	22	3	3	0	3	5	21	28	34	9	7	51	51	54	58	48	49
25	20	12	19	79	6	10	0	1	1	11	26	24	5	5	52	73	72	67	32	34
26	41	56	97	69	37	19	13	2	0	4	19	18	16	4	18	74	65	58	26	23
27	78	98	99	99	96	22	12	8	0	3	18	21	18	5	21	59	65	70	50	27
28	90	95	90	83	47	17	12	26	8	6	10	17	15	19	44	47	51	66	72	47
29	75	78	83	86	92	16	20	15	1	6	6	8	6	2	24	44	48	53	53	32
30	75	66	32	8	67	27	34	12	7	9	8	7	2	0	7	39	62	66	48	66
31	76	72	59	92	73	30	27	49	74	56	34	16	7	5	10	49	76	79	69	71
32	76	79	88	86	95	76	56	74	79	72	61	31	20	18	18	31	72	77	72	68
33	80	91	92	77	53	57	82	38	33	44	36	29	24	22	17	44	65	73	72	72
34	73	86	98	75	59	55	52	20	33	32	31	28	27	22	0	24	56	64	69	74
35	39	47	43	36	23	14	19	25	2	27	31	27	27	22	17	44	65	66	74	79
36	19	16	19	20	18	7	12	37	24	19	15	12	32	47	54	66	61	84	87	80

Texture of materials between midpoint of layers 2 and 3 -- percentage coarse-grained

Row	Column																			
1	--	--	--	--	19	19	18	22	24	25	28	27	24	30	48	56	56	59	62	62
2	--	--	--	--	19	19	19	20	20	19	11	5	8	18	49	56	55	60	66	61
3	--	--	--	19	19	19	19	20	20	21	8	0	3	12	41	58	62	77	71	54
4	--	19	19	19	19	20	20	20	20	20	13	5	7	13	21	53	81	91	85	56
5	17	19	20	20	21	21	22	22	22	20	17	16	16	13	12	29	80	99	92	73
6	--	--	18	22	26	31	35	35	34	34	29	21	19	14	11	21	46	85	90	81
7	12	13	15	23	31	41	49	52	53	53	48	26	20	19	24	23	11	30	66	64
8	12	13	15	19	28	38	47	54	57	58	59	47	27	23	16	2	2	27	57	58
9	12	13	14	16	24	35	47	54	52	54	57	44	28	12	10	14	37	54	64	56
10	11	13	15	14	18	29	45	57	51	40	23	18	16	9	10	28	47	53	75	63
11	11	12	17	14	13	19	35	66	51	31	9	13	7	5	8	20	11	66	76	90
12	11	12	21	11	16	21	37	62	58	13	4	14	9	5	11	25	33	80	80	70
13	5	11	14	2	6	28	43	51	58	27	31	48	38	25	34	41	58	60	58	34
14	1	2	3	10	21	31	25	27	42	47	55	58	56	43	39	40	62	64	50	15
15	0	11	4	65	73	42	14	56	54	49	53	57	58	49	34	31	65	73	61	62
16	6	98	98	81	84	44	47	68	54	42	43	54	60	54	30	26	42	45	58	57
17	83	94	92	71	75	67	50	40	37	42	41	47	55	48	31	25	22	21	49	62
18	96	71	33	63	59	61	38	30	32	47	49	48	37	24	21	11	28	26	61	62
19	60	61	55	56	57	51	46	37	42	44	46	47	27	20	22	7	12	50	59	65
20	52	56	44	43	36	45	49	42	39	34	45	49	51	27	41	18	2	88	95	81
21	50	48	45	40	18	30	31	20	36	46	45	35	63	51	56	52	64	90	79	59
22	44	41	46	36	22	26	10	8	23	35	35	1	24	45	56	59	83	87	61	45
23	49	54	67	56	22	24	23	21	25	32	29	29	23	29	62	86	92	82	77	89
24	53	54	52	37	9	26	36	35	31	25	19	15	25	26	69	96	99	93	83	84
25	52	51	51	70	16	27	36	34	27	17	11	8	21	28	65	96	99	96	92	92
26	51	51	52	30	36	41	35	24	21	19	14	12	14	27	39	96	91	85	94	97
27	49	49	45	39	43	31	23	23	21	20	15	15	15	26	35	79	78	65	77	92
28	40	52	52	51	27	22	18	29	25	21	16	14	13	19	41	68	71	62	57	64
29	29	49	63	60	29	9	15	29	28	27	18	10	8	6	22	70	71	68	43	45
30	21	37	74	84	40	32	34	39	52	47	24	10	6	5	17	64	76	82	54	64
31	20	31	73	78	53	51	54	63	77	54	17	12	11	11	22	65	90	94	76	67
32	25	47	86	93	88	55	53	69	80	52	9	10	20	26	33	56	88	91	80	70
33	50	78	93	93	89	64	37	36	45	41	13	17	31	23	33	56	69	81	80	73
34	64	81	98	89	60	56	35	30	38	39	37	35	40	30	65	71	69	72	75	74
35	53	55	44	36	38	30	23	28	59	41	39	38	40	45	65	75	71	72	76	80
36	36	31	24	23	20	5	9	48	53	50	44	41	42	50	62	68	72	78	83	85

Texture of materials between midpoint of layers 3 and 4 – percentage coarse-grained

Row	Column																			
	1	2	3	4	5	6	7	8	9	10	11	12	13	14	15	16	17	18	19	20
1	23	21	20	19	18	17	12	10	11	26	39	38	34	40	57	63	64	65	68	70
2	25	24	22	21	20	19	17	13	14	15	11	6	11	23	58	65	66	67	75	78
3	27	27	26	23	20	20	19	17	15	15	6	0	2	11	42	63	67	71	78	85
4	30	30	31	31	27	24	22	20	18	16	11	4	3	5	14	44	68	73	74	85
5	32	32	34	36	35	30	24	23	27	28	21	7	2	4	5	17	62	76	76	79
6	33	33	35	36	36	29	21	21	30	34	27	2	0	3	4	5	32	67	74	77
7	33	32	33	33	31	24	21	21	27	31	21	1	0	2	1	2	14	31	65	75
8	34	31	26	22	18	16	21	25	29	30	16	3	2	2	5	15	17	39	71	76
9	36	33	26	14	12	10	26	48	45	36	25	10	3	1	3	23	49	64	73	77
10	38	37	33	24	17	18	56	67	44	36	32	27	11	4	9	45	59	64	89	68
11	39	38	38	37	39	56	77	77	36	32	30	35	25	24	22	46	43	73	72	63
12	39	39	39	39	40	42	71	72	64	30	27	33	27	25	26	43	56	81	73	51
13	39	37	39	41	44	48	58	64	65	40	41	49	43	30	26	27	59	75	47	21
14	46	45	52	74	75	57	55	55	58	50	53	55	52	32	25	25	45	69	85	19
15	74	76	84	86	84	56	52	52	50	42	47	51	43	26	28	31	31	32	79	62
16	82	88	96	92	92	50	50	49	41	36	34	35	18	12	24	33	34	54	87	85
17	70	48	71	74	83	74	53	38	39	38	33	36	16	9	13	17	57	71	80	84
18	49	46	46	43	67	65	47	34	36	54	49	45	28	19	16	15	63	69	84	84
19	32	42	44	35	44	50	38	38	47	47	44	44	35	34	29	21	34	85	88	87
20	26	30	16	16	18	19	14	27	33	23	24	35	36	34	31	24	21	91	94	81
21	29	29	21	16	14	9	11	12	21	27	31	43	43	32	31	32	69	93	74	67
22	32	33	31	20	10	8	11	12	19	30	30	48	46	29	22	28	79	90	72	69
23	29	30	27	23	10	11	15	16	17	28	31	33	24	31	29	29	64	79	69	67
24	22	20	25	21	15	19	23	20	19	18	12	6	4	21	38	73	88	85	71	72
25	19	16	15	13	8	15	22	22	19	16	10	4	6	25	60	89	92	89	83	81
26	19	17	15	6	7	10	18	20	18	19	23	28	27	70	80	84	87	85	85	84
27	28	30	33	24	12	20	28	28	18	20	28	31	36	72	79	72	67	82	85	84
28	54	66	68	72	31	26	31	46	34	26	28	29	30	35	50	58	46	66	82	66
29	75	76	78	75	38	21	29	46	43	38	28	18	11	6	22	65	47	42	32	34
30	73	77	85	94	20	12	27	45	62	55	29	12	7	5	16	54	51	44	39	58
31	66	69	71	69	38	35	38	67	85	60	21	13	9	8	18	41	46	45	50	61
32	57	53	46	37	36	39	42	82	92	58	11	12	12	12	13	23	42	45	49	55
33	52	48	42	37	39	54	59	69	70	53	15	13	16	13	11	12	22	39	47	52
34	51	50	49	53	70	75	70	60	57	57	32	20	22	16	8	10	13	25	39	47
35	56	56	59	65	73	75	73	72	71	68	51	25	23	20	11	11	14	23	37	46
36	59	61	63	65	66	66	72	80	83	77	67	35	22	19	16	17	26	39	49	53

Texture of materials between midpoint of layers 4 and 5 – percentage coarse-grained

Row	Column																			
	1	2	3	4	5	6	7	8	9	10	11	12	13	14	15	16	17	18	19	20
1	55	55	57	60	61	52	25	13	14	30	43	43	43	51	65	69	70	70	71	71
2	59	62	64	68	72	73	60	30	25	28	23	19	23	35	65	71	72	73	77	75
3	59	61	64	68	73	74	68	43	30	30	20	14	16	27	56	71	74	81	81	77
4	58	59	60	62	65	66	55	33	26	28	23	16	16	28	41	63	78	84	84	77
5	54	56	57	57	57	50	31	21	17	16	15	10	12	31	36	49	75	81	82	79
6	50	54	55	57	57	41	21	18	15	16	12	2	1	29	36	52	67	79	80	78
7	41	48	51	51	47	30	19	18	14	12	11	2	1	27	55	60	69	73	70	65
8	21	31	37	32	25	21	20	18	15	12	10	8	11	19	47	72	73	70	58	60
9	7	11	17	19	18	18	19	20	18	16	19	16	13	20	27	65	75	69	52	62
10	2	3	8	16	18	19	23	24	20	18	23	24	16	19	24	66	77	71	46	49
11	1	2	4	12	22	25	27	26	19	12	21	30	9	5	12	61	72	67	33	42
12	0	0	4	7	24	25	27	26	18	11	13	23	10	5	8	37	68	69	57	47
13	0	0	4	9	25	27	29	28	21	16	20	24	20	13	16	24	56	65	54	51
14	4	5	10	65	73	44	32	31	28	23	26	27	25	19	16	17	60	57	76	58
15	22	26	59	85	81	48	32	31	31	27	26	26	25	22	19	25	69	73	57	50
16	31	29	84	45	83	45	42	37	35	27	25	26	25	25	26	35	70	71	33	29
17	36	42	64	26	47	64	49	44	42	30	24	28	26	25	28	32	65	75	84	63
18	45	54	56	50	46	51	48	45	45	40	39	37	27	25	30	31	59	73	87	86
19	43	48	43	42	45	47	43	44	43	43	42	39	24	22	27	17	19	60	72	79
20	28	23	11	23	28	20	13	30	45	50	49	39	27	27	55	27	6	87	97	84
21	24	22	21	21	14	7	8	12	34	45	40	30	31	58	79	71	34	72	79	62
22	23	24	23	19	8	5	8	10	22	39	40	26	29	59	66	66	59	62	61	60
23	23	23	23	17	9	7	13	17	19	35	36	33	41	54	58	62	62	61	60	60
24	23	23	21	17	12	12	15	17	19	30	33	34	47	50	54	59	61	62	62	64
25	23	22	21	19	18	16	16	17	20	30	32	30	44	52	63	65	63	65	69	70
26	24	24	25	26	26	25	23	22	24	31	34	36	48	71	75	74	63	59	73	76
27	30	30	30	29	29	29	28	27	27	34	39	45	58	72	75	73	64	45	54	72
28	39	37	34	31	30	30	30	29	29	34	41	47	52	56	63	71	79	54	36	54
29	50	48	43	37	32	31	32	31	28	28	33	41	43	41	50	68	79	76	57	57
30	60	60	59	56	49	43	40	35	27	21	24	32	40	41	47	68	76	79	63	59
31	67	70	72	73	71	65	55	40	25	20	20	24	37	44	52	70	83	85	79	67
32	70	73	76	79	79	74	65	44	23	19	17	20	41	57	62	68	81	83	80	73
33	--	74	77	79	79	75	67	48	25	21	19	29	54	62	63	65	71	78	78	75
34	--	--	74	75	75	71	66	53	36	27	34	49	62	63	65	64	66	70	75	74
35	--	--	68	69	68	67	64	58	47	41	47	57	63	63	64	64	64	65	66	66
36	--	--	68	64	66	66	64	59	54	50	53	59	62	63	63	63	63	62	61	61

Matrix (modflow ibound array) indicating distribution of potentially active cells for layers 1-5

[0, inactive, 1, potentially active]

Row	Column																			
1	0	0	0	0	0	0	0	0	0	0	1	1	0	0	0	0	0	0	0	0
2	0	0	0	0	0	0	0	0	0	1	1	1	1	0	0	0	0	0	0	0
3	0	0	0	0	0	0	0	1	1	1	1	1	1	0	0	0	0	0	0	0
4	0	0	0	0	1	1	1	1	1	1	1	1	1	1	0	0	0	0	0	0
5	0	0	0	0	1	1	1	1	1	1	1	1	1	1	1	0	0	0	0	0
6	0	0	0	0	1	1	1	1	1	1	1	1	1	1	1	1	0	0	0	0
7	0	0	0	0	1	1	1	1	1	1	1	1	1	1	1	1	0	0	0	0
8	0	0	0	0	1	1	1	1	1	1	1	1	1	1	1	1	1	0	0	0
9	0	0	0	0	1	1	1	1	1	1	1	1	1	1	1	1	1	1	0	0
10	0	0	0	1	1	1	1	1	1	1	1	1	1	1	1	1	1	1	1	0
11	0	0	0	1	1	1	1	1	1	1	1	1	1	1	1	1	1	1	1	0
12	0	0	0	1	1	1	1	1	1	1	1	1	1	1	1	1	1	1	1	0
13	0	0	1	1	1	1	1	1	1	1	1	1	1	1	1	1	1	1	1	0
14	0	0	1	1	1	1	1	1	1	1	1	1	1	1	1	1	1	1	1	1
15	0	1	1	1	1	1	1	1	1	1	1	1	1	1	1	1	1	1	1	1
16	0	1	1	1	1	1	1	1	1	1	1	1	1	1	1	1	1	1	1	1
17	0	1	1	1	1	1	1	1	1	1	1	1	1	1	1	1	1	1	1	1
18	0	1	1	1	1	1	1	1	1	1	1	1	1	1	1	1	1	1	1	1
19	0	1	1	1	1	1	1	1	1	1	1	1	1	1	1	1	1	1	1	0
20	0	1	1	1	1	1	1	1	1	1	1	1	1	1	1	1	1	1	1	0
21	1	1	1	1	1	1	1	1	1	1	1	1	1	1	1	1	1	1	1	0
22	0	1	1	1	1	1	1	1	1	1	1	1	1	1	1	1	1	1	0	0
23	0	1	1	1	1	1	1	1	1	1	1	1	1	1	1	1	1	1	0	0
24	0	0	1	1	1	1	1	1	1	1	1	1	1	1	1	1	1	1	0	0
25	0	0	0	1	1	1	1	1	1	1	1	1	1	1	1	1	1	1	0	0
26	0	0	0	1	1	1	1	1	1	1	1	1	1	1	1	1	1	1	1	0
27	0	0	0	1	1	1	1	1	1	1	1	1	1	1	1	1	1	1	1	0
28	0	0	0	1	1	1	1	1	1	1	1	1	1	1	1	1	1	1	1	1
29	0	0	0	0	1	1	1	1	1	1	1	1	1	1	1	1	1	1	1	1
30	0	0	0	0	1	1	1	1	1	1	1	1	1	1	1	1	1	1	1	1
31	0	0	0	0	1	1	1	1	1	1	1	1	1	1	1	1	1	1	1	0
32	0	0	0	0	1	1	1	1	1	1	1	1	1	1	1	1	1	1	1	0
33	0	0	0	0	1	1	1	1	1	1	1	1	1	1	1	1	1	1	1	0
34	0	0	0	1	1	1	1	1	1	1	1	1	1	1	1	1	1	1	0	0
35	0	0	0	1	1	1	1	1	1	1	1	1	1	1	0	0	0	0	0	0
36	0	0	1	1	1	1	1	1	1	0	0	0	0	0	0	0	0	0	0	0

Matrix (modflow ibound array) indicating distribution of active cells for layer 6

[0, inactive; 1, active]

Row	Column																			
1	0	0	0	0	0	0	0	0	0	0	0	1	1	0	0	0	0	0	0	0
2	0	0	0	0	0	0	0	0	0	0	1	1	1	1	0	0	0	0	0	0
3	0	0	0	0	0	0	0	0	0	1	1	1	1	1	1	0	0	0	0	0
4	0	0	0	0	0	1	1	1	1	1	1	1	1	1	1	1	0	0	0	0
5	0	0	0	1	1	1	1	1	1	1	1	1	1	1	1	1	1	0	0	0
6	0	0	1	1	1	1	1	1	1	1	1	1	1	1	1	1	1	1	0	0
7	0	0	1	1	1	1	1	1	1	1	1	1	1	1	1	1	1	1	0	0
8	0	0	1	1	1	1	1	1	1	1	1	1	1	1	1	1	1	1	1	0
9	0	0	1	1	1	1	1	1	1	1	1	1	1	1	1	1	1	1	1	0
10	0	0	1	1	1	1	1	1	1	1	1	1	1	1	1	1	1	1	1	0
11	0	0	1	1	1	1	1	1	1	1	1	1	1	1	1	1	1	1	1	0
12	0	1	1	1	1	1	1	1	1	1	1	1	1	1	1	1	1	1	1	0
13	0	1	1	1	1	1	1	1	1	1	1	1	1	1	1	1	1	1	1	0
14	1	1	1	1	1	1	1	1	1	1	1	1	1	1	1	1	1	1	1	1
15	1	1	1	1	1	1	1	1	1	1	1	1	1	1	1	1	1	1	1	1
16	1	1	1	1	1	1	1	1	1	1	1	1	1	1	1	1	1	1	1	1
17	1	1	1	1	1	1	1	1	1	1	1	1	1	1	1	1	1	1	1	1
18	0	1	1	1	1	1	1	1	1	1	1	1	1	1	1	1	1	1	1	1
19	1	1	1	1	1	1	1	1	1	1	1	1	1	1	1	1	1	1	1	0
20	1	1	1	1	1	1	1	1	1	1	1	1	1	1	1	1	1	1	1	0
21	1	1	1	1	1	1	1	1	1	1	1	1	1	1	1	1	1	1	1	0
22	0	1	1	1	1	1	1	1	1	1	1	1	1	1	1	1	1	1	1	0
23	0	1	1	1	1	1	1	1	1	1	1	1	1	1	1	1	1	1	1	0
24	0	0	1	1	1	1	1	1	1	1	1	1	1	1	1	1	1	1	1	0
25	0	0	0	1	1	1	1	1	1	1	1	1	1	1	1	1	1	1	1	0
26	0	0	0	1	1	1	1	1	1	1	1	1	1	1	1	1	1	1	1	0
27	0	0	0	1	1	1	1	1	1	1	1	1	1	1	1	1	1	1	1	0
28	0	0	0	1	1	1	1	1	1	1	1	1	1	1	1	1	1	1	1	1
29	0	0	0	0	1	1	1	1	1	1	1	1	1	1	1	1	1	1	1	1
30	0	0	0	0	1	1	1	1	1	1	1	1	1	1	1	1	1	1	1	1
31	0	0	0	0	1	1	1	1	1	1	1	1	1	1	1	1	1	1	1	0
32	0	0	0	0	1	1	1	1	1	1	1	1	1	1	1	1	1	1	1	0
33	0	0	0	0	1	1	1	1	1	1	1	1	1	1	1	1	1	1	1	0
34	0	0	0	1	1	1	1	1	1	1	1	1	1	1	1	1	1	1	1	0
35	0	0	0	1	1	1	1	1	1	1	1	1	1	1	1	1	1	1	0	0
36	0	0	1	1	1	1	1	1	1	1	1	1	1	1	0	0	0	0	0	0

APPENDIX D: DATA GENERATED FROM MEASURED WATER LEVELS AND USED FOR COMPARISON WITH SIMULATION RESULTS

Cells subject to bare-soil evaporation (water table within 7 ft of land surface) from October 1972 through October 1988 are tabulated below, "1" signifying that the cell is subject to bare-soil evaporation. Data are given for July and October conditions for each year, except July 1977.

Cells subject to bare-soil evaporation in October 1974

Row	Column																			
1	0	0	0	0	0	0	0	0	0	0	0	0	0	0	0	0	0	0	0	0
2	0	0	0	0	0	0	0	0	0	1	1	1	1	0	0	0	0	0	0	0
3	0	0	0	0	0	0	0	0	0	1	1	1	1	1	0	0	0	0	0	0
4	0	0	0	0	0	0	0	0	0	1	1	1	1	1	0	0	0	0	0	0
5	0	0	0	0	0	0	0	0	0	0	1	1	1	1	1	0	0	0	0	0
6	0	0	0	0	0	0	0	0	0	0	1	1	1	1	1	0	0	0	0	0
7	0	0	0	0	0	1	0	1	0	0	0	0	1	1	1	1	0	0	0	0
8	0	0	0	0	0	0	0	0	0	0	0	0	1	1	1	1	1	0	0	0
9	0	0	0	0	0	0	0	0	0	0	0	0	1	1	0	0	1	1	0	0
10	0	0	0	0	0	0	0	0	0	0	0	0	1	1	0	0	1	1	1	0
11	0	0	0	0	0	0	0	0	0	0	0	0	1	1	1	1	1	0	0	0
12	0	0	0	0	0	0	0	0	0	0	0	0	0	1	1	1	1	0	0	0
13	0	0	0	0	0	0	0	0	0	0	0	0	0	0	1	1	1	0	0	0
14	0	0	0	0	0	0	0	0	0	0	0	0	0	0	1	1	0	0	0	0
15	0	0	0	0	0	0	0	0	0	0	0	0	0	0	1	1	1	0	0	0
16	0	0	0	0	0	0	0	0	0	0	0	0	0	1	1	1	1	0	0	0
17	0	0	0	0	0	0	0	0	0	0	0	0	0	1	1	0	1	0	0	0
18	0	0	0	0	0	0	0	0	0	0	0	0	0	0	1	0	0	0	0	0
19	0	0	0	0	0	0	0	0	0	0	0	0	0	0	0	1	1	0	0	0
20	0	0	0	0	0	0	0	0	0	1	0	0	1	1	1	0	0	0	0	0
21	0	0	0	0	0	0	0	0	0	0	0	0	0	1	1	1	0	0	0	0
22	0	0	0	0	0	0	1	0	0	0	0	0	0	1	1	0	0	0	0	0
23	0	0	0	0	0	0	0	0	0	0	0	0	0	0	1	1	0	0	0	0
24	0	0	0	0	0	0	0	0	0	0	0	0	0	1	1	1	1	0	0	0
25	0	0	0	0	0	0	0	0	0	0	0	0	0	1	1	1	0	0	0	0
26	0	0	0	0	0	0	0	0	0	0	0	0	0	1	1	0	0	0	0	0
27	0	0	0	0	0	0	0	0	0	0	0	0	0	1	1	1	0	0	0	0
28	0	0	0	0	0	0	0	0	0	0	0	0	0	1	1	1	0	0	0	0
29	0	0	0	0	0	0	0	0	0	1	0	0	1	1	1	0	0	0	0	0
30	0	0	0	0	0	0	0	0	0	0	0	0	0	1	1	1	0	0	0	0
31	0	0	0	0	0	0	0	0	0	1	0	0	1	1	0	1	0	0	0	0
32	0	0	0	0	0	0	0	0	0	0	0	0	0	0	0	0	0	0	0	0
33	0	0	0	0	0	0	0	0	0	0	0	0	0	0	0	0	0	0	0	0
34	0	0	0	0	0	0	0	0	0	0	0	0	0	0	1	1	0	0	0	0
35	0	0	0	0	0	0	0	0	0	0	0	0	0	0	1	0	0	0	0	0
36	0	0	0	0	0	0	0	0	0	0	0	0	0	0	0	0	0	0	0	0

Cells subject to bare-soil evaporation in October 1975

Row	Column																			
1	0	0	0	0	0	0	0	0	0	0	0	0	0	0	0	0	0	0	0	0
2	0	0	0	0	0	0	0	0	0	0	1	1	1	1	0	0	0	0	0	0
3	0	0	0	0	0	0	0	0	0	0	1	1	0	1	1	0	0	0	0	0
4	0	0	0	0	0	0	0	0	0	0	1	1	0	1	1	1	0	0	0	0
5	0	0	0	0	0	0	0	0	0	0	1	1	1	1	1	1	0	0	0	0
6	0	0	0	0	0	0	0	0	0	0	1	1	1	1	1	1	1	0	0	0
7	0	0	0	0	0	0	0	0	0	0	0	0	0	0	0	0	0	0	0	0
8	0	0	0	0	0	0	0	0	0	0	0	0	0	0	0	0	1	1	1	0
9	0	0	0	0	0	0	0	0	0	0	0	0	0	0	0	0	1	1	1	0
10	0	0	0	0	0	0	0	0	0	0	0	0	0	0	0	0	0	0	1	1
11	0	0	0	0	0	0	0	0	0	0	0	0	0	0	0	0	0	1	1	0
12	0	0	0	0	0	0	0	0	0	0	0	0	0	0	0	0	0	1	1	0
13	0	0	0	0	0	0	0	0	0	0	0	0	0	0	0	0	0	1	1	0
14	0	0	0	0	0	0	0	0	0	0	0	0	0	0	0	0	0	1	1	0
15	0	0	0	0	0	0	0	0	0	0	0	0	0	0	0	0	0	1	1	0
16	0	0	0	0	0	0	0	0	0	0	0	0	0	0	0	0	0	1	1	0
17	0	0	0	0	0	0	0	0	0	0	0	0	0	0	0	0	0	1	1	0
18	0	0	0	0	0	0	0	0	0	0	0	0	0	0	0	0	0	1	1	0
19	0	0	0	0	0	0	0	0	0	0	0	0	0	0	0	0	0	1	1	0
20	0	0	0	0	0	0	0	0	0	0	0	0	0	0	0	0	0	1	1	0
21	0	0	0	0	0	0	0	0	0	0	0	0	0	0	0	0	0	1	1	0
22	0	0	0	0	0	0	0	0	0	0	0	0	0	0	0	0	0	1	1	0
23	0	0	0	0	0	0	0	0	0	0	0	0	0	0	0	0	0	1	1	0
24	0	0	0	0	0	0	0	0	0	0	0	0	0	0	0	0	0	1	1	0
25	0	0	0	0	0	0	0	0	0	0	0	0	0	0	0	0	0	1	1	0
26	0	0	0	0	0	0	0	0	0	0	0	0	0	0	0	0	0	1	0	0
27	0	0	0	0	0	0	0	0	0	0	0	0	0	0	0	0	0	1	1	0
28	0	0	0	0	0	0	0	0	0	0	0	0	0	0	0	0	0	1	1	0
29	0	0	0	0	0	0	0	0	0	0	0	0	0	0	0	0	0	1	0	0
30	0	0	0	0	0	0	0	0	0	0	0	0	0	0	0	0	0	1	1	0
31	0	0	0	0	0	0	0	0	0	0	0	0	0	0	0	0	0	1	1	0
32	0	0	0	0	0	0	0	0	0	0	0	0	0	0	0	0	0	1	1	0
33	0	0	0	0	0	0	0	0	0	0	0	0	0	0	0	0	0	0	0	0
34	0	0	0	0	0	0	0	0	0	0	0	0	0	0	0	0	0	0	0	0
35	0	0	0	0	0	0	0	0	0	0	0	0	0	0	0	0	0	0	0	0
36	0	0	0	0	0	0	0	0	0	0	0	0	0	0	0	0	0	0	0	0

Cells subject to bare-soil evaporation in July 1975

Row	Column																			
1	0	0	0	0	0	0	0	0	0	0	1	1	0	0	0	0	0	0	0	0
2	0	0	0	0	0	0	0	0	0	1	1	1	0	0	0	0	0	0	0	0
3	0	0	0	0	0	0	0	0	0	1	1	1	1	1	0	0	0	0	0	0
4	0	0	0	0	0	0	0	0	0	1	1	1	1	1	0	0	0	0	0	0
5	0	0	0	0	0	0	0	0	0	1	1	1	1	1	1	0	0	0	0	0
6	0	0	0	0	0	0	0	0	0	1	1	1	1	1	1	1	0	0	0	0
7	0	0	0	0	0	1	1	1	1	1	1	1	1	1	1	0	0	0	0	0
8	0	0	0	0	0	0	0	0	0	0	1	1	1	1	1	1	0	0	0	0
9	0	0	0	0	0	0	0	0	0	0	0	1	1	1	1	1	1	0	0	0
10	0	0	0	0	0	0	0	0	0	0	0	1	1	1	1	1	0	0	0	0
11	0	0	0	0	0	0	0	0	0	0	0	0	1	1	1	1	1	0	0	0
12	0	0	0	0	0	0	0	0	0	0	0	0	0	1	1	1	1	0	0	0
13	0	0	0	0	0	0	0	0	0	0	0	0	0	0	1	1	1	0	0	0
14	0	0	0	0	0	0	0	0	0	0	0	0	0	0	0	0	0	1	1	0
15	0	0	0	0	0	0	0	0	0	0	0	0	0	0	1	0	0	1	1	0
16	0	0	0	0	0	0	0	0	0	0	0	0	0	0	1	1	1	1	0	0
17	0	0	0	0	0	0	0	0	0	0	0	0	0	0	1	1	1	1	0	0
18	0	0	0	0	0	0	0	0	0	0	0	0	0	0	1	0	0	0	0	0
19	0	0	0	0	0	0	0	0	0	0	0	0	0	0	1	1	1	0	0	0
20	0																			

Cells subject to bare-soil evaporation in October 1976

Row	Column																			
1	0	0	0	0	0	0	0	0	0	0	0	1	1	0	0	0	0	0	0	0
2	0	0	0	0	0	0	0	0	0	1	1	1	1	0	0	0	0	0	0	0
3	0	0	0	0	0	0	0	0	0	1	1	0	1	1	0	0	0	0	0	0
4	0	0	0	0	0	0	0	0	1	1	1	1	1	0	0	0	0	0	0	0
5	0	0	0	0	0	0	0	0	1	1	1	1	1	1	0	0	0	0	0	0
6	0	0	0	0	0	0	1	1	1	1	1	1	1	1	1	0	0	0	0	0
7	0	0	0	0	0	1	1	1	1	0	1	1	1	1	1	0	0	0	0	0
8	0	0	0	0	0	0	0	0	0	0	1	1	1	1	1	1	0	0	0	0
9	0	0	0	0	0	0	0	0	0	0	0	1	1	1	1	0	0	0	0	0
10	0	0	0	0	0	0	0	0	0	0	1	1	0	0	0	0	0	0	0	0
11	0	0	0	0	0	0	0	0	0	0	0	0	1	1	1	1	0	0	0	0
12	0	0	0	0	0	0	0	0	0	0	0	1	1	1	1	1	1	0	0	0
13	0	0	0	0	0	0	0	0	0	0	0	1	1	1	1	1	0	0	0	0
14	0	0	0	0	0	0	0	0	0	0	0	1	1	1	1	1	0	0	0	0
15	0	0	0	0	0	0	0	0	0	0	0	0	1	1	0	0	0	0	0	0
16	0	0	0	0	0	0	0	0	0	0	0	1	1	1	0	0	0	0	0	0
17	0	0	0	0	0	0	0	0	0	0	0	0	1	1	0	0	0	0	0	0
18	0	0	0	0	0	0	0	0	0	0	0	0	1	0	0	0	0	0	0	0
19	0	0	0	0	0	0	0	0	0	0	0	1	1	1	0	0	0	0	0	0
20	0	0	0	0	0	0	0	0	0	0	1	1	1	0	0	0	0	0	0	0
21	0	0	0	0	0	0	0	0	0	0	1	1	1	1	1	1	0	0	0	0
22	0	0	0	0	0	0	0	0	0	1	0	0	1	1	1	0	0	0	0	0
23	0	0	0	0	0	0	0	0	0	1	1	1	1	1	1	0	0	0	0	0
24	0	0	0	0	0	0	0	0	0	1	1	1	1	0	0	0	0	0	0	0
25	0	0	0	0	0	0	0	0	0	0	1	1	1	1	0	0	0	0	0	0
26	0	0	0	0	0	0	0	0	0	0	0	1	1	1	0	0	0	0	0	0
27	0	0	0	0	0	0	1	1	0	0	0	1	1	1	0	0	0	0	0	0
28	0	0	0	0	0	0	0	1	0	0	0	1	1	1	0	0	0	0	0	0
29	0	0	0	0	0	0	0	0	1	0	0	1	1	1	1	0	0	0	0	0
30	0	0	0	0	0	0	0	0	0	0	1	1	1	1	0	0	0	0	0	0
31	0	0	0	0	0	0	0	0	0	0	0	1	1	1	0	0	0	0	0	0
32	0	0	0	0	0	0	0	0	0	0	0	1	0	1	0	0	0	0	0	0
33	0	0	0	0	0	0	0	0	0	0	0	0	0	0	0	0	0	0	0	0
34	0	0	0	0	0	0	0	0	0	0	0	0	1	0	0	0	0	0	0	0
35	0	0	0	0	0	0	0	0	0	0	0	0	0	0	0	0	0	0	0	0
36	0	0	0	0	0	0	0	0	0	0	0	0	0	0	0	0	0	0	0	0

Cells subject to bare-soil evaporation in July 1978

Row	Column																			
1	0	0	0	0	0	0	0	0	0	0	1	1	0	0	0	0	0	0	0	0
2	0	0	0	0	0	0	0	0	0	1	1	1	0	0	0	0	0	0	0	0
3	0	0	0	0	0	0	0	0	1	1	1	1	1	1	0	0	0	0	0	0
4	0	0	0	0	0	0	0	1	1	1	1	1	1	1	1	0	0	0	0	0
5	0	0	0	0	0	0	0	1	1	1	1	1	1	1	1	1	0	0	0	0
6	0	0	0	0	0	1	0	1	1	1	1	1	1	1	1	1	0	0	0	0
7	0	0	0	0	0	1	1	1	1	1	1	1	1	1	1	1	0	0	0	0
8	0	0	0	0	0	0	0	0	0	1	1	1	1	1	1	1	1	0	0	0
9	0	0	0	0	0	0	0	0	0	0	0	1	1	1	1	1	1	0	0	0
10	0	0	0	0	0	0	0	0	0	0	0	1	1	1	1	1	1	0	0	0
11	0	0	0	0	0	0	0	0	0	0	0	0	1	1	1	1	1	0	0	0
12	0	0	0	0	0	0	0	0	0	0	0	0	0	1	1	1	1	0	0	0
13	0	0	0	0	0	0	0	0	0	0	0	0	0	1	1	1	1	0	0	0
14	0	0	0	0	0	0	0	0	0	0	0	0	0	0	1	1	1	1	0	0
15	0	0	0	0	0	0	0	0	0	0	0	0	0	0	1	1	1	0	0	0
16	0	0	0	0	0	0	0	0	0	0	0	0	0	0	0	1	0	0	0	0
17	0	0	0	0	0	0	0	0	0	0	0	0	0	0	0	0	1	0	0	0
18	0	0	0	0	0	0	0	0	0	0	0	0	0	0	0	0	1	1	0	0
19	0	0	0	0	0	0	0	0	0	0	0	0	0	0	0	0	1	1	0	0
20	0	0	0	0	0	0	0	0	0	0	0	0	0	0	0	0	1	1	1	0
21	0	0	0	0	0	0	0	0	0	0	0	1	0	0	1	1	0	0	0	0
22	0	0	0	0	0	0	0	0	0	0	0	0	0	0	0	0	1	1	0	0
23	0	0	0	0	0	0	0	0	0	0	0	0	0	0	0	0	1	0	1	0
24	0	0	0	0	0	0	0	0	0	0	0	1	1	1	1	1	1	0	0	0
25	0	0	0	0	0	0	0	0	0	0	1	1	0	1	1	1	1	0	0	0
26	0	0	0	0	0	0	0	0	0	0	1	1	0	0	1	1	1	0	0	0
27	0	0	0	0	0	0	1	0	0	0	1	0	1	0	1	1	0	0	0	0
28	0	0	0	0	0	0	0	1	0	0	0	1	0	0	1	1	0	0	0	0
29	0	0	0	0	0	0	0	0	1	0	0	1	0	0	1	1	0	0	0	0
30	0	0	0	0	0	0	0	0	0	0	1	1	1	1	0	0	0	0	0	0
31	0	0	0	0	0	0	0	0	0	0	0	1	1	0	1	0	0	0	0	0
32	0	0	0	0	0	0	0	0	0	0	0	0	0	0	0	1	0	1	0	0
33	0	0	0	0	0	0	0	0	0	0	0	0	0	0	0	0	0	0	0	0
34	0	0	0	0	0	0	0	0	0	0	0	0	0	0	0	0	1	0	0	0
35	0	0	0	0	0	0	0	0	0	0	0	0	0	0	0	0	0	1	0	0
36	0	0	0	0	0	0	0	0	0	0	0	0	0	0	0	0	0	0	0	0

Cells subject to bare-soil evaporation in October 1977

Row	Column																			
1	0	0	0	0	0	0	0	0	0	0	1	1	0	0	0	0	0	0	0	0
2	0	0	0	0	0	0	0	0	0	1	1	1	0	0	0	0	0	0	0	0
3	0	0	0	0	0	0	0	0	1	1	0	1	1	0	0	0	0	0	0	0
4	0	0	0	0	0	0	0	0	1	0	0	1	1	1	0	0	0	0	0	0
5	0	0	0	0	0	0	0	0	1	1	1	1	1	1	0	0	0	0	0	0
6	0	0	0	0	0	0	1	1	0	1	1	1	1	1	0	0	0	0	0	0
7	0	0	0	0	0	0	1	1	0	0	1	1	1	1	1	0	0	0	0	0
8	0	0	0	0	0	0	0	0	0	0	1	1	1	0	0	0	0	0	0	0
9	0	0	0	0	0	0	0	0	0	0	0	1	1	0	0	0	0	0	0	0
10	0	0	0	0	0	0	0	0	0	0	0	1	1	0	0	0	0	0	0	0
11	0	0	0	0	0	0	0	0	0	0	0	1	0	0	0	0	0	0	0	0
12	0	0	0	0	0	0	0	0	0	0	0	0	1	0	0	0	0	0	0	0
13	0	0	0	0	0	0	0	0	0	0	0	0	0	1	0	0	0	0	0	0
14	0	0	0	0	0	0	0	0	0	0	0	0	0	0	0	0	0	0	0	0
15	0	0	0	0	0	0	0	0	0	0	0	0	0	0	0	0	0	0	0	0
16	0	0	0	0	0	0	0	0	0	0	0	0	0	0	1	0	0	0	0	0
17	0	0	0	0	0	0	0	0	0	0	0	0	0	0	0	1	0	0	0	0
18	0	0	0	0	0	0	0	0	0	0	0	0	0	0	1	0	0	0	0	0
19	0	0	0	0	0	0	0	0	0	0	0	0	1	1	0	0	0	0	0	0
20	0	0																		

Cells subject to bare-soil evaporation in July 1983

Row	Column																			
1	0	0	0	0	0	0	0	0	0	0	0	0	0	0	0	0	0	0	0	0
2	0	0	0	0	0	0	0	0	0	1	1	1	1	0	0	0	0	0	0	0
3	0	0	0	0	0	0	0	0	1	1	1	1	1	0	0	0	0	0	0	0
4	0	0	0	0	0	0	0	0	1	1	1	1	1	1	0	0	0	0	0	0
5	0	0	0	0	0	0	0	1	1	1	1	1	1	1	0	0	0	0	0	0
6	0	0	0	0	0	0	1	1	0	1	1	1	1	1	1	0	0	0	0	0
7	0	0	0	0	1	0	1	1	0	0	1	1	1	1	1	0	0	0	0	0
8	0	0	0	0	1	0	0	0	0	0	1	1	1	1	1	0	0	0	0	0
9	0	0	0	0	0	0	0	0	0	0	0	1	1	1	1	1	0	0	0	0
10	0	0	0	0	0	0	0	0	0	0	0	1	1	1	1	1	0	0	0	0
11	0	0	0	0	0	0	0	0	0	0	0	1	1	1	1	1	0	0	0	0
12	0	0	0	0	0	0	0	0	0	0	0	1	1	1	1	1	0	0	0	0
13	0	0	0	0	0	0	0	0	0	0	0	0	1	1	1	1	1	0	0	0
14	0	0	0	0	0	0	0	0	0	0	0	0	0	1	1	1	1	0	0	0
15	0	0	0	0	0	0	0	0	0	0	0	0	0	1	1	1	1	0	0	0
16	0	0	0	0	0	0	0	0	0	0	0	0	1	0	1	1	1	0	0	0
17	0	0	0	0	0	0	0	0	0	0	0	0	1	1	1	1	1	0	0	0
18	0	0	0	0	0	0	0	0	0	0	0	0	1	1	1	1	1	0	0	0
19	0	0	0	0	0	0	0	0	0	0	0	0	1	1	1	1	1	0	0	0
20	0	0	0	0	0	0	0	0	0	0	0	1	1	1	1	0	0	0	0	0
21	0	0	0	0	0	0	0	0	0	0	1	1	0	0	0	0	0	0	0	0
22	0	0	0	0	0	0	0	0	1	1	0	1	0	0	0	0	0	0	0	0
23	0	0	0	0	0	0	0	0	1	1	0	1	1	0	0	0	0	0	0	0
24	0	0	0	0	0	0	0	0	0	1	1	1	1	0	0	0	0	0	0	0
25	0	0	0	0	0	0	1	1	1	1	0	1	0	1	0	0	0	0	0	0
26	0	0	0	0	0	1	0	0	0	1	1	0	0	0	0	0	0	0	0	0
27	0	0	0	0	0	0	1	0	1	1	1	1	0	0	0	0	0	0	0	0
28	0	0	0	0	0	0	1	1	1	1	1	1	1	0	0	0	0	0	0	0
29	0	0	0	0	0	0	0	1	1	1	1	1	1	1	1	0	0	0	0	0
30	0	0	0	0	0	0	0	1	1	1	1	1	1	1	0	0	0	0	0	0
31	0	0	0	0	0	0	0	1	1	1	1	1	1	1	0	0	0	0	0	0
32	0	0	0	0	0	0	0	1	0	0	1	1	0	1	0	0	0	0	0	0
33	0	0	0	0	0	0	0	0	0	0	0	0	0	0	0	0	0	0	0	0
34	0	0	0	0	0	0	0	0	0	0	0	0	0	0	0	0	0	0	0	0
35	0	0	0	0	0	0	0	0	0	0	0	1	0	0	0	0	0	0	0	0
36	0	0	0	0	0	0	0	0	0	0	0	0	0	0	0	0	0	0	0	0

Cells subject to bare-soil evaporation in July 1984

Row	Column																			
1	0	0	0	0	0	0	0	0	0	0	1	1	0	0	0	0	0	0	0	0
2	0	0	0	0	0	0	0	0	0	1	1	1	1	0	0	0	0	0	0	0
3	0	0	0	0	0	0	0	0	1	1	1	1	1	0	0	0	0	0	0	0
4	0	0	0	0	0	0	0	0	1	1	1	1	1	1	0	0	0	0	0	0
5	0	0	0	0	0	0	0	1	1	1	1	1	1	1	0	0	0	0	0	0
6	0	0	0	0	0	0	1	1	1	1	1	1	1	1	1	0	0	0	0	0
7	0	0	0	0	1	0	0	0	1	1	1	1	1	1	1	1	0	0	0	0
8	0	0	0	0	1	0	0	0	0	1	1	1	1	1	1	1	0	0	0	0
9	0	0	0	0	0	0	0	0	0	0	0	0	1	1	1	1	1	0	0	0
10	0	0	0	0	0	0	0	0	0	0	0	0	0	1	1	1	1	1	0	0
11	0	0	0	0	0	0	0	0	0	0	0	0	0	1	1	1	1	1	0	0
12	0	0	0	0	0	0	0	0	0	0	0	0	0	0	1	1	1	1	0	0
13	0	0	0	0	0	0	0	0	0	0	0	0	0	0	0	1	1	1	1	0
14	0	0	0	0	0	0	0	0	0	0	0	0	0	0	1	1	1	1	1	0
15	0	0	0	0	0	0	0	0	0	0	0	0	0	0	1	1	1	1	1	0
16	0	0	0	0	0	0	0	0	0	0	0	0	0	0	1	0	1	1	1	0
17	0	0	0	0	0	0	0	0	0	0	0	0	0	0	1	0	1	1	1	0
18	0	0	0	0	0	0	0	0	0	0	0	0	0	0	1	1	1	1	1	0
19	0	0	0	0	0	0	0	0	0	0	0	0	0	0	1	1	0	1	1	0
20	0	0	0	0	0	0	0	0	0	0	0	0	0	1	1	1	0	0	0	0
21	0	0	0	0	0	0	0	0	0	1	1	1	1	1	0	0	0	0	0	0
22	0	0	0	0	0	0	0	0	1	1	0	1	0	0	0	0	0	0	0	0
23	0	0	0	0	0	0	0	0	1	1	1	1	1	0	1	0	0	0	0	0
24	0	0	0	0	0	0	0	0	0	1	1	1	1	0	1	1	0	0	0	0
25	0	0	0	0	0	0	0	0	0	1	1	0	1	0	1	0	1	0	0	0
26	0	0	0	0	0	1	0	0	0	1	1	1	1	0	0	0	0	0	0	0
27	0	0	0	0	0	0	1	1	1	1	1	1	1	0	0	0	0	0	0	0
28	0	0	0	0	0	0	1	1	1	1	1	1	1	1	0	0	0	0	0	0
29	0	0	0	0	0	0	0	1	1	1	1	1	1	1	1	0	0	0	0	0
30	0	0	0	0	0	0	0	1	1	1	1	1	1	1	1	0	0	0	0	0
31	0	0	0	0	0	0	0	1	1	1	1	1	1	1	1	0	0	0	0	0
32	0	0	0	0	0	0	0	1	0	0	1	1	0	1	0	0	0	0	0	0
33	0	0	0	0	0	0	0	0	0	0	0	0	0	0	0	0	0	0	0	0
34	0	0	0	0	0	0	0	0	0	0	0	0	0	0	0	0	0	0	0	0
35	0	0	0	0	0	0	0	0	0	0	0	0	0	0	0	1	0	0	0	0
36	0	0	0	0	0	0	0	0	0	0	0	0	0	0	0	0	0	0	0	0

Cells subject to bare-soil evaporation in October 1983

Row	Column																			
1	0	0	0	0	0	0	0	0	0	0	1	1	0	0	0	0	0	0	0	0
2	0	0	0	0	0	0	0	0	0	1	1	1	1	0	0	0	0	0	0	0
3	0	0	0	0	0	0	0	0	1	1	1	1	1	0	0	0	0	0	0	0
4	0	0	0	0	0	0	0	1	1	1	1	1	1	0	0	0	0	0	0	0
5	0	0	0	0	0	0	1	0	0	1	1	1	1	1	0	0	0	0	0	0
6	0	0	0	0	0	0	1	0	0	1	1	1	1	1	1	0	0	0	0	0
7	0	0	0	0	1	0	0	0	0	1	1	1	1	1	1	0	0	0	0	0
8	0	0	0	0	0	0	0	0	0	1	1	1	1	1	1	0	0	0	0	0
9	0	0	0	0	0	0	0	0	0	0	1	1	1	1	1	0	0	0	0	0
10	0	0	0	0	0	0	0	0	0	0	1	1	1	1	1	1	0	0	0	0
11	0	0	0	0	0	0	0	0	0	0	1	1	1	1	1	0	0	0	0	0
12	0	0	0	0	0	0	0	0	0	0	1	1	1	1	1	0	0	0	0	0
13	0	0	0	0	0	0	0	0	0	0	0	1	1	1	1	1	0	0	0	0
14	0	0	0	0	0	0	0	0	0	0	0	0	1	1	1	0	0	0	0	0
15	0	0	0	0	0	0	0	0	0	0	0	0	1	1	1	0	0	0	0	0
16	0	0	0	0	0	0	0	0	0	0	1	0	0	1	0	0	0	0	0	1
17	0	0	0	0	0	0	0	0	0	0	0	0	0	1	0	1	0	1	1	1
18	0	0	0	0	0	0	0	0	0	0	0	1	0	0	1	1	1	1	1	1
19	0	0	0	0	0	0	0	0	0	0	0	1	0	0	1	1	0	0	1	0
20	0																			

Cells subject to bare-soil evaporation in July 1987

Row	Column																			
1	0	0	0	0	0	0	0	0	0	0	0	1	1	0	0	0	0	0	0	0
2	0	0	0	0	0	0	0	0	1	1	1	0	0	0	0	0	0	0	0	0
3	0	0	0	0	0	0	0	0	1	1	1	0	0	0	0	0	0	0	0	0
4	0	0	0	0	0	0	0	0	1	1	1	0	0	0	0	0	0	0	0	0
5	0	0	0	0	0	0	1	1	1	1	1	1	1	1	0	0	0	0	0	0
6	0	0	0	0	0	0	1	1	1	1	1	1	1	0	1	0	0	0	0	0
7	0	0	0	0	1	0	1	1	1	1	1	1	1	1	0	0	0	0	0	0
8	0	0	0	0	0	0	1	1	1	1	1	1	1	1	1	1	0	0	0	0
9	0	0	0	0	0	0	0	0	0	1	1	1	1	1	1	1	0	0	0	0
10	0	0	0	0	0	0	0	0	0	1	1	1	1	1	1	1	0	0	0	0
11	0	0	0	0	0	0	0	0	0	0	1	1	1	1	1	1	1	0	0	0
12	0	0	0	0	0	0	0	0	0	0	1	1	1	1	1	1	0	0	0	0
13	0	0	0	0	0	0	0	0	0	0	1	1	1	1	1	1	0	0	0	0
14	0	0	0	0	0	0	0	0	0	0	0	1	1	1	1	1	1	0	0	0
15	0	0	0	0	0	0	0	0	0	0	0	1	1	1	1	1	1	0	0	0
16	0	0	0	0	0	0	0	0	0	0	1	1	1	1	1	1	1	0	0	0
17	0	0	0	0	0	0	0	0	0	0	1	0	0	1	1	1	1	0	0	0
18	0	0	0	0	0	0	0	0	0	0	0	1	1	1	1	1	1	0	0	0
19	0	0	0	0	0	0	0	0	0	1	1	1	1	1	1	0	1	0	0	0
20	0	0	0	0	0	0	0	0	0	1	1	1	1	1	1	0	1	0	0	0
21	0	0	0	0	0	0	0	1	1	1	0	1	0	1	0	0	0	0	0	0
22	0	0	0	0	0	0	1	1	1	1	1	1	1	0	0	0	0	0	0	0
23	0	0	0	0	0	0	0	1	1	1	0	0	0	0	0	0	0	0	0	0
24	0	0	0	0	0	0	0	0	1	1	0	0	0	0	0	0	0	0	0	0
25	0	0	0	0	0	1	0	0	1	1	1	0	1	0	0	0	0	0	0	0
26	0	0	0	0	0	1	0	0	1	1	1	0	0	0	0	0	0	0	0	0
27	0	0	0	0	0	0	1	0	1	1	1	1	0	0	0	0	0	0	0	0
28	0	0	0	0	0	0	1	1	1	1	1	1	0	0	0	0	0	0	0	0
29	0	0	0	0	0	0	1	1	1	1	1	1	1	0	0	0	0	0	0	0
30	0	0	0	0	0	0	1	1	1	0	1	1	1	1	0	0	0	0	0	0
31	0	0	0	0	0	0	0	1	1	1	1	0	1	0	0	0	0	0	0	0
32	0	0	0	0	0	0	0	1	0	0	1	0	1	0	1	0	0	0	0	0
33	0	0	0	0	0	0	0	0	0	0	0	1	0	0	0	0	0	0	0	0
34	0	0	0	0	0	0	0	0	0	0	0	0	0	0	0	0	0	0	0	0
35	0	0	0	0	0	0	0	0	0	0	0	1	0	0	0	0	0	0	0	0
36	0	0	0	0	0	0	0	0	0	0	0	0	0	0	0	0	0	0	0	0

Cells subject to bare-soil evaporation in July 1988

Row	Column																			
1	0	0	0	0	0	0	0	0	0	0	0	1	1	0	0	0	0	0	0	0
2	0	0	0	0	0	0	0	0	0	1	1	1	0	0	0	0	0	0	0	0
3	0	0	0	0	0	0	0	0	1	1	1	1	0	0	0	0	0	0	0	0
4	0	0	0	0	0	0	0	0	1	1	1	1	1	0	0	0	0	0	0	0
5	0	0	0	0	0	0	1	1	0	1	1	1	1	1	1	1	0	0	0	0
6	0	0	0	0	0	0	1	1	1	1	1	1	1	1	1	1	0	0	0	0
7	0	0	0	0	0	0	1	1	1	1	1	1	1	1	1	1	0	0	0	0
8	0	0	0	0	0	0	0	1	1	1	1	1	1	1	1	1	1	0	0	0
9	0	0	0	0	0	0	0	0	1	1	1	1	1	1	1	1	1	0	0	0
10	0	0	0	0	0	0	0	0	0	1	1	1	1	1	1	1	1	0	0	0
11	0	0	0	0	0	0	0	0	0	0	1	1	1	1	1	1	1	1	0	0
12	0	0	0	0	0	0	0	0	0	0	0	1	1	1	1	1	1	0	0	0
13	0	0	0	0	0	0	0	0	0	0	0	1	1	1	1	1	1	0	0	0
14	0	0	0	0	0	0	0	0	0	0	0	0	1	1	1	1	1	1	0	0
15	0	0	0	0	0	0	0	0	0	0	0	0	1	1	1	1	1	0	0	0
16	0	0	0	0	0	0	0	0	0	0	0	0	1	1	1	1	1	0	0	0
17	0	0	0	0	0	0	0	0	0	0	0	0	0	1	1	1	1	0	0	0
18	0	0	0	0	0	0	0	0	0	0	0	0	0	1	1	1	1	0	0	0
19	0	0	0	0	0	0	0	0	0	0	0	0	0	1	1	1	1	0	0	0
20	0	0	0	0	0	0	0	0	0	0	0	0	1	1	1	1	1	0	0	0
21	0	0	0	0	0	0	0	0	1	1	1	1	1	0	1	0	0	0	0	0
22	0	0	0	0	0	0	0	1	1	1	1	1	0	1	1	0	1	0	0	0
23	0	0	0	0	0	0	0	1	1	1	0	0	0	0	0	0	0	0	0	0
24	0	0	0	0	0	0	0	0	1	1	0	0	0	0	0	0	0	0	0	0
25	0	0	0	0	0	1	0	0	1	1	0	0	1	0	0	1	0	0	0	0
26	0	0	0	0	0	1	0	0	1	1	1	0	0	0	0	0	0	0	0	0
27	0	0	0	0	0	0	1	0	1	1	1	1	0	0	0	0	0	0	0	0
28	0	0	0	0	0	0	1	1	1	1	1	1	0	0	0	0	0	0	0	0
29	0	0	0	0	0	0	1	1	1	1	1	1	1	0	0	0	0	0	0	0
30	0	0	0	0	0	0	1	1	1	0	1	1	1	1	0	0	0	0	0	0
31	0	0	0	0	0	0	0	1	1	1	1	0	1	0	0	0	0	0	0	0
32	0	0	0	0	0	0	0	1	0	0	1	0	1	0	1	0	0	0	0	0
33	0	0	0	0	0	0	0	0	0	0	0	1	0	0	0	0	0	0	0	0
34	0	0	0	0	0	0	0	0	0	0	0	0	0	0	0	0	0	0	0	0
35	0	0	0	0	0	0	0	0	0	0	0	0	0	0	0	0	0	0	0	0
36	0	0	0	0	0	0	0	0	0	0	0	0	0	0	0	0	0	0	0	0

Cells subject to bare-soil evaporation in October 1987

Row	Column																			
1	0	0	0	0	0	0	0	0	0	1	1	0	0	0	0	0	0	0	0	0
2	0	0	0	0	0	0	0	0	1	1	1	0	0	0	0	0	0	0	0	0
3	0	0	0	0	0	0	0	1	1	0	1	0	0	0	0	0	0	0	0	0
4	0	0	0	0	0	0	0	1	1	0	1	1	0	0	0	0	0	0	0	0
5	0	0	0	0	0	0	0	1	1	1	1	0	0	0	0	0	0	0	0	0
6	0	0	0	0	0	0	0	1	1	1	0	0	0	0	0	0	0	0	0	0
7	0	0	0	0	1	0	0	0	1	1	1	0	0	0	0	0	0	0	0	0
8	0	0	0	0	1	0	0	0	1	1	1	1	1	0	0	0	0	0	0	0
9	0	0	0	0	0	0	0	0	1	1	1	1	1	1	0	0	0	0	0	0
10	0	0	0	0	0	0	0	0	0	1	1	1	1	1	0	0	0	0	0	0
11	0	0	0	0	0	0	0	0	0	1	1	1	1	1	0	0	0	0	0	0
12	0	0	0	0	0	0	0	0	0	0	1	1	1	1	1	0	0	0	0	0
13	0	0	0	0	0	0	0	0	0	0	0	1	0	1	1	0	0	0	0	0
14	0	0	0	0	0	0	0	0	0	0	0	1	0	1	1	0	0	0	0	0
15	0	0	0	0	0	0	0	0	0	0	0	0	0	1	0	0	1	0	0	0
16	0	0	0	0	0	0	0	0	0	0	0	0	0	0	0	0	0	0	0	0
17	0	0	0	0	0	0	0	0	0	0	0	0	0	0	0	0	0	0	0	0
18	0	0	0	0	0	0	0	0	0	0	0	0	1	1	1	1	0	0	0	0
19	0	0	0	0	0	0	0	0	0	0	0	0	1	1	1	1	0	0	0	0
20	0																			